PERFORMANCE ANALYSIS OF FS3P INVERTER FED INDUCTION MOTOR DRIVE USING SVPWM TECHNIQUE

A DISSERTATION

SUBMITTED IN PARTIAL FULFILLMENT OF REQUIREMENTS OF THE AWARD FOR THE DEGREE

OF

MASTER OF TECHNOLOGY

IN

POWER SYSTEMS

SUBMITTED BY

ASHRAY SAINI

2K18/PSY/12

UNDER THE SUPERVISION OF

PROF. DHEERAJ JOSHI

DEPARTMENT OF ELECTRICAL ENGINEERING

DELHI TECHNOLOGICAL UNIVERSITY

(Formely Delhi College of Engineering)

Bawana Road, Delhi-110042

2020

DEPARTMENT OF ELECTRICAL ENGINEERING

DELHI TECHNOLOGICAL UNIVERSITY

(Formely Delhi College of Engineering)

Bawana Road, Delhi-110042

CANDIDATE'S DECLARATION

I, ASHRAY SAINI, Roll No. 2K18/PSY/12 student of M.Tech. (Power System), hereby declare that the project Dissertation titled "**PERFORMANCE ANALYSIS OF FS3P INVERTER FED INDUCTION MOTOR DRIVES USING SVPWM TECHNIQUE**" which is submitted by me to the Department of Electrical Engineering Department, Delhi Technological University, Delhi in partial fulfillment of the requirement for the award of the degree of Master of Technology, is original and not copied from any source without proper citation. This work has not previously formed the basis for the award of any Degree, Diploma Associate ship, Fellowship or other similar title or recognition.

Place: Delhi

Date:

(ASHRAY SAINI)

DEPARTMENT OF ELECTRICAL ENGINEERING

DELHI TECHNOLOGICAL UNIVERSITY

(Formely Delhi College of Engineering)

Bawana Road, Delhi-110042

CERTIFICATE

I hereby certify that the major project titled **"PERFORMANCE ANALYSIS OF FS3P INVERTER FED INDUCTION MOTOR DRIVES USING SVPWM TECHNIQUE"** which is submitted by ASHRAY SAINI, Roll No-2K18/PSY/12 ELECTRICAL ENGINEERING DEPARTMENT, Delhi Technological University, Delhi, in partial fulfilment of the requirement for the award of the degree of Master of Technology, is a record of the project work carried out by the students under my supervision. To the best of my knowledge this work has not been submitted in part or full for any Degree to this University or elsewhere.

Place: Delhi

Date:

PROF. DHEERAJ JOSHI

(PROJECT SUPERVISOR)

Professor

Department of Electrical Engineering

Delhi Technological University

DEPARTMENT OF ELECTRICAL ENGINEERING

DELHI TECHNOLOGICAL UNIVERSITY

(Formely Delhi College of Engineering)

Bawana Road, Delhi-110042

ACKNOWLEDGEMENT

I want to convey my deepest gratitude to Professor Dheeraj Joshi for their continuous support in the dissertation. I am highly indebted to him for allowing me to work under his mentorship, and for providing all the necessary guidance and equipments required for my project. It would have not been possible to conclude my project in absence of their valuable time and advice. I sincerely appreciate their readiness to address all my doubts and queries regarding the project work and their consistent encouragement to carry my work forward. Working under him has been a great experience and it aided me in gaining a lot of personal as well as professional insight.

I am thankful to Prof. Uma Nangia, Head of Department, Electrical Engineering, faculties in Electrical Department, DTU for their kind help, encouragement and knowledge throughout this course which helped me in completing my project work.

I am also indebted to my seniors Mr. Kailash Rana, Mr. Shreyansh Upadhyaya, Mr. Ajay Kumar Sahu and Mr. Animesh Patra for their constant emotional and technical support in every part of stages in completion of my project work, without them this dissertation would have been incomplete. I would be failing in my duty if I don't mention Ms. Annu Ahlawat and Mr. Shobhit Sharma for their continuous moral and technical support and all other colleagues for helping me in all possible way.

Finally, I am appreciative of my family for their love and encouragement. They have always provided me with all the needful resources and guidance to excel in life. I am fortunate to have them. All my capabilities are because of them and all my achievements truly belongs to them.

Place: Delhi **ASHRAY SAINI**

Date:

ABSTRACT

Electric Vehicles is call for today and tomorrow and induction motor drives are best chosen for the motional part in the system because of their enormous advantages. Three phase inverter fed induction motor drives are being used in the vehicles that have been made yet and research are still going to reduce the cost and complexity along with increased reliability to meet it at consumer ends without compromising its performance. In this dissertation an effort is made to reduce the cost of system by utilizing four-switch three phase inverter to feed induction motor drive. Also if conventional six switch inverter system incurred a fault in any one leg then shifting the motor load to four switch three phase alternatives would increase the reliability to great extent. Performance analysis for three induction motor drives with FS3P topology is presented along with the comparison between the conventional six-switch and proposed four switch inverter is made and discussed. Space Vector Pulse Width Modulation technique is used in proposed topology to produce three phase voltages at the output of four switch inverter, also SVPWM has advantages like better DC voltage utilization, Switching losses reduction and easier digital implementation. The validity of FS3P topology and performance of induction motor drives is verified by simulated results and MATLAB/SIMULINK platform has been utilized for simulation purpose.

CONTENTS

LIST OF FIGURES

LIST OF TABLES

List of Symbols

Parameters	Definition
R_s	Stator Resistance
R_r	Rotor Resistance
L_{ls}	Stator Self Inductance
L_{lr}	Rotor self Inductance
L_m	Magnetizing Inductance
ω_b	Base Frequency
P	Number of Poles
J	Moment of Inertia
T_e	Electromagnetic Torque
T_l	Load Torque
ω_m	Rotor Mechanical Speed
ω_r	Rotor angular Electrical Speed
ω_e	Supply Frequency
$\varphi_{qs}, \varphi_{qr}$	q-axis stator and rotor flux linkages
$\varphi_{ds}, \varphi_{dr}$	d-axis stator and rotor flux linkages
φ_{qm}	q-axis mutual flux linkage
φ_{dm}	d-axis mutual flux linkage
X_{ls}	Stator Impedance
X_{lr}	Rotor Impedance
X_m	Mutual Impedance
V_{qs}, i_{qs}	q-axis stator voltage and current
V_{ds}, i_{ds}	d-axis stator voltage and current
V_{qr}, i_{qr}	q-axis rotor voltage and current
V_{dr}, i_{dr}	d-axis rotor voltage and current
W	Watts
HP	Horse Power

CHAPTER 1

INTRODUCTION

This section includes the discussion over the four-switch three-phase Induction Motor drive system and how it is gaining attention for scientists due to its low cost and comparatively less complexity in controlling four-switches over six-switches voltage source inverter. The description of dissertation and Literature review is also included in the present chapter.

1.1 Motivation

Induction Motors forms an integral part in many industries since they are to be easy build, robust, and generally provides satisfactory efficiency. In many other applications such as air-conditioning, heating and also the need of present time "Electric Vehicles" controllable speed drives forms a major part and plays a vital role in recent years.

Defence and Custom services such as Submarines and Merchant ships the major locomotive work is performed using Induction Motor drives because of their reliability and performance. Conventionally in these major applications the induction motor drives are fed using six-switch three-phase inverter but at the same time looking into a economically beneficial aspect the reduced number of inverter switches is most promising solution to achieve.

The below shown figure shows the block diagram of cost effective and sustained drive system.

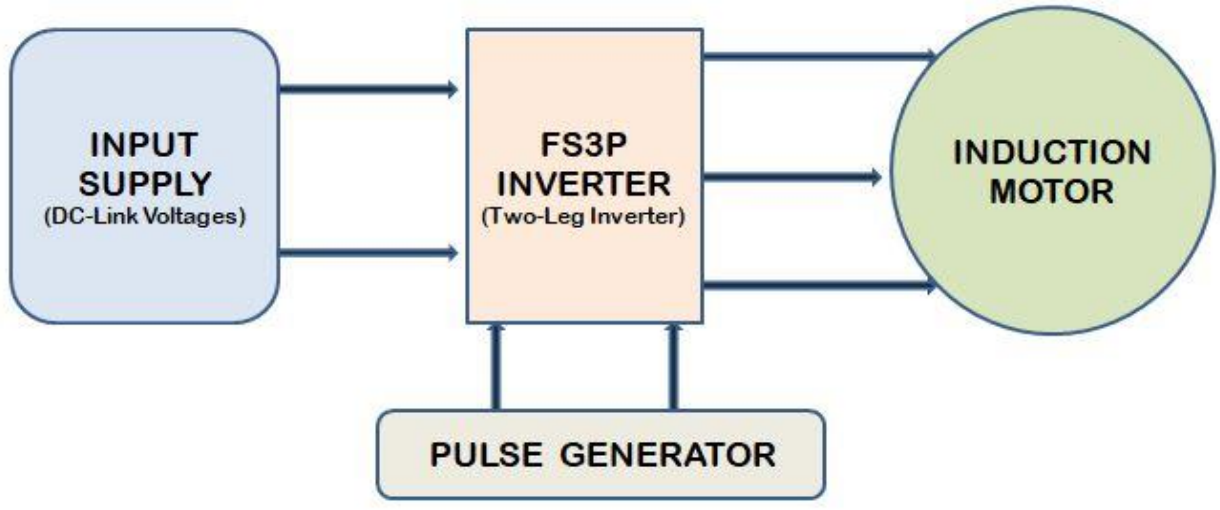

Fig.1.1 Block Diagram of Proposed Drive System

Moreover in emergency situations for example if one of the leg of three-phase inverter encounters a fault and simultaneously work using induction motor drive need to be performed immediately since controllable drives are back-bone for many industries (example- automobile assembly), here proposed drive system can prove to play a vital role and continuation of drive performance for an industry is achieved and thus forming a little part in unfloundered Nation's economy.

1.2 Proposed Topology

Fig.1.2 presents proposed topology of VSI Fed Unbalanced Induction motor drive using four-switch three-phase inverter.

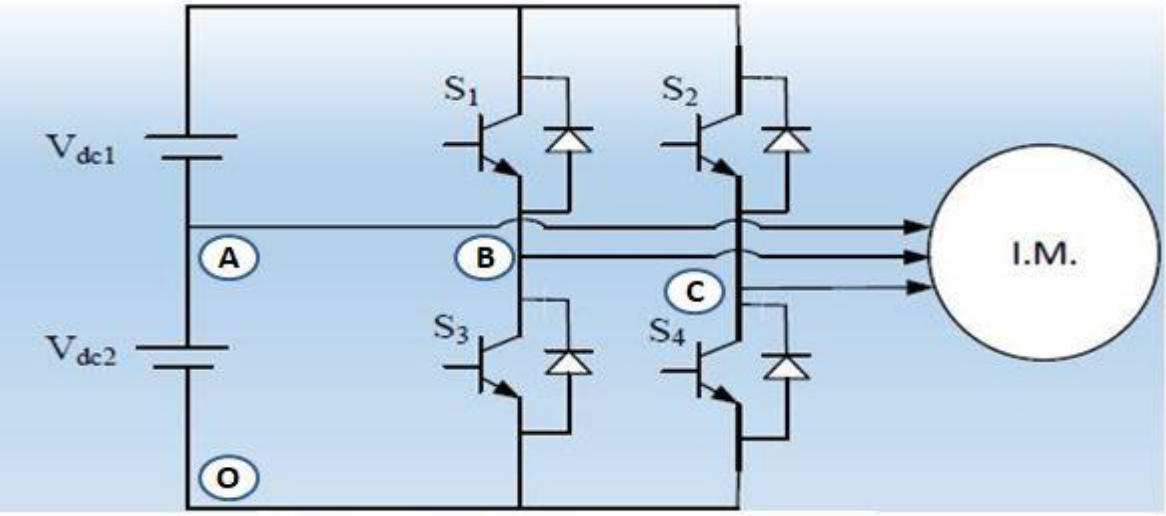

Fig.1.2 Proposed Topology for FS3P VSI-Fed Induction Motor Drive

The proposed topology shown to fed three-phase induction motor drive using four-switch inverter constitutes two phases i.e phase B and phase C from the two legs of VSI, and the third phase A is taken from the mid-point of two dc voltages V_{dc1} and V_{dc2}.

The point O which is shown in Fig.1.2 is zero-potential point and thus we can define phase-to-zero voltages V_{AO}, V_{BO}, V_{CO} depending upon the switching states of S_1, S_2 and V_{dc1} and V_{dc2} i.e dc-link Voltages.

1.3 Literature Survey

The FS3P inverter, which is suggested topology to produce three output phases from 2-leg voltage source Inverter and making it cost effective thus instead of conventional three-phase inverters using six-switches, the inverters producing three phases at output using four-switches were introduced[1]-[3].

This inverter is found advantageous [4]; since switches get reduces or one leg is totally removed so the driver circuits involved controls only the two branches there by reducing the complexity in control algorithms also. The switches of FS3P inverter must have higher withstand-able voltage (increase in cost of switches) but still it cost lower than six-switch inverter and thus thanking to price ratio of four-switch to six-switch inverter which is less than 3/2.

Besides having cost-effective topology, it includes major drawbacks of decrement in voltage and unbalanced output currents. While using split-capacitors for creating dc-link which is suggested topology by many authors a large variation of voltages across two-capacitors is caused due to circulating current of one phase through capacitor bank[4]-[6]. Decrement of maximum output voltage[7] and also voltage ripples caused by dc-link capacitors reports a major problem in FS3P topologies, the author of [8] proposed a solution to compensate dc-link voltage ripple without additional filtering in 3-leg inverters using a special modulation technique and effort also put by [6] for 2-leg three phase inverters.

In order to remove these drawbacks in FS3P inverters the different researchers moved their attention towards modulation techniques. A Sinusoidal Pulse Width Modulation (SPWM) method is used in [9] by generating two sinusoidal reference signals shifted by 60-degree for FS3P inverter.

SVPWM gain very much popularity because of its better harmonics performance, high DC-voltage utilization and also for 15% higher linear modulation range[10], many modulation strategies are developed which are based on space vectors[11]-[17]. In [4] authors presented space vector modulation strategy producing minimum torque ripple and was based on flux-trajectories.

By using space vector techniques the maximum output voltage obtained is limited to linear modulation and efforts are made by author of [18]-[21] to achieve linearity or continuous control in the over-modulation region. A similar effort to obtain linearity in over-modulation is also made by authors of [22] using Carrier Based PWM for FS3P inverters which is very simple way to generate the pulses for four switches and desired output voltage can be obtained from the intersection of reference signals with triangular signals, also the extension of linearity in the over-modulation region is greatly achieved. The effectiveness of proposed FS3P topology as a reliable topology to fed three phase Induction Motor Drive is being tested for three Induction Machines (1HP,3HP and 5.4HP), authors of [23] worked on 1HP 380V star connected Induction

Machine for constant voltage and constant frequency operation and authors of [24] worked on 3HP 220V delta connected Induction motor to incorporate the main flux saturation effect.

1.4 Dissertation Composition

The dissertation is organized in five parts. The first part of dissertation includes Chapter-1 which outlines the literature review, the need for choosing the proposed system and motivation behind it. The drawbacks and benefits of proposed system is mentioned and idea of topology proposed in research has been clearly described. Second part of dissertation describes various techniques to pulse the inverter in proposed topology, Chapter-2, Chapter-3 and Chapter-4 details the concepts, methodology and principle of different pulse width modulation techniques.

The third part includes Chapter-5 which shows the implementation of SVPWM technique in proposed topology using Matlab/Simulink.

The next part of our dissertation includes chapter-6 which shows how dc-links in FS3P topology is created using DC-DC boost conversion and describes the advantage of using the method since it is cost effective and minimizes the need of high rated dc-voltage batteries. Next with the flow dissertation includes modeling of Induction Motor drive in Chapter 7 which includes the basic equations of Flux, Voltage and Current in d-q frame and how different motor parameters are taken into account to model the machine and its implementation in Matlab/Simulink.

The Last section of the work includes the results of different topologies to fed IM Drives, the comparative analysis is also done between the conventional six switch three phase inverter topology to fed IM drive and four switch three phase inverter topology. The study of results is done for three induction motors and comments on the reliability of proposed method are discussed. Chapter 8 includes the conclusion of the dissertation along with the future work of the proposed system needed to obtain a sustainable and reliable system at the consumer end.

CHAPTER 2

SVPWM FOR THREE LEG INVERTERS

2.1 Introduction to PWM Inverters

PWM inverters started gaining much popularity over square wave inverters due to two main reasons:

(i) Control over output voltage magnitude.

(ii) It provides satisfactory reduction in unwanted harmonics in output voltages.

But at the same time it was shown that lower magnitude of output voltage of fundamental frequency is resulted using PWM inverters. In the context of SPWM good quality of output voltage is resulted when modulation index (m)≤1 for m>1 (over-modulation) the magnitude of fundamental voltage increases but at poor quality of output voltage waveform. Only 78.5% of fundamental voltage of square wave inverter can be resulted from the SPWM inverter output at maximum (without over-modulation). Because of high switching frequency of PWM inverters, the switches of PWM inverters encounters significantly higher switching loss as compared to square wave inverters thus switches in PWM inverters is made over-sized in terms of its current rating so that total sum of conduction and switching loss remains well within the heat dissipation capability of switch and its associated heat sink.

As due to high fundamental voltage at output and less switching loss the VA rating (VA rating of inverter is equals the maximum VA of load power) of square wave inverters is higher than PWM inverters, also due to use of slower switches, simpler control circuit the cost of square wave inverters comes down further. But at the same time better quality of output voltage and current makes the PWM inverters unavoidable.

Let us take example of three phase 400 volts rated induction motor is to be fed from a PWM inverter. The three phase diode rectifier followed by a large filter capacitor in often cases used to get dc bus voltage whose magnitude is considered to be peak of supply line voltage i.e for 400 volts, 50Hz, three phase supply system the dc bus voltage will be 566 volts ($400\sqrt{2}$ volts) at output. Now by using SPWM based inverter with 566 volts as dc-link voltage, maximum rms line voltage one can output is only 347 volts ($=0.612V_{dc}$), thus it will not be able to meet the rated voltage demand of 400 volts for the motor. Instead if one had used square wave inverter the maximum rms line voltage that can get at inverter output would have been 441 volts ($0.78V_{dc}$). Thus on lower output voltage account the SPWM inverters found unsuitable in certain applications besides having better output voltage and current.

Fortunately, there are some other PWM techniques that are developed or being used which provides higher output voltage magnitude at output along with good quality of line voltage and current waveforms.

2.1.1 Sine+3rd Harmonic PWM Technique

The idea of sine+3rd harmonic PWM technique is based on the fact that three phase ac load (star-connected) does not provides the path for zero sequence current.

The neutral point of star-connected load is always floating, however for a balanced three phase load fundamental component of phase voltage is identical to fundamental component of inverter's pole voltage and floating neutral has the advantage that no zero sequence currents (dc, third and integral multiples of third harmonics) will flow through the load. So if inverter's pole voltage is distorted by 3rd harmonic and its multiples, the load side phase voltage and line voltages will not be affected by these distortions.

The sine+3rd harmonic PWM technique is the modification of SPWM technique, where some amount of third harmonic voltage is introduced in inverters pole voltage deliberately. A suitable amount of third harmonic signal is added to the sinusoidal modulating signal and resultant waveform is compared with triangular carrier waveform of high frequency. Low frequency component or fundamental component of inverter pole voltage will be identical to the modified modulating signal if:

(i) Peak magnitude of carrier signal is always greater than instantaneous magnitude of modified modulating signal.

(ii) Carrier frequency should be significantly higher than modulating signal frequency.

The addition of small percentage of 3rd harmonic to the fundamental sinusoidal modulating wave having peak magnitude equal to the peak magnitude of triangular carrier wave, cause peak magnitude of combined modulating wave to become lower than peak magnitude of triangular wave, the modified modulating waveform now appears to be more flat-topped as shown in fig.2.1

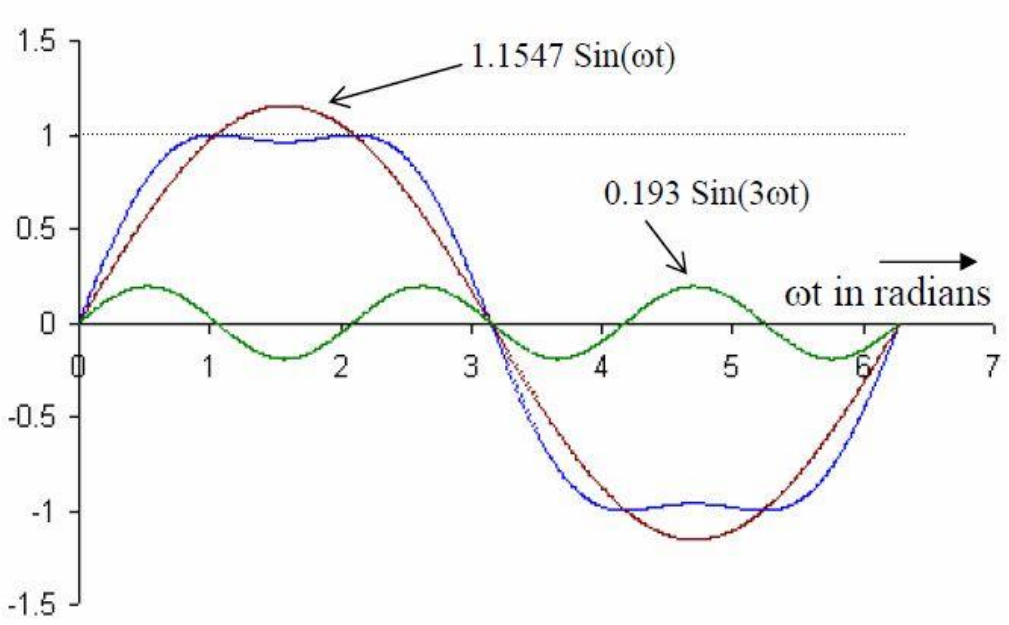

Fig.2.1 Modulating signal for Sine+3rd harmonic PWM

If peak magnitude of fundamental sinusoidal modulating wave is made slightly higher and 3rd harmonic amount is chosen suitably such that it results in a modified signal of peak magnitude not exceeding the carrier signal, thus the peak of modulating signal remains lower than peak of carrier signal and still fundamental component of output voltage is still higher than SPWM can output with m=1 as load sees only the fundamental component of inverter pole voltage and not third harmonics. Thus higher load voltage is achieved as compared to SPWM inverter without compromising the quality of output waveform.

Fig.2.1 Illustrates that [1.1547sin(ωt) + 0.193sin(3ωt)] is resulting modulating wave whose peak magnitude is 1.The fundamental voltage output of an inverter employing sine+3rd harmonics PWM techniques can be higher by nearly 15.47% than a SPWM based inverter, so considering example of 400 volts rated three phase induction motor as discussed earlier, the maximum rms line voltage output can now be 347*1.157 volts = 400 volts thus meeting the peak voltage requirement of the drive.

2.2 Space Vector PWM

The principle of SVPWM is similar to that of other PWM techniques such as Sine+3rd harmonic PWM and SPWM but the concept behind and implementation technique is somewhat different.

2.2.1 Concept

When three phase sinusoidal current is fed to stator windings of three phase ac machine, a revolving mmf is produced in the air-gap, the revolving mmf is a example of space vector. Similarly with the analogy of flux vector, a rotating voltage space vector will a resultant if a three phase balanced voltage is applied to the windings of three phase ac machine. The resultant voltage space vector will be rotating at a synchronous speed (depending upon frequency of applied three phase voltage) and will have a magnitude equal to the 1.5 times the magnitude (peak or rms) of phase voltage.

Thus looking other way around if voltage vector rotating at some synchronous speed (particular frequency) and magnitude can be generated, then it is a implication of three phase sinusoidal voltages having magnitude of each phase is 1.5 times lower than magnitude of space voltage vector and same particular frequency.

2.2.2 Inverter States and Voltage Vectors.

Let us consider three phase voltage source inverter as shown in fig.2.2.

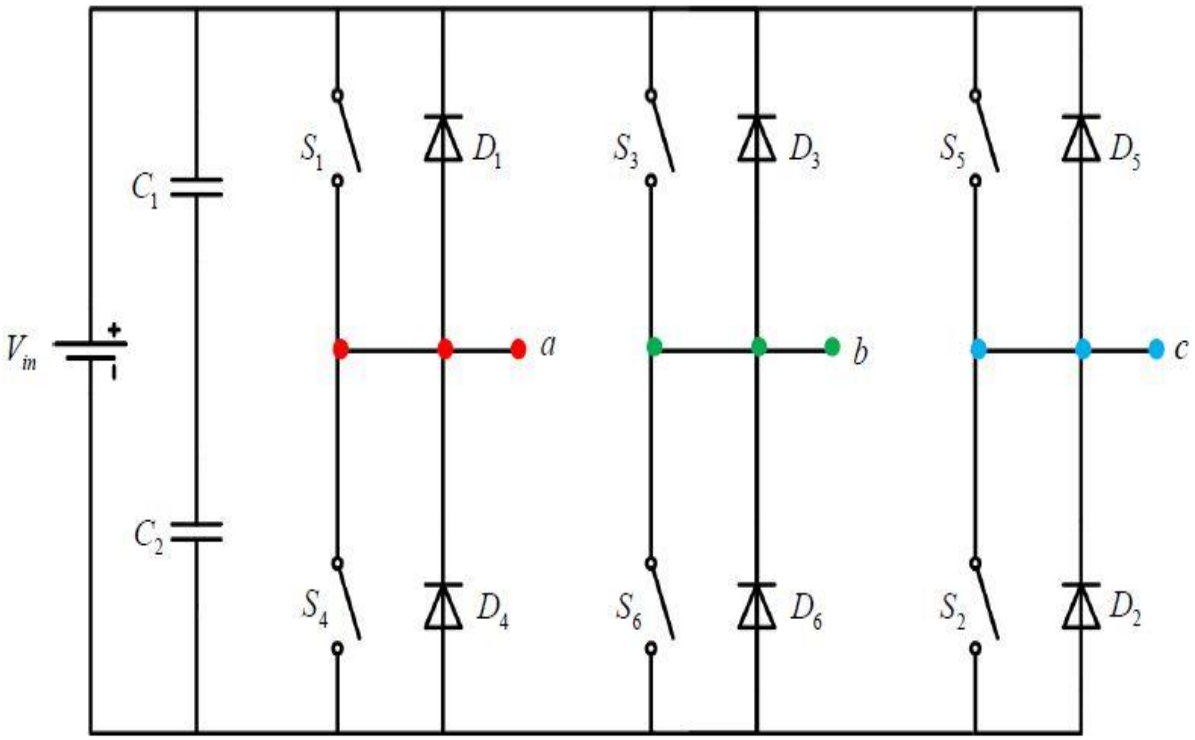

Fig.2.2 Three Phase Inverter Configuration

The given configuration has total of six switches namely S_1, S_2, S_3, S_4, S_5, S_6. Both the switches of same leg if ON represents the short-circuit condition thus here switching will be complementary i.e if S_1 is ON then S_4 is OFF and vice-versa. Since both the switches cannot have same state at the same time therefore the upper switches can be used to determine the switching states of three-phase inverter.

A switch can have two states i.e ON and OFF thus combination of upper three switches (from 2^3) will yield eight switching states where S_x=1 (x=1,3,5) implies switch is in ON state and S_x=0 implies switch is OFF, for example a switching state [101] represents switch S_1 and S_5 is ON and switch S_3 is OFF while their corresponding lower switches will follow a complementary fashion i.e same state [101] represents S_4 and S_2 is OFF and switch S_6 is ON. Fig.2.3 shows combination of different switching states of three leg inverter.

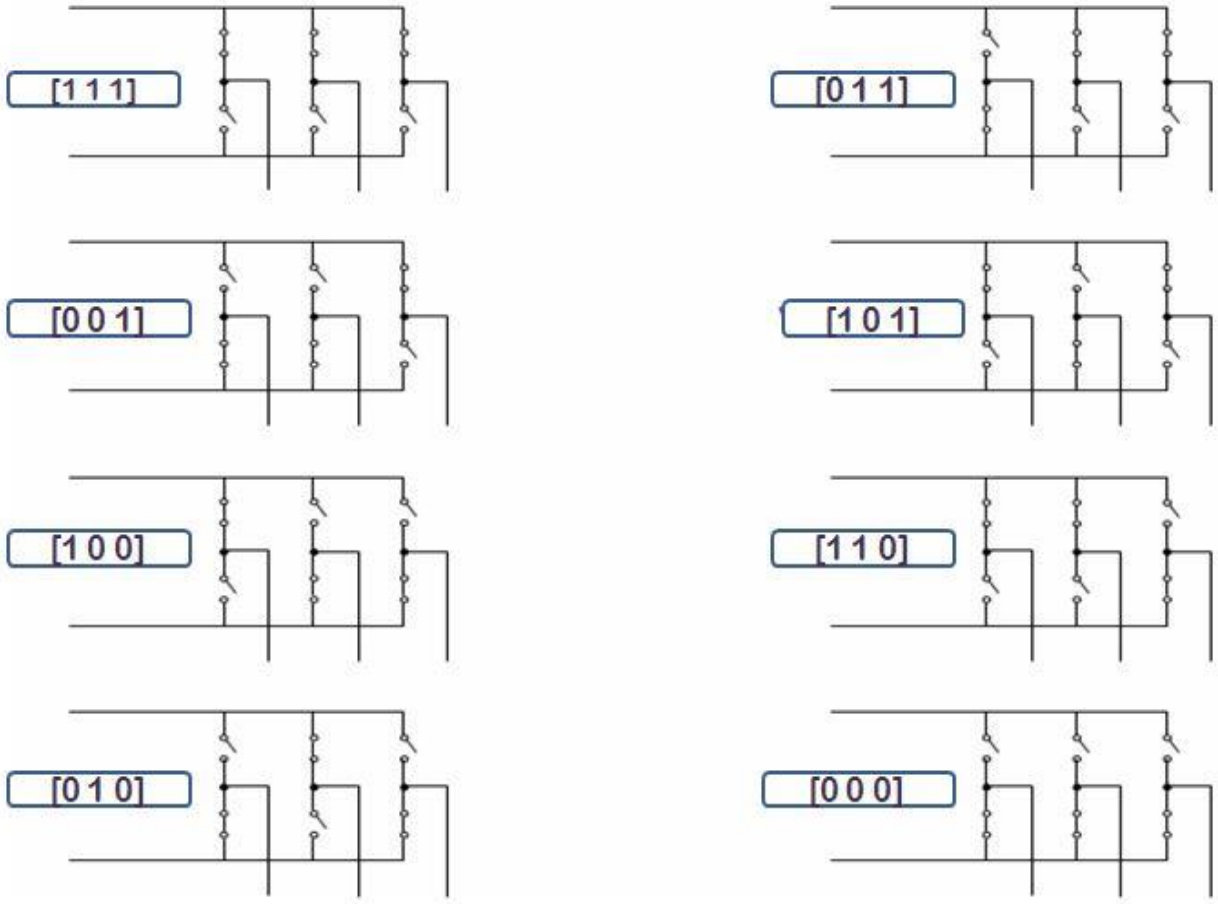

Fig.2.3 The Eight Inverter Switching States

Let us now consider the three phase inverter with star connected resistive load as shown in Fig.2.4(a). This configuration of three phase inverter showing the switching state [101] i.e switch S_1, S_6 and S_5 are turned ON, as a result terminals ***a*** and ***c*** are connected to the positive terminal of input DC source and ***b*** is connected to the negative terminal of DC source, the direction of current through R_a, R_b and R_c is shown in Fig.2.4(a) and the equivalent circuit formed is shown in Fig.2.4(b).

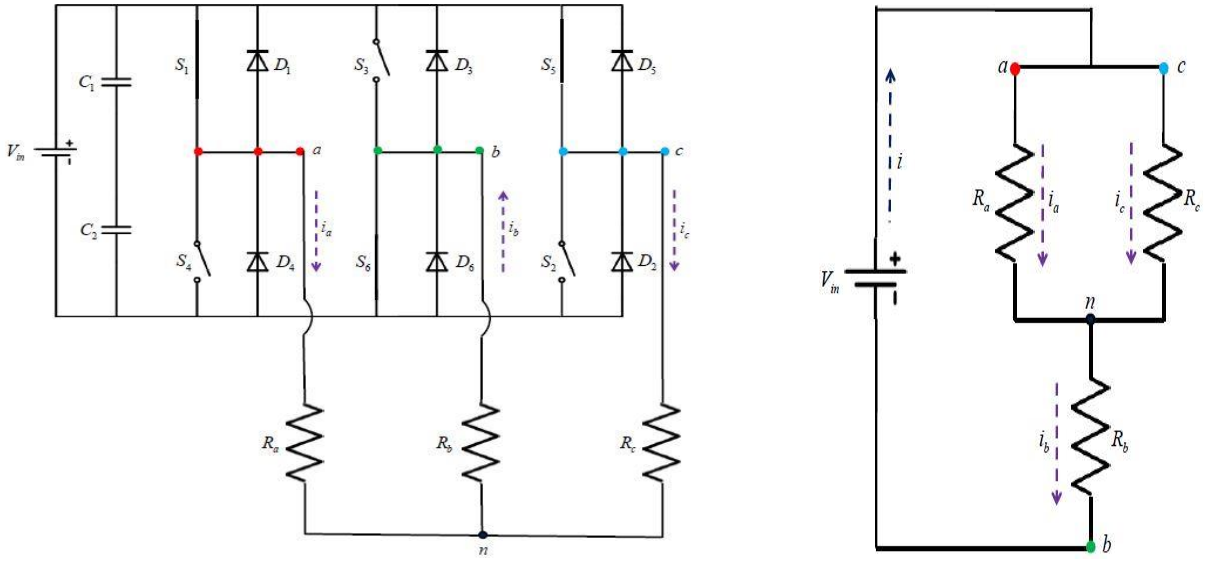

(a) **(b)**

Fig.2.4 (a) Current through load for state [101] (b) Equivalent circuit for state [101]

From Fig.2.4(b) the equivalent resistance of the circuit is ($R_a = R_b = R_c = R$)

$$R_{eq} = R + \frac{R}{2} = \frac{3R}{2} \tag{2.1}$$

The current delivered by input DC source

$$i = \frac{V_{in}}{R_{eq}} = \frac{2}{3}\frac{V_{in}}{R} \tag{2.2}$$

The current i_a and i_c are

$$i_a = i_c = \frac{1}{3}\frac{V_{in}}{R} \tag{2.3}$$

While current i_b is

$$i_b = \frac{2}{3}\frac{V_{in}}{R} \tag{2.4}$$

Thus V_{an}, V_{bn} and V_{cn} are given by

$$V_{an} = V_{cn} = \frac{V_{in}}{3} \; and \; V_{bn} = -\frac{2}{3}V_{in} \tag{2.5}$$

These values of phase voltages obtained are for the inverter configuration whose switching state is [101], the different values of phase voltages and line voltages for different switching states have been summarized in Table 2.1.

Table 2.1 Voltage Vector, Switching States, Phase Voltage and Output Line-Line Voltages

Voltage Vectors	Switching States			Phase Voltage			Line to Line Voltage		
	S_1	S_2	S_3	V_{an}	V_{bn}	V_{cn}	V_{ab}	V_{bc}	Vca
V_0	0	0	0	0	0	0	0	0	0
V_1	1	0	0	2/3	-1/3	-1/3	1	0	-1
V_2	1	1	0	1/3	1/3	-2/3	0	1	-1
V_3	0	1	0	-1/3	2/3	-1/3	-1	1	0
V_4	0	1	1	-2/3	1/3	1/3	-1	0	1
V_5	0	0	1	-1/3	-1/3	2/3	0	-1	1
V_6	1	0	1	1/3	-2/3	1/3	1	-1	0
V_7	1	1	1	0	0	0	0	0	0

The respective fraction should be multiplied by the input DC voltage to get the magnitude of output phase and line voltages.

Out of eight combinations, there are two combinations where all the upper switches are simultaneously OFF or ON, these states are being referred as null states of inverter as they results in zero output voltage from the inverter. The remaining states where two of upper and one of lower switch conduct or vice-versa are active states, the output phase and line voltages during these six states are detailed in Table 2.1

Let us consider Fig.2.5(a), it shows set of three phase balanced sinusoidal voltages being applied to the windings of three phase ac machine as shown in Fig.2.5(b). During each time period of these phase voltages six different time instants can be identified when one of the phase voltage have maximum positive or negative instantaneous magnitude and the resultant of space voltage at these instants have been named or signified V_1 to V_6 and are called as voltage vectors. Fig.2.5(b) shows the spatial positions of voltage space vectors.

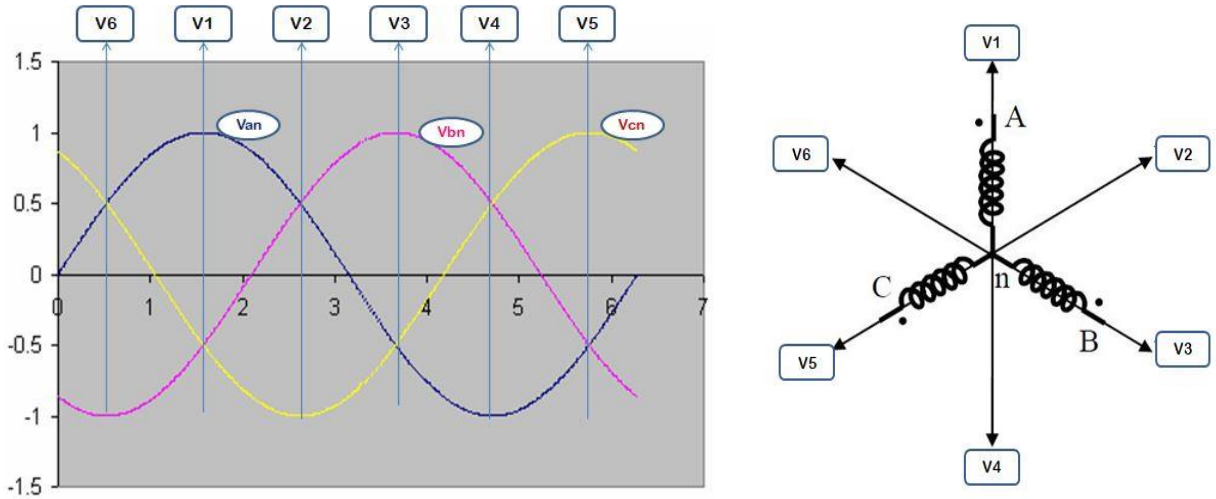

(a) (b)

Fig.2.5 (a) Three phase Balanced Sinusoidal Voltages (b) The spatial Position of Voltage Space Vectors

The instantaneous voltage output from three phase inverter as we have discussed for a star-connected resistive load cannot be matched to three phase sinusoidal phase voltages of Fig.2.5(a) at all time instants since inverter outputs are obtained from a rectangular pole voltages and contain apart from fundamental, harmonic voltages also. But however at six discrete instants the inverter output and sinusoidal voltages can be made to match because at these six discrete instants the phase voltage is at its positive or negative peak magnitude and the other two have half of the peak magnitude and also polarity of peak phase voltage is opposite to that of other phase voltages. For example, taking switching state [101] we have $V_{an} = V_{cn} = 1/3V_{dc}$ and $V_{bn} = -2/3V_{dc}$ the resulting voltage pattern is identical to the voltage pattern of the space vector voltage V_6, since $2/3V_{dc}$ represents peak magnitude of inverter output phase voltage and is assumed to be

equal to phase voltage peak in Fig.2.5(a). Table 2.1 shows how space voltage vectors V_1 to V_6 is produced from six active states of the inverter and can be matched with the six voltage vectors of Fig.2.5

Fig.2.6 shows the voltage space vector plane formed by the null state and six active states. The space vector PWM technique aims to realize synchronously rotating voltage space vector (corresponding to the fundamental component of output voltage) from six active and two null voltage vectors, the active states have the magnitude equal to V_{dc} and points along the fixed directions while null voltage vectors have zero magnitude and are each represented by a dot at the origin of voltage space vector plane.

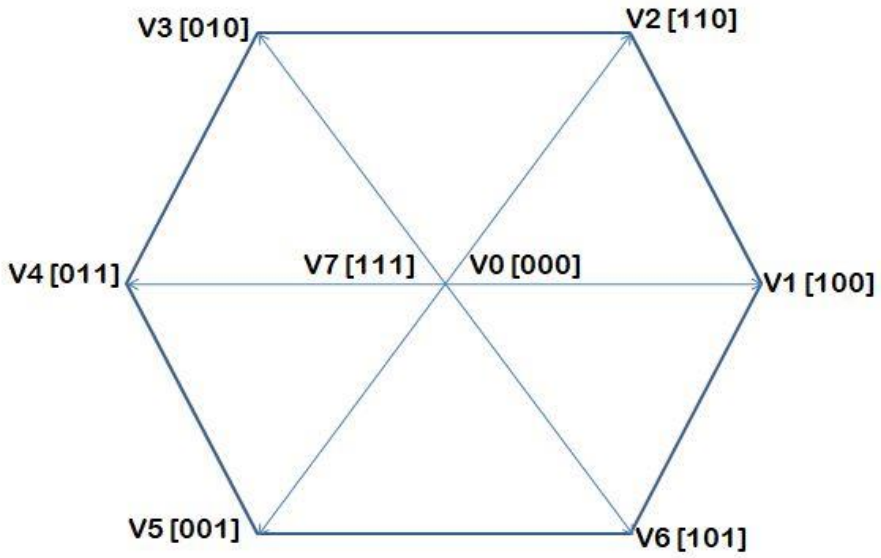

Fig.2.6 Voltage Space Vector Plane

2.2.3 The α-β Transformation

The implementation of space vector need transformation from three phase reference frame into a stationary α-β reference frame that consists of horizontal α-axes and vertical β-axes. The magnitude of voltage vector for each switching state is V_{dc} and can be easily calculated from two axes reference frame. The switching time calculations for the sysnthesis of $|V_{ref}|$ (synchronously rotating required voltage vector at output) would became easy if active voltage vectors gets divided into its respective α-β components.

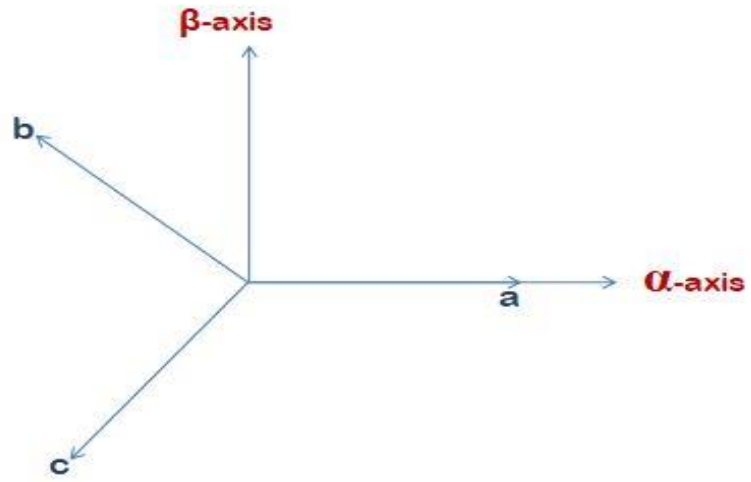

Fig.2.7 The Relationship between *abc* reference frame and stationary *α-β* reference frame

From Fig.2.7

$$V_\alpha = V_{an} - V_{bn}\cos 60 - V_{cn}\cos 60 \tag{2.6}$$

$$V_\alpha = V_{an} - \frac{1}{2}V_{bn} - \frac{1}{2}V_{cn} \tag{2.7}$$

And

$$V_\beta = 0 + V_{bn}\cos 30 - V_{cn}\cos 30 \tag{2.8}$$

$$V_\beta = 0 + \frac{\sqrt{3}}{2}V_{bn} - \frac{\sqrt{3}}{2}V_{cn} \tag{2.9}$$

From (2.7) and (2.9)

$$\begin{bmatrix} V_\alpha \\ V_\beta \end{bmatrix} = \begin{bmatrix} 1 & -\frac{1}{2} & -\frac{1}{2} \\ 0 & \frac{\sqrt{3}}{2} & -\frac{\sqrt{3}}{2} \end{bmatrix} \begin{bmatrix} V_{an} \\ V_{bn} \\ V_{cn} \end{bmatrix} \tag{2.10}$$

Using Table 2.1 and equation (2.10) one can find that for any switching state the magnitude of voltage vectors is V_{dc}.

There are total six-active voltage vectors thus voltage space vector plane is divided into six equally spaced sectors with angle between any two consecutive voltage vectors being 60 degree. If V_1 is considered to be at 0 degree and anti-clockwise direction is taken to be in increasing sense then different sectors can be represented as shown in Fig.2.8

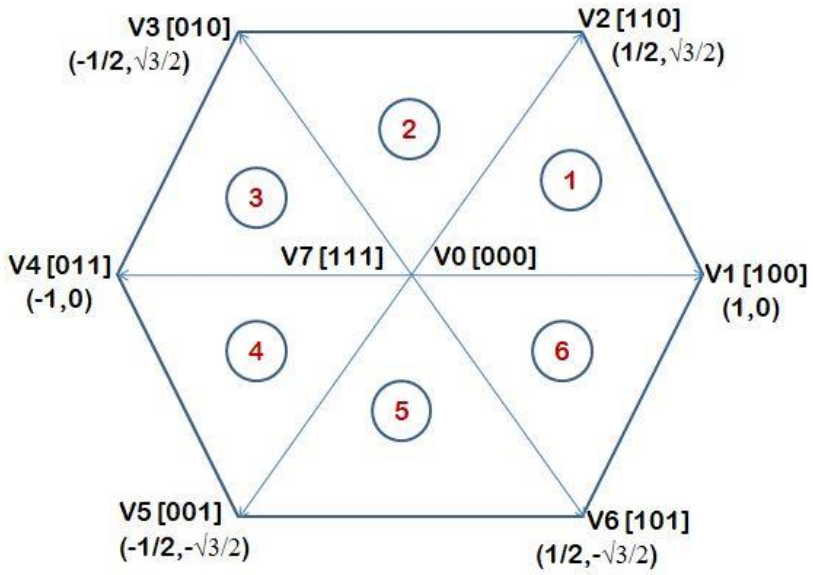

Fig.2.8 Sectors in Voltage Space Vector Plane

The α-β components of different voltage vectors can be calculated using (2.10) and their values for respective voltage vector is shown in Fig.2.8.

2.2.4 $\left|\overrightarrow{V_{ref}}\right|$ Synthesis

Let $\left|\overrightarrow{V_{ref}}\right|$ be the magnitude of the phase voltage at the output of three phase inverter. If a voltage vector whose magnitude is $1.5\left|\overrightarrow{V_{ref}}\right|$ synchronously rotating corresponding to the fundamental component of output frequency can be realized then it represents the three phase balanced sinusoidal voltages at the output of the three phase inverter, thus we need to synthesize a voltage vector whose magnitude is $1.5\left|\overrightarrow{V_{ref}}\right|$ rotating synchronously.

The required voltage vector can be synthesize using any two consecutive voltage vectors depending upon the sector in which it lies, however there will be a instant when the required voltage vector lies along any of six active voltage vectors whose magnitude being V_{dc}, so the maximum value it can take is $1.5\left|\overrightarrow{V_{ref}}\right| = V_{dc}$, thus if $1.5\left|\overrightarrow{V_{ref}}\right| = aV_{dc}$, (where a = modulation index) it implies a magnitude of required voltage vector being realized for a given value of modulation index is "aV_{dc}".

For a given Modulation index 'a' the $\left|\overrightarrow{V_{ref}}\right| = aV_{dc}$, thus by using voltage vectors whose magnitude is $2/3V_{dc}$ we can generate a required voltage vector which will result in a output phase voltage magnitude being equal to $\left|\overrightarrow{V_{ref}}\right|$ for a given value of V_{dc} which is analogous to the generation of required voltage vector of magnitude $1.5\left|\overrightarrow{V_{ref}}\right|$ from voltage vectors whose magnitude being V_{dc}. The voltage space vector plane with active voltage vector magnitude being $2/3V_{dc}$ and α-β components of respective voltage vectors is shown in Fig.2.9.

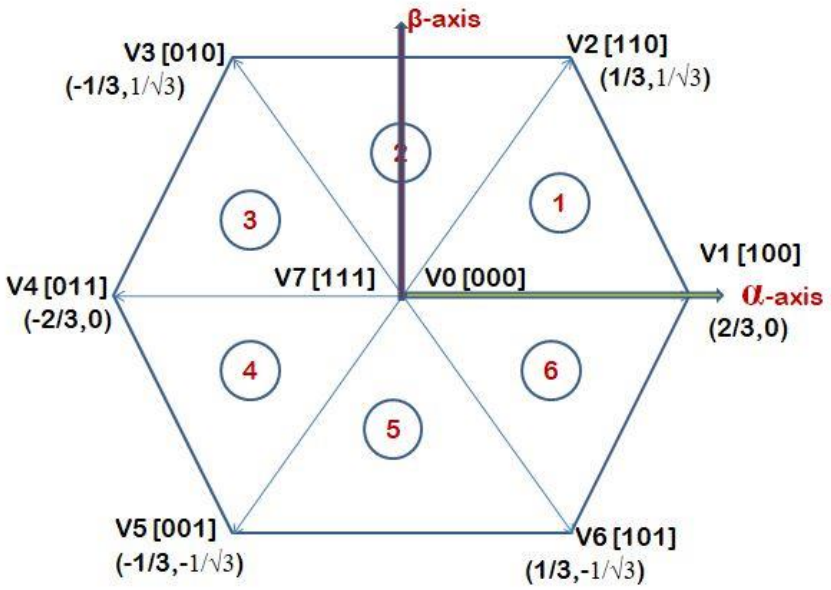

Fig.2.9 Voltage Space Vector Plane for $|V_{ref}|$ Synthesis

The reference voltage vector or required voltage vector can be synthesize by two consecutive vectors depending upon the sector in which it lies. Fig.2.10 shows the synthesis of reference voltage vector by two adjacent voltage vectors when reference vector is lying in sector 1.

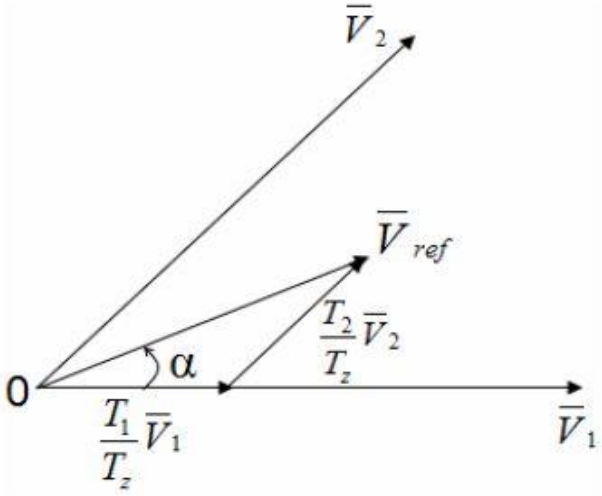

Fig.2.10 Reference Voltage Vector as a Combination of Adjacent Vectors.

$|\overrightarrow{V_{ref}}|$ is being realized using $|\overrightarrow{V_1}|$ and $|\overrightarrow{V_2}|$, let us assume that T_z being the sampling interval i.e after evry T_z time the $|\overrightarrow{V_{ref}}|$ will be sampled and the frequency at which $|\overrightarrow{V_{ref}}|$ is being sampled is called the sampling frequency.

So, to realize $|\overrightarrow{V_{ref}}|$ let us assume that $|\overrightarrow{V_1}|$ is applied for T_1 seconds and $|\overrightarrow{V_2}|$ is applied for T_2 seconds and for the remaining time the Null vectors will be applied since they results in zero voltage output where $T_z = T_1 + T_2 + T_0$ and T_0 being the time for which Null vectors are applied and to limit the prolonged conduction from the same switch, V_0 is applied for $T_0/2$ and V_7 is applied for $T_0/2$.

The switching state of $|\overrightarrow{V_1}|$ is [100] and switching state of $|\overrightarrow{V_2}|$ is [110] thus for sector 1 switch S_1 is applied for $T_1 + T_2 + T_0/2$, S_3 is applied for $T_2 + T_0/2$ and S_5 is applied for $T_0/2$. Similarly if for sector 2, $|\overrightarrow{V_2}|$[110] is applied for T_1 seconds and $|\overrightarrow{V_3}|$[010] is applied for T_2 seconds and remaining time being Null vectors for a given sampling interval T_z, then for sector 2 Switch S_1 is applied is applied or tuned ON for $T_1 + T_0/2$ time, Switch S_3 is turned ON for $T_1 + T_2 + T_0/2$ and switch S_5 is turned ON for $T_0/2$ time. Also the corresponding switches in lower arm will follow the complementary fashion i.e if S_1 is turning ON for time $T_1 + T_0/2$ then S_4 will turn ON for $T_2 + T_0/2$ in this way the time for all the switches at different sectors to synthesize $|\overrightarrow{V_{ref}}|$ can be obtained. Table 2.2 summarizes the switching timings at each sector.

Table 2.2 Switches Time for each Sector

Sectors	Upper Switches (S_1, S_2, S_3)	Lower Switches (S_4, S_6, S_2)
1	$S_1 = T_1 + T_2 + T_0/2$ $S_3 = T_2 + T_0/2$ $S_5 = T_0/2$	$S_4 = T_0/2$ $S_6 = T_1 + T_0/2$ $S_2 = T_1 + T_2 + T_0/2$
2	$S_1 = T_1 + T_0/2$ $S_3 = T_1 + T_2 + T_0/2$ $S_5 = T_0/2$	$S_4 = T_2 + T_0/2$ $S_6 = T_0/2$ $S_2 = T_1 + T_2 + T_0/2$
3	$S_1 = T_0/2$ $S_3 = T_1 + T_2 + T_0/2$ $S_5 = T_2 + T_0/2$	$S_4 = T_1 + T_2 + T_0/2$ $S_6 = T_0/2$ $S_2 = T_1 + T_0/2$
4	$S_1 = T_0/2$ $S_3 = T_1 + T_0/2$ $S_5 = T_1 + T_2 + T_0/2$	$S_4 = T_1 + T_2 + T_0/2$ $S_6 = T_2 + T_0/2$ $S_2 = T_0/2$
5	$S_1 = T_2 + T_0/2$ $S_3 = T_0/2$ $S_5 = T_1 + T_2 + T_0/2$	$S_4 = T_1 + T_0/2$ $S_6 = T_1 + T_2 + T_0/2$ $S_2 = T_0/2$
6	$S_1 = T_1 + T_2 + T_0/2$ $S_3 = T_0/2$ $S_5 = T_1 + T_0/2$	$S_1 = T_0/2$ $S_2 = T_1 + T_2 + T_0/2$ $S_2 = T_2 + T_0/2$

2.2.4.1 Determination of Time Duration T_1, T_2, and T_0

Let us consider our required voltage vector $\overrightarrow{V_{ref}}$ lies in sector 1,

$$\int_0^{T_z} \overrightarrow{V_{ref}} dt = \int_0^{T_1} \overrightarrow{V_1} dt + \int_{T_1}^{T_1+T_2} \overrightarrow{V_2} dt + \int_{T_1+T_2}^{T_z} \overrightarrow{V_0} dt \tag{2.11}$$

$$T_z . \overrightarrow{V_{ref}} = (T_1 . \overrightarrow{V_1} + T_2 \overrightarrow{V_2} \tag{2.12}$$

$$T_z . |\overrightarrow{V_{ref}}| \begin{bmatrix} \cos\alpha \\ \sin\alpha \end{bmatrix} = T_1 \frac{2}{3} V_{dc} \begin{bmatrix} 1 \\ 0 \end{bmatrix} + T_1 \frac{2}{3} V_{dc} \begin{bmatrix} \cos\frac{\pi}{3} \\ \sin\frac{\pi}{3} \end{bmatrix} \tag{2.13}$$

Here, $0 \leq \alpha \leq \frac{\pi}{3}$ since $|\overrightarrow{V_{ref}}|$ lies in sector 1,

$$T_z |\overrightarrow{V_{ref}}| [\cos\alpha + j \sin\alpha] = T_1 \frac{2}{3} V_{dc} + T_2 \frac{2}{3} V_{dc} \left[\cos\frac{\pi}{3} + j \sin\frac{\pi}{3}\right] \tag{2.14}$$

Comparing real and imaginary terms from (2.14) we have,

$$T_1 = T_z a \frac{\sin(\frac{\pi}{3} - \alpha)}{\sin\frac{\pi}{3}} \tag{2.15}$$

$$T_2 = T_z a \frac{\sin(\alpha)}{\sin\frac{\pi}{3}} \tag{2.16}$$

And

$$T_0 = T_z - (T_1 + T_2) \tag{2.17}$$

Where,

$$a = \frac{|\overrightarrow{V_{ref}}|}{\frac{2}{3} V_{dc}} \tag{2.18}$$

Also switching timing duration for any Sector is

$$T_1 = \frac{\sqrt{3} . T_z |\overrightarrow{V_{ref}}|}{V_{dc}} \left(\sin\left(\frac{n\pi}{3} - \alpha\right)\right) \tag{2.19}$$

$$T_2 = \frac{\sqrt{3} . T_z |\overrightarrow{V_{ref}}|}{V_{dc}} \left(\sin\left(\alpha - \frac{(n-1)\pi}{3}\right)\right) \tag{2.20}$$

Where "*n* = Sector", example for sector 2 the *n* = 2.

Equation (2.19), (2.20) and (2.17) gives the values of time T_1, T_2 and T_0 and depending upon the switching time at each sector for different switches as mentioned in Table 2.2 the gate pulses of corresponding timings will be fed to the three phase inverter switches which as a result will generate a synchronously rotating vector of magnitude $1.5\left|\overrightarrow{V_{ref}}\right|$ at output and thus magnitude of phase voltage that will obtained at output of the inverter will be $\left|\overrightarrow{V_{ref}}\right|$.

Assume V_{dc} = 400 volts and need to fed three phase motor load of rating 400 volts from a three phase voltage source inverter, it implies phase voltage at inverter output should be 230 volts so, from $1.5\left|\overrightarrow{V_{ref}}\right|$ = a*V_{dc}, we have 1.5*230 = a*400 we obtained a = 0.862. Thus 230 volts as output phase voltage of inverter will be obtained with modulation index being 0.862 (modulation index greater than 1 implies $1.5\left|\overrightarrow{V_{ref}}\right|$ is greater than V_{dc} and thus required voltage vector cannot be generated since magnitude of voltage vectors for input dc voltage V_{dc} is "V_{dc}") if SVPWM implementation procedure as discussed is followed.

CHAPTER 3

SVPWM FOR FOUR SWITCH THREE PHASE INVERTERS

3.1 Introduction

The cost and size of ac drives with improved waveform quality have significantly reduced with the improvements in Power Semiconductor switching technology. In order to further reduce the cost of inverter a number of topologies have been developed which uses the four switches to generate the three-phase voltage instead of conventional six-switch inverters.

Space Vector Pulse Width Modulation among all the PWM strategies is found best since it aims to switching the switches in a way to generate three-phase sinusoidal voltages at the output, using the basic fundamental principle that three-phase voltage or current will generate the rotating vector having same fundamental frequency and 1.5 times the magnitude of parent three-phase voltage or current. This chapter presents a technique to generate SVPWM signals for control of the four switch three-phase inverter based on the principle of SVPWM for six switch three-phase voltage source inverters.

3.2 Proposed Topology

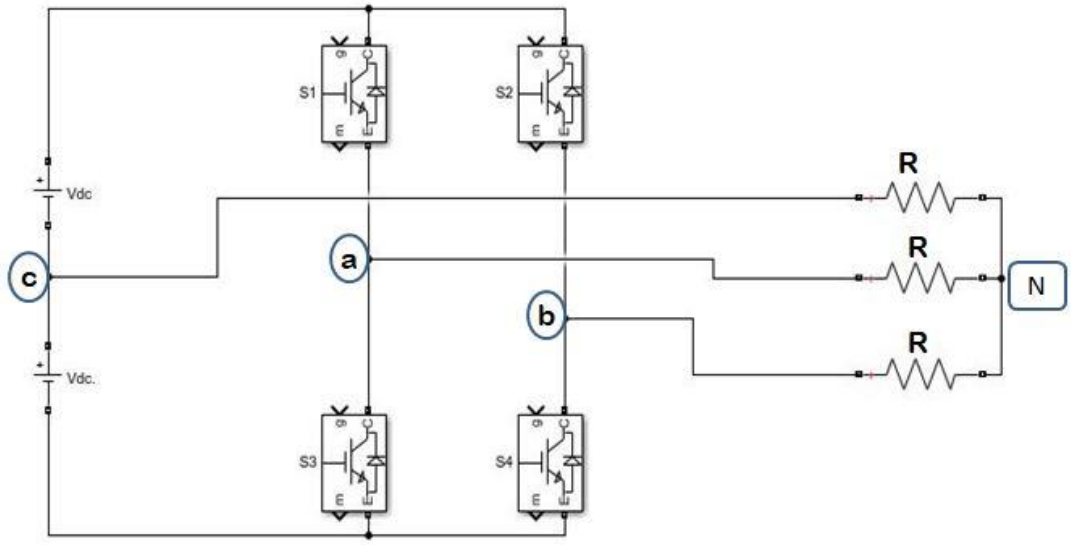

Fig.3.1 Proposed FS3P Inverter Topology

Fig.3.1 shows the power circuit of proposed system. The given topology consists of four switches that provides two output phases ‘a’ and ‘b’ of the inverter and the third phase is fed by the dc-link from the center of two dc voltages, also this dc-link can be obtained using split capacitor bank in which capacitors of high vaue is used to maintained the dc voltage across them to be constant.

In the proposed topology we are following the ‘abc' sequence for example in topology shown in fig.3.1 phase ‘a’ can take place of phase ‘b’, phase ‘b’ can take place of phase ‘c’ and phase ‘c’ can take place of phase ‘a’, still we will have the sequence ‘cab’ which is same ‘abc’. However if two terminals are interchanged disturbing the sequence ‘abc’ the direction of flux reverses thereby causing the motor to rotate in opposite direction.

3.3 Inverter States and Corresponding Voltage Vectors

3.3.1 Phase to Neutral Voltages

With respect to the circuit of fig.3.1 the phase voltages at the three-phase load terminals depends upon the conduction states of te power switches. When switch is closed its state is set to ‘1’and it is set to ‘0’ when switch is open. Also the switch in one inverter branch are controlled complementary to avoid the short-circuit condition thus, $(S_1+S_3) = 1$ and $(S_2+S_4) = 1$.

Depending upon the switching states of switch ‘S_1’ and ‘S_2’ whether ‘0’ or ‘1’ there are total of four states possible. Table 3.1 shows the four inverter states.

Table 3.1 Possible states of inverter

States	S_1	S_2
1	0	0
2	1	0
3	0	1
4	1	1

The phase to neutral voltages can be derived from the simplified circuit obtained for a particular state of the inverter. Fig.3.2 shows the simplified diagram for inverter state '00'.

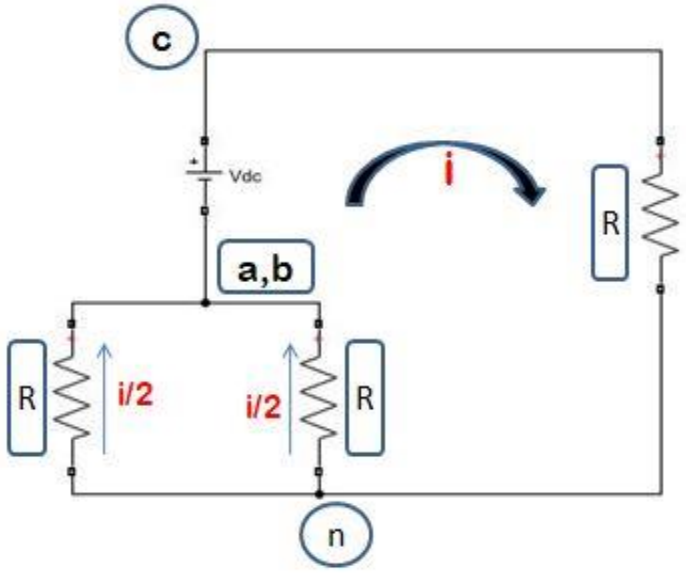

Fig.3.2 Simplified Circuit diagram for state '00'

From fig.3.2 one can derive the phase to neutral voltages easily by using the basic Kirchoff's Laws.

Net Resistance of Circuit

$$R + \left(\frac{R}{2}\right) = \frac{3R}{2} \tag{3.1}$$

Now,

$$i = \frac{V_{dc}}{\frac{3R}{2}} = \frac{2V_{dc}}{3R} \tag{3.2}$$

$$\frac{i}{2} = \frac{V_{dc}}{3R} \tag{3.3}$$

Thus,

$$V_{cn} = \frac{2V_{dc}}{3R} \times R = \frac{2V_{dc}}{3} \tag{3.4}$$

$$V_{an} = \frac{-V_{dc}}{3R} \times R = \frac{-V_{dc}}{3} \tag{3.5}$$

$$V_{bn} = \frac{-V_{dc}}{3R} \times R = \frac{-V_{dc}}{3} \tag{3.6}$$

Similarly phase to neutral voltages 'V_{an}', 'V_{bn}' and 'V_{cn}' can be derived for other inverter states in a manner using the simplified circuit diagram as done above for the state '00'. Table 3.2 summarizes the phase to neutral voltages of all the possible states of the inverter.

Table 3.2 Inverter States and Phase to Neutral Voltages

State	S_1	S_2	V_{an}	V_{bn}	V_{cn}
1	0	0	$-V_{dc}/3$	$-V_{dc}/3$	$2V_{dc}/3$
2	1	0	V_{dc}	$-V_{dc}$	0
3	0	1	$-V_{dc}$	V_{dc}	0
4	1	1	$V_{dc}/3$	$V_{dc}/3$	$-2V_{dc}/3$

3.3.2 Voltage Vectors

Table 3.2 shows the phase to neutral voltages for all possible states of the inverter. The three-phase voltages can be represented in a α-β plane using Clark's Transformation, Thus there would be particular 'V_α' and 'V_β' for a particular 'V_{an}', 'V_{bn}' and 'V_{cn}' for a given inverter state which can be represented as a phasor in a α-β plane with definite phase and magnitude thus forming a vector of a particular inverter state.

The Orthogonal Components of three-phase voltages is given by:

$$V_\alpha = (V_{an} - 0.5V_{bn} - 0.5V_{cn}) \tag{3.7}$$

$$V_\beta = \frac{\sqrt{3}}{2}(V_{bn} - V_{cn}) \tag{3.8}$$

The different 'V_α' and 'V_β' value for different phase to neutral voltages depending upon the inverter states has been summarized in table 3.3.

The phase of a vector is given by

$$\tan\theta = \frac{V_\alpha}{V_\beta} \tag{3.9}$$

The magnitude of a vector is given by

$$|V| = \sqrt{{V_\alpha}^2 + {V_\beta}^2} \tag{3.10}$$

The phase and magnitude of different vectors according to different values of 'V_α' and 'V_β' depending upon the states of the inverter has also been summarized in table 3.3.

Table 3.3 Inverter states and corresponding Voltages and Vectors

Vectors	**S_1**	**S_2**	**V_α**	**V_β**	**Phase**	**|V|**
V_1	0	0	$-V_d/2$	$-\sqrt{3}V_d/2$	240	V_d
V_2	1	0	$3V_d/2$	$-\sqrt{3}V_d/2$	330	$\sqrt{3}V_d$
V_3	0	1	$-3V_d/2$	$\sqrt{3}V_d/2$	150	$\sqrt{3}V_d$
V_4	1	1	$V_d/2$	$\sqrt{3}V_d/2$	60	V_d

The representation of different vectors in α-β plane is shown in figure 3.3.

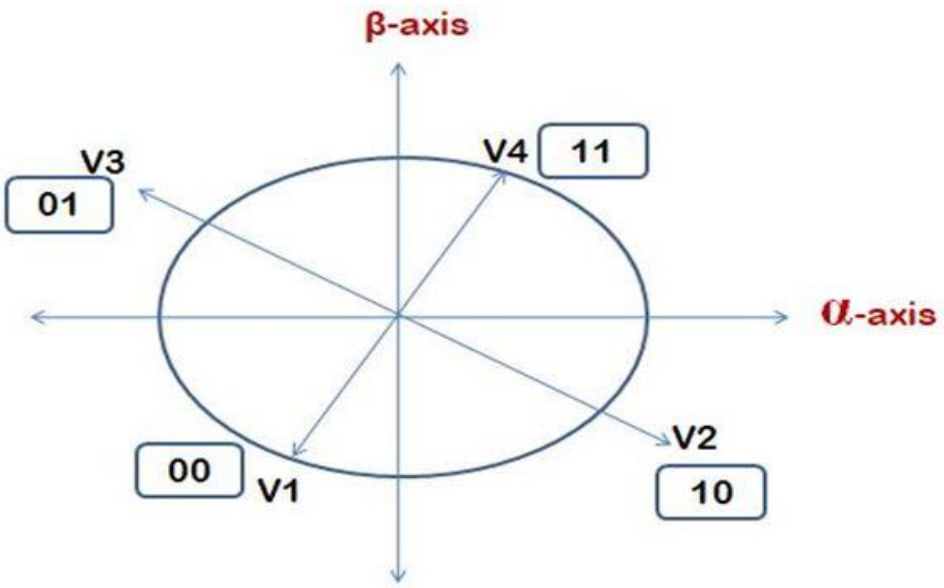

Fig.3.3 Space Vector Voltages in α-β Plane

3.4 Obtaining Sectors

Conventionally there are four sectors when obtaining SVPWM signals for four switch three phase inverters, also as we can see from fig.3.3 there are four vectors which are responsible to divide α-β plane into four sectors. The technique presented in this chapter is based on the principle of similarity of six switch three phase inverters, where α-β plane is divided into six sectors, here also instead of four sectors the V_{ref} synthesis is done using six sectors similarly as in case of six switch three phase inverters.

Fig.3.4 shows the new vectors with aiding the four vectors show in fig.3.3. Here all the six vectors are of equal length and displaced by 60 degree as in case of six switch inverters, but here the magnitude of each vector is V_{dc}.

The new vectors are

$V_{24m} = 1/2V_{24}$; where V_{24} is resultant of V_2 and V_4.

$V_{34m} = 1/2V_{34}$; where V_{34} is resultant of V_3 and V_4.

$V_{13m} = 1/2V_{13}$; where V_{13} is resultant of V_1 and V_3.

$V_{12m} = 1/2V_{12}$; where V_{12} is resultant of V_1 and V_2.

Table 3.4 consists of orthogonal representation of new vectors along with the phase and magnitude so that it becomes easier to plot new obtained vectors in α-β plane.

Table 3.4 New Vectors and corresponding Orthogonal Components

Vectors	V_α	V_β	Angle	|V|
V_{24m}	V_d	0	0	V_d
V_4	$V_d/2$	$\sqrt{3}V_d/2$	60	V_d
V_{34m}	$-V_d/2$	$\sqrt{3}V_d/2$	120	V_d
V_{13m}	$-V_d$	0	180	V_d
V_1	$-V_d/2$	$-\sqrt{3}V_d/2$	240	V_d
V_{12m}	$V_d/2$	$-\sqrt{3}V_d/2$	300	V_d

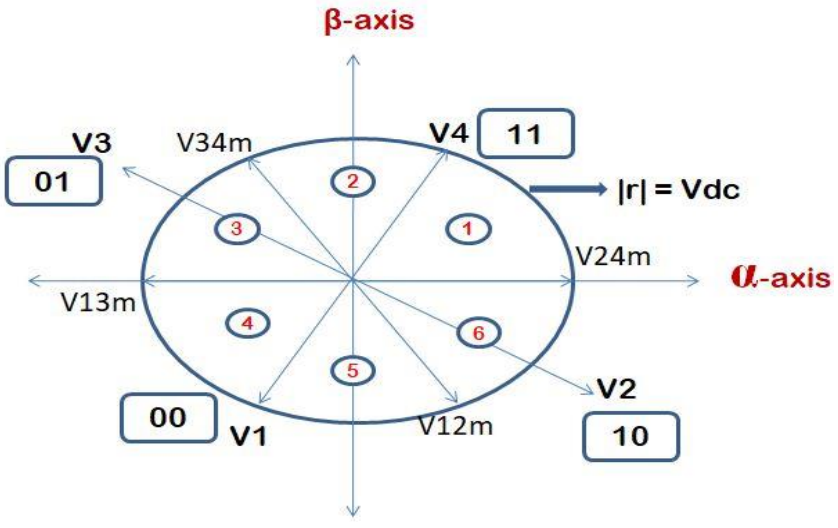

Fig.3.4 Four Switch SVPWM on the principle of conventional Six Switches SVPWM

Table 3.5 shows the similarity between vectors that we have obtained using the presented technique with the conventional six switch SVPWM inverter, and fig.3.5 shows the vectors in α-β plane similar we have in case of six switch SVPWM based inverters.

Table 3.5 Similarity in vectors between FS3P SVPWM and Conventional SVPWM

Four Switches SVPWM	**Six Switches SVPWM**
V_{24m}	V_1
V_4	V_2
V_{34m}	V_3
V_{13m}	V_4
V_1	V_5
V_{12m}	V_6
V_0	V_0 and V_7

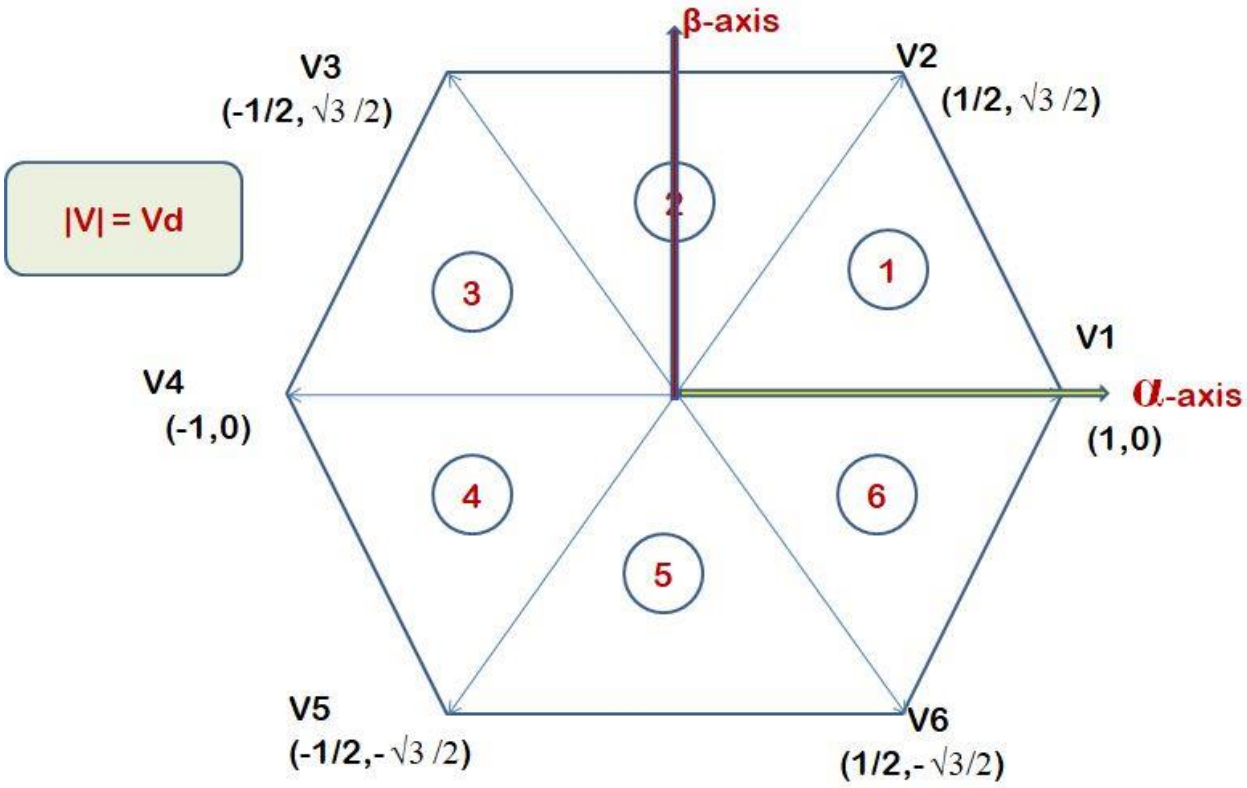

Fig.3.5 Vectors in α-β Plane

3.5 Concept of Zero Vectors

In conventional SVPWM we have vectors V_0 and V_7 which corresponds to the state that gives zero voltage at output. These zero vectors runs for the remaining time T_0 from the sampling time T_s to give zero value of voltage at output (since V_{ref} is already been synthesized in a time "T_s – T_0"). In FS3P SVPWM there is no state that is available to give zero voltage at output thus question may arise that which vector should be rum for the remaining time T_0 to give zero value voltage at output. The concept that lies here is if two equally opposite vectors are being run for same or equal time the resultant would be zero at the output.

From FS3P inverter the pair of opposite vectors are "V_3[01] and V_2[10]" and "V_4[11] and V_1[00]". So if T_0 is the remaining time then 'V_3 and V_2' must run for time $T_0/2$ equally or 'V_1 and V_4' if run for time $T_0/2$ equally, gives zero voltage at output. In any of the case if one employ 'V_3 and V_2' or 'V_1 and V_4' for reaming time T_0 the switch S_1 will run for $T_0/2$ and switch S_2 will run for $T_0/2$ and gives zero value of voltage at output.

3.6 Concept of Modulation Index

Assuming that magnitude of phase voltage that is needed at output be $|V_{ref}|$, then the rotating vector which is being synthesized must have the magnitude to be 1.5 times the $|V_{ref}|$. The length of each vector which are responsible to synthesize V_{ref} is V_d where V_d is the value of any dc-link voltage. So if $1.5|V_{ref}|$ equal to V_d, the magnitude of output phase voltage will be $|V_{ref}|$ and in this case modulation index is said to be 1.

Thus,

$$\frac{3}{2}|V_{ref}| = a \times V_d \tag{3.11}$$

Impies

$$|V_{ref}| = a \times \frac{2}{3} V_d \tag{3.12}$$

This is the reason we can also take radius of circle being $2/3V_d$, with this concept we will synthesize directly $|V_{ref}|$ required at the output.

Here, "a = Modulation Index"

Equation (3.11) shows the significance of modulation index in generation of V_{ref}, $a < 1$ implies that length of available vectors (V_d) is sufficient to generate rotating vector of length $3/2|V_{ref}|$ which gives phase voltage magnitude to be $|V_{ref}|$. For example, output phase voltage required to be 230 volts and V_d available say 350 volts then modulation index from equation (3.11) is 0.986, $a>1$ signifies the over-modulation case when rotating vector of length $1.5|V_{ref}|$ is exceeding the boundary of available vectors of length V_d.

3.7 V_{ref} Synthesis and vector time calculation

Fig.3.6 shows V_{ref} is synthesized using V_1 and V_2, here V_1 is run for time T_1 and V_2 is being run for time T_2 the resultant that obtained is required V_{ref}.

T_s is the sampling time which is maximum time provided to synthesize the V_{ref}, T_1 and T_2 are the vector timings of the respective vector V_1 and V_2 to obtain required V_{ref}. Also "$T_0 = T_s - (T_1 + T_2)$" is the remaining time where it is needed to run zero vector or two opposite vectors (in this case) equally to get zero voltage since required voltage V_{ref} is already being synthesized in time "$T_1 + T_2$".

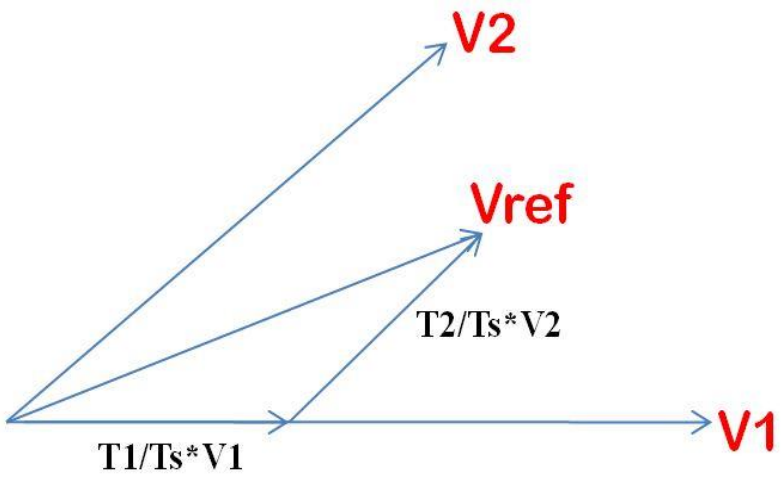

Fig.3.6 V_{ref} Synthesis using V_1 and V_2

Now,

Considering Sector '1'

$$\int_0^{T_s} \frac{3}{2} V_{ref}\, dt = \int_0^{T_1} V_1\, dt + \int_{T_1}^{T_1+T_2} V_2\, dt + \int_{T_1+T_2}^{T_s} V_0\, dt \tag{3.12}$$

$$T_s \frac{3}{2} |V_{ref}| \begin{bmatrix} \cos\alpha \\ \sin\alpha \end{bmatrix} = T_1 V_d \begin{bmatrix} 1 \\ 0 \end{bmatrix} + T_2 V_d \begin{bmatrix} \cos\frac{\pi}{3} \\ \sin\frac{\pi}{3} \end{bmatrix} \tag{3.13}$$

$$T_s \frac{3}{2} |V_{ref}| (\cos\alpha + \mathrm{j}\sin\alpha) = T_1 V_d (1 + j0) + T_2 V_d \left(\frac{1}{2} + j\frac{\sqrt{3}}{2}\right) \tag{3.14}$$

Comparing real and imaginary terms,

$$T_1 = T_s \frac{3V_{ref}}{2V_d} \frac{\sin\left(\frac{\pi}{3} - \alpha\right)}{\sin\left(\frac{\pi}{3}\right)} = T_s \frac{\sqrt{3}V_{ref}}{V_d} \sin\left(\frac{\pi}{3} - \alpha\right) \tag{3.15}$$

And

$$T_2 = T_s \frac{\sqrt{3}V_{ref}}{V_d} \sin(\alpha) \tag{3.16}$$

Also

$$T_0 = T_s - T_1 - T_2 \tag{3.17}$$

Vector Timings for sector 'n'

$$T_1 = T_s \frac{\sqrt{3}|V_{ref}|}{V_d} \sin\left(\frac{n\pi}{3} - \alpha\right) \quad (3.18)$$

$$T_2 = T_s \frac{\sqrt{3}V_{ref}}{V_d} \sin\left(\alpha - \left(\frac{n-1}{3}\right)\pi\right) \quad (3.19)$$

$$T_0 = T_s - T_1 - T_2 \quad (3.20)$$

Where, n = 1 to 6

Equation (3.18), (3.19), (3.20) generalizes the vector timings for any sector 1 to 6.

3.8 Switching Time Calculation

Considering that V_{ref} lies in sector 1, then the vectors that are responsible to synthesize the V_{ref} are V_1 and V_2. Let us suppose if V_1 is applied for T_1 and V_2 is applied for applied for T_2 time, since V_1 which is V_{24m} is composed of state [10] and [11] being run equally so, state [10] will run for time $T_1/2$ and state [11] will also run for time $T_1/2$ to give vector V_1 or V_{24m} being run for time T_1 and the state of V_2 is [11] is to be run for time T_2. The timings for switches in this case are S_1 to be run for "$T_1 + T_2 + T_0/2$" and switch S_2 to be run for "$T_1/2 + T_2 + T_0/2$" time to synthesize the V_{ref} if it lies in sector 1. Fig.3.7 shows the process to derive the timings of switches S_1 and S_2 to synthesize the V_{ref} for sector 1, 2 and 3 using same procedure the timings of switches S_1 and S_2 for other sectors can also be derived.

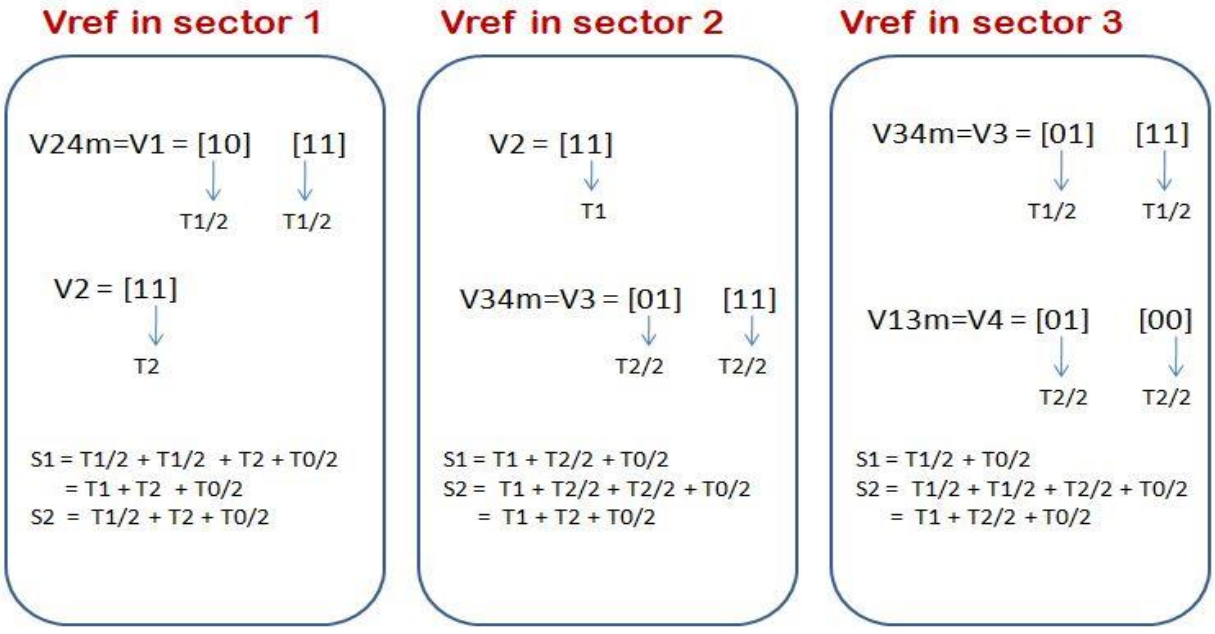

Fig.3.7 Derivation of Switches Timings

Table 3.6 Summarizes the Switches Timings at each sectors.

Table 3.6 Switching Time at each Sector

Sector	Switch (S_1)	Switch (S_2)
1	$T_1 + T_2 + T_0/2$	$T_1/2 + T_2 + T_0/2$
2	$T_1 + T_2/2 + T_0/2$	$T_1 + T_2 + T_0/2$
3	$T_1/2 + T_0/2$	$T_1 + T_2/2 + T_0/2$
4	$T_0/2$	$T_1/2 + T_0/2$
5	$T_2/2 + T_0/2$	$T_0/2$
6	$T_1/2 + T_2 + T_0/2$	$T_2/2 + T_0/2$

Timings of switch S_3 and S_4 will be complementary to the switches S_1 and S_2 respectively since both the switches of same leg cannot be made close at the same time to avoid the short circuit condition.

CHAPTER 4

Adaptive Carrier Based PWM Technique under DC-Link Voltage Ripples

4.1 Introduction

The Four Switch Three Phase Inverter topology insures the low cost for inverter fed ac motor drives since it involves only four switches which also reduces the switching losses and complexity due to interface and driver circuits. Space Vector Pulse Width Modulation for Four Switch Three Phase Inverter which has been discussed in chapter 3 considers constant dc voltages and calculations are being done by considering the constant dc-link voltages.

Practically a dc-link is created using two split capacitors which results in decrements of output voltages and unbalancing in output currents also arises due to variation of voltage across split capacitors. Comparatively with other modulation strategies such as SPWM method, SVPWM has been shown to generate less total harmonic distortion in output voltages and currents and provides wide linear modulation region but did not considers the effects of two unbalanced dc-link voltages to output currents.

With time some Adaptive SVPWM techniques developed which considers the voltages ripples due to split capacitors and provides balancing in output currents but maximum obtainable output voltage is still limited under linear modulation region (m<1). Carrier based PWM is proposed to be used for FS3P inverters and found to provide linearity in over modulation region to some extent.

This chapter discusses the Adaptive Carrier based PWM technique for FS3P Inverter, and proposed a simple way to generate the switching pulses from intersection reference signal with triangular signals and develop the equations for reference signals to be compared and discuss how the effect of variation of voltage in dc-link capacitors can be compensated.

Fig.2.1 shows the FS3P inverter topology with split capacitors to provide dc-link, from where the third phase, phase A has been taken whereas in fig.3.1 during SVPWM discussion dc-link has been provided using constant dc voltages in the proposed topology.

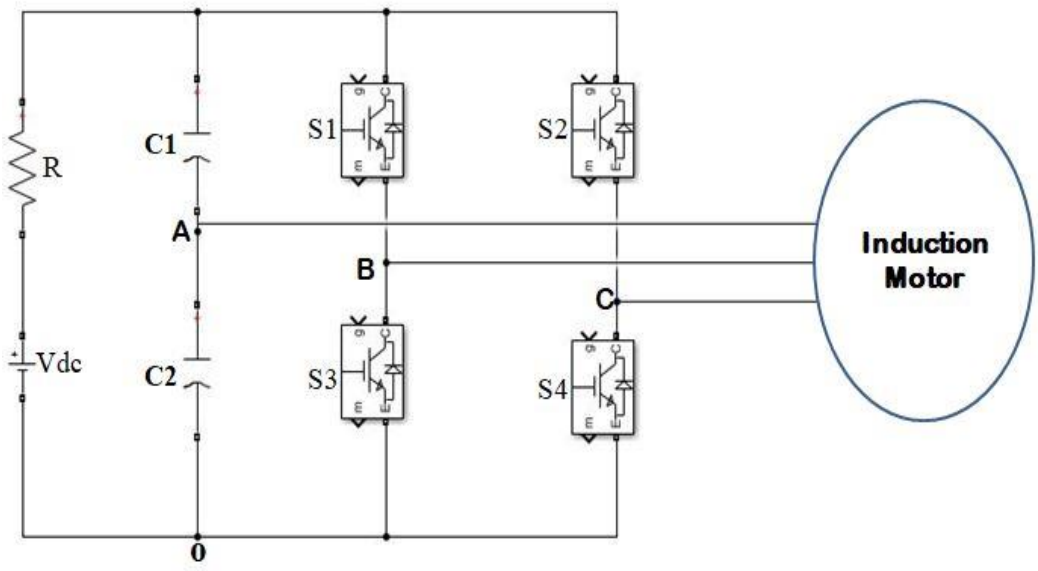

Fig.4.1 FS3P Inverter Topology with DC-Link Split Capacitors

4.2 Space Vector Analysis

Fig.4.1 shows FS3P inverter topology that provides two inverter output phases B and C from two inverter legs and third phase, Phase A, is connected to the mid-point of the two split capacitors.

The phase-to-zero voltages V_{AO}, V_{BO} and V_{CO} where 'O' is zero potential point as shown in fig.4.1, depends upon the switching states of S_1 and S_2 (S_3 and S_4 being complementary respectively) and the value of voltages across two dc-link capacitors. If V_{dc1} and V_{dc2} being voltage across capacitors C_1 and C_2 respectively then:

$$V_{AO} = V_{dc2} \tag{4.1}$$

$$V_{BO} = S_1(V_{dc1} + V_{dc2}) \tag{4.2}$$

$$V_{CO} = S_2(V_{dc1} + V_{dc2}) \tag{4.3}$$

When switch S_x is OFF then $S_x = 0$ and $S_x = 1$ when switch S_x is ON where 'X = 1,2'.

Under balanced load conditions:

$$V_{AN} + V_{BN} + V_{CN} = 0 \tag{4.4}$$

$$V_{AO} + V_{BO} + V_{CO} - 3V_{NO} = 0 \tag{4.5}$$

$$V_{NO} = \frac{V_{AO} + V_{BO} + V_{CO}}{3} \tag{4.6}$$

Thus phase-to-neutral voltages can be derived from phase-to-zero voltages as:

$$V_{AN} = V_{AO} - V_{NO} = \frac{2}{3}V_{AO} - \frac{1}{3}(V_{BO} + V_{CO}) \quad (4.7)$$

$$V_{BN} = V_{BO} - V_{NO} = \frac{2}{3}V_{BO} - \frac{1}{3}(V_{AO} + V_{CO}) \quad (4.8)$$

$$V_{CN} = V_{CO} - V_{NO} = \frac{2}{3}V_{CO} - \frac{1}{3}(V_{AO} + V_{BO}) \quad (4.9)$$

So, phase-to-zero voltages which depend upon switching states s shown in equations (4.1), (4.2) and (4.3) can be utilized to derive the phase-to-neutral voltages from equations (4.7), (4.8) and (4.9). Table 4.1 summarizes the phase-to-zero and phase-to-neutral voltages for different switching states of inverter.

Table 4.1 Phase-to-Zero and Phase-to-Neutral Voltages for all Switching states

States		**Phase-to-zero**			**Phase-to-Neutral**		
S_1	**S_2**	**V_{AO}**	**V_{BO}**	**V_{CO}**	**V_{AN}**	**V_{BN}**	**V_{CN}**
0	0	V_{dc2}	0	0	$2V_{dc2}/3$	$-V_{dc2}/3$	$-V_{dc2}/3$
1	0	V_{dc2}	$V_{dc1}+V_{dc2}$	0	$V_{dc2}/3-V_{dc1}/3$	$2V_{dc1}/3+V_{dc2}/3$	$-V_{dc1}/3-2V_{dc2}/3$
1	1	V_{dc2}	$V_{dc1}+V_{dc2}$	$V_{dc1}+V_{dc2}$	$-2V_{dc1}/3$	$V_{dc1}/3$	$V_{dc1}/3$
0	1	V_{dc2}	0	$V_{dc1}+V_{dc2}$	$V_{dc2}/3-V_{dc1}/3$	$-V_{dc1}/3-2V_{dc2}/3$	$2V_{dc1}/3+V_{dc2}/3$

From expression (4.10) one can transform phase-to-neutral voltages in two dimensional α-β plane where for particular switching state the definite value of real and imaginary axis voltages defines a space vector.

$$\begin{bmatrix} V_\alpha \\ V_\beta \end{bmatrix} = \frac{2}{3}\begin{bmatrix} 1 & -\frac{1}{2} & -\frac{1}{2} \\ 0 & \frac{\sqrt{3}}{2} & -\frac{\sqrt{3}}{2} \end{bmatrix}\begin{bmatrix} V_{AN} \\ V_{BN} \\ V_{CN} \end{bmatrix} \tag{4.10}$$

Using all the switching combinations of S_1 and S_2 the four active vectors or space vectors can be generated which are summarized in table 4.2 along with their real and imaginary values.

Table 4.2 Voltage Vectors in 2-D Plane

S_1	S_2	Vector	V_α	V_β
0	0	V_1	$2V_{dc2}/3$	0
1	0	V_2	$(V_{dc2}-V_{dc1})/3$	$(V_{dc1}+V_{dc2})/\sqrt{3}$
1	1	V_3	$-2V_{dc1}/3$	0
0	1	V_4	$(V_{dc2}-V_{dc1})/3$	$-(V_{dc1}+V_{dc2})/\sqrt{3}$

The condition of $V_{dc1} = V_{dc2} = V_{dc}/2$ is achieved when capacitance of two split capacitors is large enough to keep V_{dc1} and V_{dc2} constant, in this condition the four voltage vectors are presented as shown in fig.4.2(a). When capacitance of two split capacitors is small, the unbalancing of two dc-link voltages will occur i.e $V_{dc1} \neq V_{dc2}$ and the switching states will produce voltage vectors as shown in fig.4.2(b)

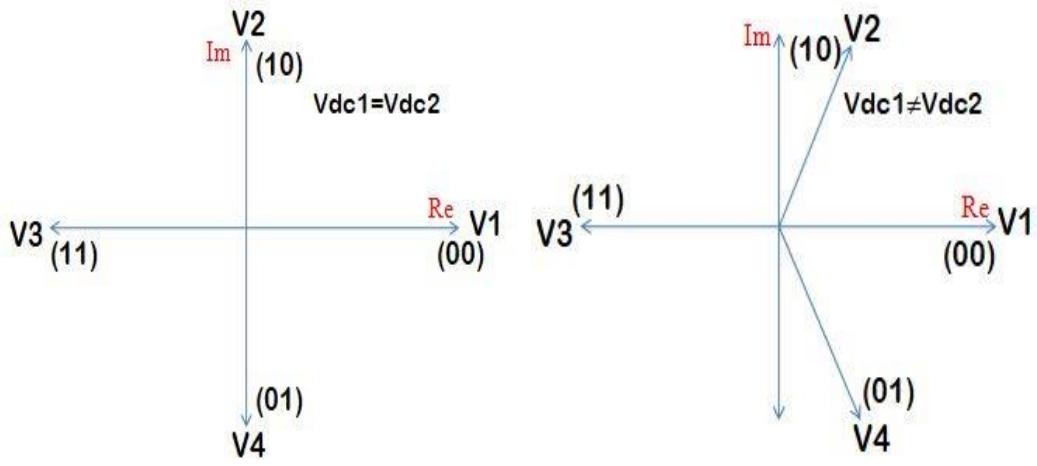

Fig.4.2 Space Vectors in 4S3P inverter (a) Balanced dc-link Voltages (b) Unbalanced dc-link Voltages

There are several reasons which are responsible for dc-link voltage ripples, the first being the rectification of power supply, the phase current circulating through split capacitors also results in dc-link voltage ripples.

However, output distortions can be minimized by increasing the capacitance of two split capacitors but it would result in increase of cost and size of inverter which is not economically feasible hence some compensation methods were suggested to generate balanced output currents without increasing the capacitance of two dc-link capacitors in FS3P inverter.

Let us consider V_m as the desired output voltage vector required as shown in fig.4.3. The desired vector V_m can be synthesized using space vector technique. In this process three vectors among four active vectors are responsible to generate the required vector V_m i.e synthesis will be done in two sectors, the first being sector 1for $(0 \leq \alpha \leq \pi)$ and vectors responsible are V_1, V_2 and V_3; the second being sector 2 for $(\pi \leq \alpha \leq 2\pi)$ and vectors responsible for synthesis are V_3, V_4 and V_1. Compared to the space vector analysis in six-switch three phase inverters there are no zero vectors in FS3P inverters thus zero vector is obtained by using two equally opposite vectors to be rum for equal time. Thus, here sectors are chosen such that it contain equal and opposite vectors also, and vectors forming pair of equal and opposite vectors are V_1 and V_3 as shown in fig.4.3.

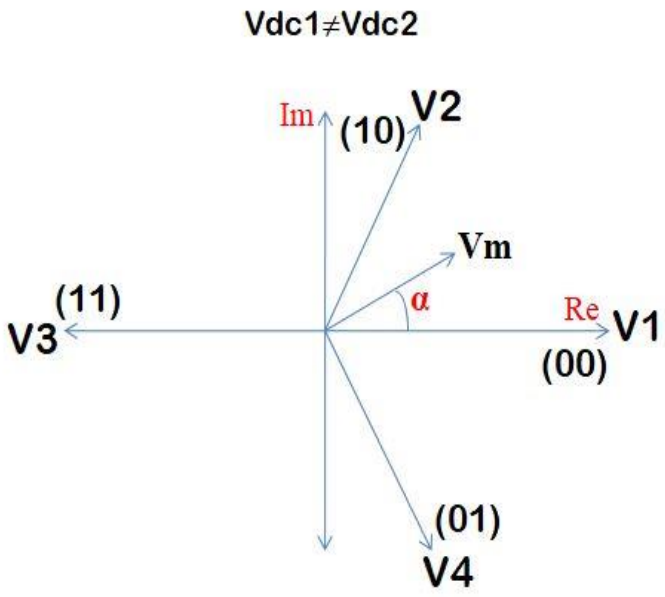

Fig.4.3 Modulation of required output voltage vector V_m

Table 4.3 shows the sectors and selected vectors for V_m synthesis.

Table 4.3 Sectors and selected Vectors

Sector	Selected Vectors
1	V_1, V_2, V_3
2	V_1, V_4, V_3

The time duration of different vectors in sector 1 can be obtained as:

$$\int_0^{T_s} V_m dt = \int_0^{T_x} V_1 dt + \int_{T_x}^{T_y+T_x} V_2 dt + \int_0^{T_z/2} V_1 dt + \int_0^{T_z/2} V_3 dt \quad (4.11)$$

Where

T_s = Sampling Time

And

$$T_s = T_x + T_y + T_z \quad (4.12)$$

Also

$$T_1 = T_x + \frac{T_z}{2} \quad (4.13)$$

$$T_2 = T_y \quad (4.14)$$

$$T_3 = \frac{T_z}{2} \tag{4.15}$$

Where,

T_1 = Time duration of vector 1

T_2 = Time duration of vector 2

T_3 = Time duration of vector 3

T_4 = Time duration of vector 4

From equations (4.11) – (4.15) the time durations of each vector in sector 1 ($0 \leq \alpha \leq \pi$) are given by:

$$T_1 = T_S \frac{V_{dc1}}{V_{dc1} + V_{dc2}} - T_S \frac{\sqrt{3}V_m}{V_{dc1} + V_{dc2}} \sin\left(\alpha - \frac{\pi}{3}\right) \tag{4.16}$$

$$T_2 = T_S \frac{\sqrt{3}V_m}{V_{dc1} + V_{dc2}} \sin(\alpha) \tag{4.17}$$

$$T_3 = T_S \frac{V_{dc2}}{V_{dc1} + V_{dc2}} - T_S \frac{\sqrt{3}V_m}{V_{dc1} + V_{dc2}} \sin\left(\alpha + \frac{\pi}{3}\right) \tag{4.18}$$

Similarly, time durations of each vector in sector 2 ($\pi \leq \alpha \leq 2\pi$) are given by:

$$T_1 = T_S \frac{V_{dc1}}{V_{dc1} + V_{dc2}} - T_S \frac{\sqrt{3}V_m}{V_{dc1} + V_{dc2}} \sin\left(\alpha - \frac{2\pi}{3}\right) \tag{4.19}$$

$$T_4 = T_S \frac{\sqrt{3}V_m}{V_{dc1} + V_{dc2}} \sin(\alpha - \pi) \tag{4.20}$$

$$T_3 = T_S \frac{V_{dc2}}{V_{dc1} + V_{dc2}} - T_S \frac{\sqrt{3}V_m}{V_{dc1} + V_{dc2}} \sin\left(\alpha - \frac{4\pi}{3}\right) \tag{4.21}$$

Table 4.4 shows the switching time duration for each sector that must be given to the switches of FS3P inverter in order to synthesize the required voltage vector V_m.

Table 4.4 Switches Timings in each Sector

Sector	**S_1**	**S_2**
1	T_2+T_3	T_3
2	T_3	T_3+T_4

4.3 Proposed Adaptive Carrier-Based PWM Technique

Let us consider desired output voltage vector V_m is located in sector 1, then the vectors that are responsible for its generation are V_1, V_2 and V_3 with timings be T_1, T_2 and T_3 respectively, table 4.4 shows timings of switches for each sector.

The concept of carrier-based PWM is to find reference voltage signals which are compared with triangular carrier signal to generate same gating pulse as the SVPWM method.

The timings of switch S_1 and S_2 for sector 1 is defined as follows:

$$T_b = T_2 + T_3 \tag{4.22}$$

$$T_c = T_3 \tag{4.23}$$

Where

T_B = Timing for switch S_1

T_C = Timing for switch S_2

Let us generate Normalized triangle signal between Peak 0 and 1 in the positive slope, this will be considered as carrier signal in the proposed method, it can be described as:

$$V_t = \frac{t}{T_s} \qquad (0 \le t \le T_s) \tag{4.24}$$

Where V_t is instantaneous carrier signal.

The reference signals that are generated using equations (4.22), (4.23) and (4.24) are as follows:

$$V_{refB} = \frac{t_B}{T_s} = \frac{V_{dc2}}{V_{dc1} + V_{dc2}} + \frac{\sqrt{3}V_m}{V_{dc1} + V_{dc2}} \sin\left(\alpha - \frac{\pi}{3}\right) \tag{4.25}$$

$$V_{refC} = \frac{t_C}{T_s} = \frac{V_{dc2}}{V_{dc1} + V_{dc2}} - \frac{\sqrt{3}V_m}{V_{dc1} + V_{dc2}} \sin\left(\alpha + \frac{\pi}{3}\right) \tag{4.26}$$

The reference signals that are generated when compared with triangular carrier signal must generate the same timings for switch S_1 and S_2 as derived in SVPWM method or described in table 4.4

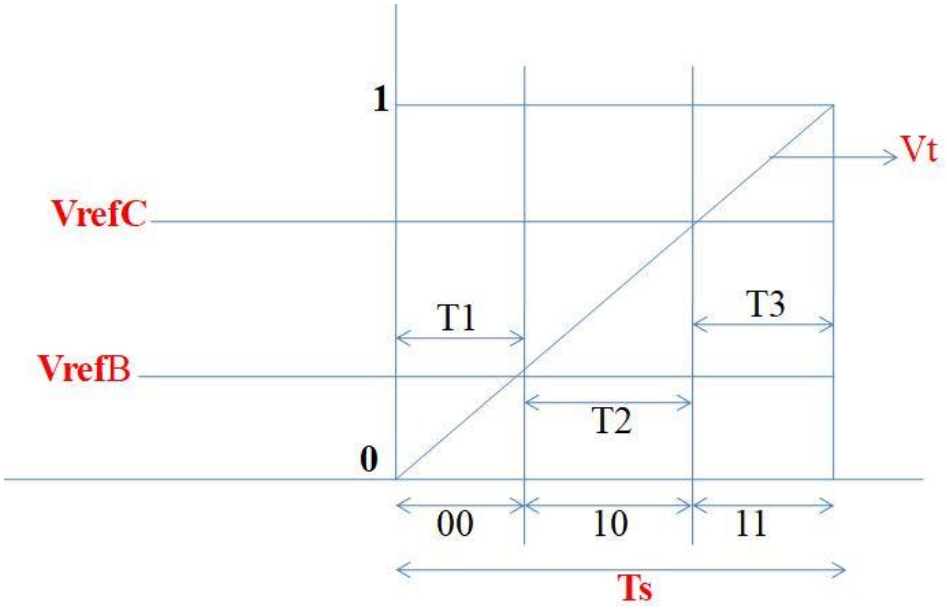

Fig.4.4 Timing of gate pulse in Carrier-Based PWM for sector 1

Fig.4.4 shows the reference signals V_{refB} and V_{refC} along with the triangular carrier signal V_t. The state (11) will run for time T_3**,** state (10) will run for time T_2 and state (00) will run for time T_1. When V_{refB} will be compare with V_t i.e time for which $V_{refB} \leq V_t$ will bring out timings to be "T_3 + T_2" which is for switch S_1 in sector 1 and time for which $V_{refC} \leq V_t$ will bring out gate pulse time to be 'T_3' which is for switch S_2 in sector 1.

Thus the proposed carrier-based PWM method brings out the timings to be same as SVPWM method to generate the required voltage vector V_m. The advantage of proposed carrier-based PWM technique can be seen in equations (4.25) and (4.26), the reference signals V_{refB} and V_{refC} contains voltage offset component which compensates the problems arising due to dc-link voltage oscillations i.e ($V_{dc2}/(V_{dc1}+V_{dc2})$) will remains approximately constant (increase or decrease of V_{dc2} take place both in numerator and denominator thereby maintaining the ratio approximately constant).

Also for sector 2

$$t_B = T_3 \tag{4.27}$$

$$t_C = T_4 + T_3 \tag{4.28}$$

The reference signals V_{refB} and V_{refC} in sector 2 are same as obtained in equation (4.25) and (4.26) respectively.

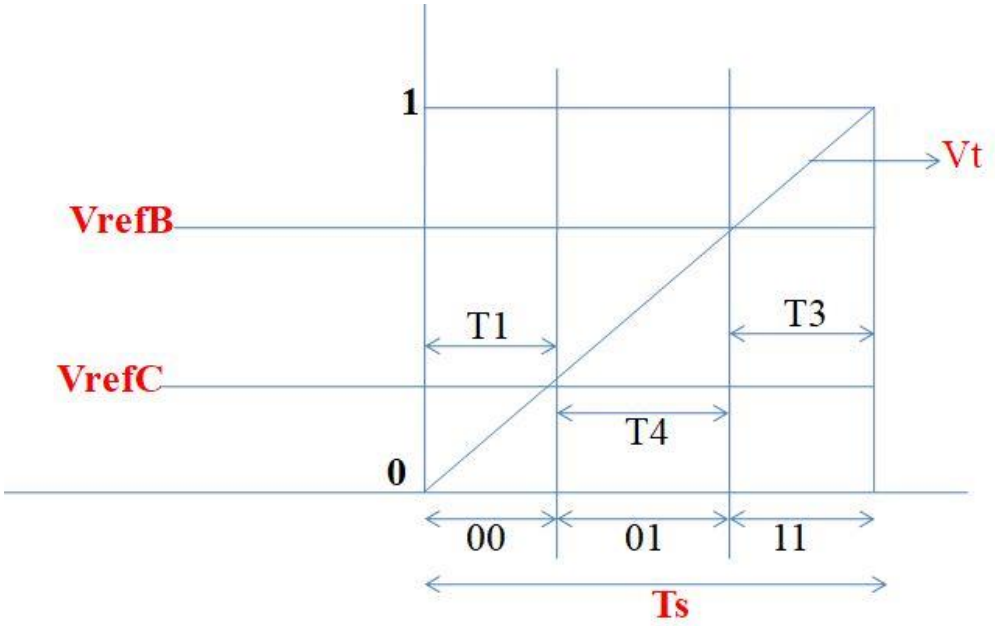

Fig.4.5 Timing of gate Pulse in Carrier-Based PWM for sector 2

Fig.4.5 shows that when triangular carrier signal is compared with reference signals V_{refB} and V_{refC} will generate same timings as obtained in SVPWM method i.e for $V_{refB} \leq V_t$ timings of switch S_1 is T_3 and when $V_{refC} \leq V_t$ the time for switch S_2 to be gated is $T_3 + T_4$ which is same as described in table 4.4.

Thus it can be seen that proposed carrier-based PWM method generates same timings as in SVPWM method along with the advantage of dc-link voltage ripples compensation due to voltage offset component in reference signals V_{refB} and $V_{refC.}$

CHAPTER 5

MATLAB IMPLEMENTATION OF SVPWM IN PROPOSED TOPOLOGIES

5.1 Introduction

This chapter discusses the implementation of space vector technique in MATLAB R2018a. The first topology in which SVPWM method is implemented is six switch three phase inverter directly feds the induction motor. The second topology implemented includes four switch three phase inverter feeding induction motor drive and SVPWM method is utilized to generate the gating pulses of FS3P inverter. The second topology has constant dc source for dc-link creation unlike the third topology which is also a FS3P inverter fed induction motor but dc-link is created using the two split capacitors, the third topology uses a adaptive carrier based PWM method to generate gating pulses of FS3P inverter which founds benefits in compensating the voltage ripples due to dc-link capacitors.

This chapter includes the discussion over basic blocks that has been used for project implementation and how the sector selection, switching time generation, α-β transformation that must be required for implementation of SVPWM technique is being done, is shown in the following sections.

5.2 Proposed Topologies of Voltage Source Inverters

5.2.1 Six Switch Three Phase Inverter

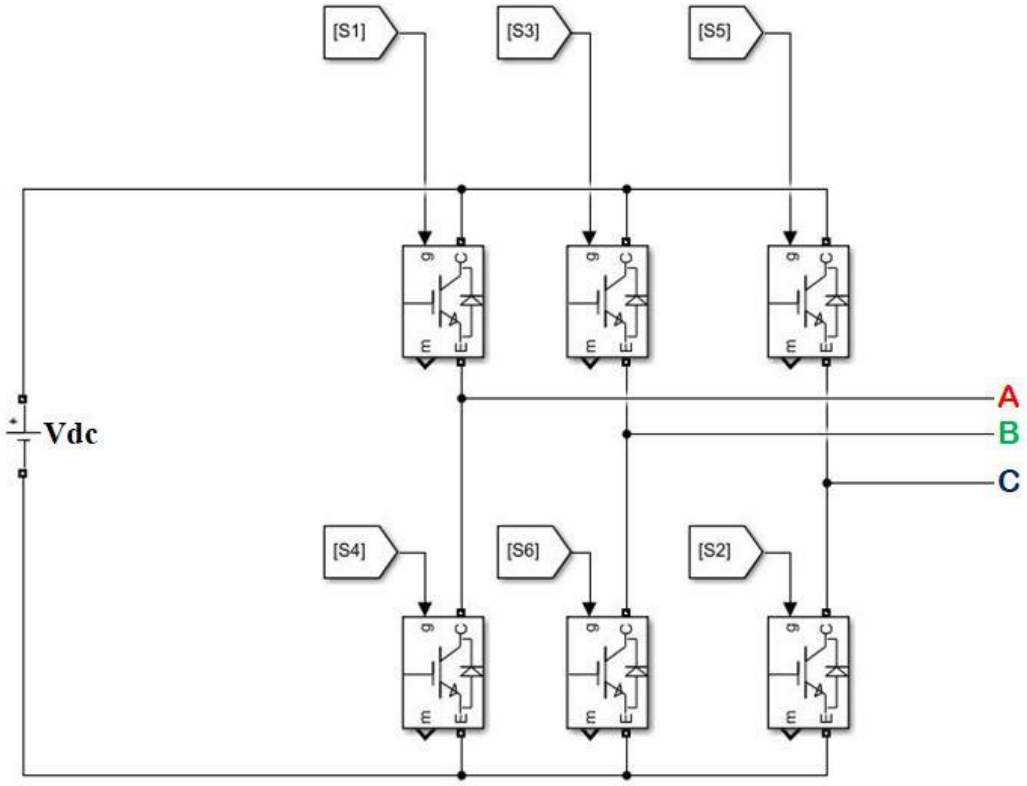

Fig.5.1 Six Switch Three Phase Inverter

Fig.5.1 shows simulated model of three legs voltage source inverter, The switches used are IGBTs with anti-parallel diode, switch S_1, S_3 and S_5 will get the gating pulse from Space Vector PWM method and switches S_4, S_6 and S_2 will follow the complementary ON/OFF fashion respectively. The three output phases of inverter will fed induction motor since its performance is used to describe or analyze the effectiveness of the Space Vector Technique.

5.2.2 Four Switch Three Phase Inverter

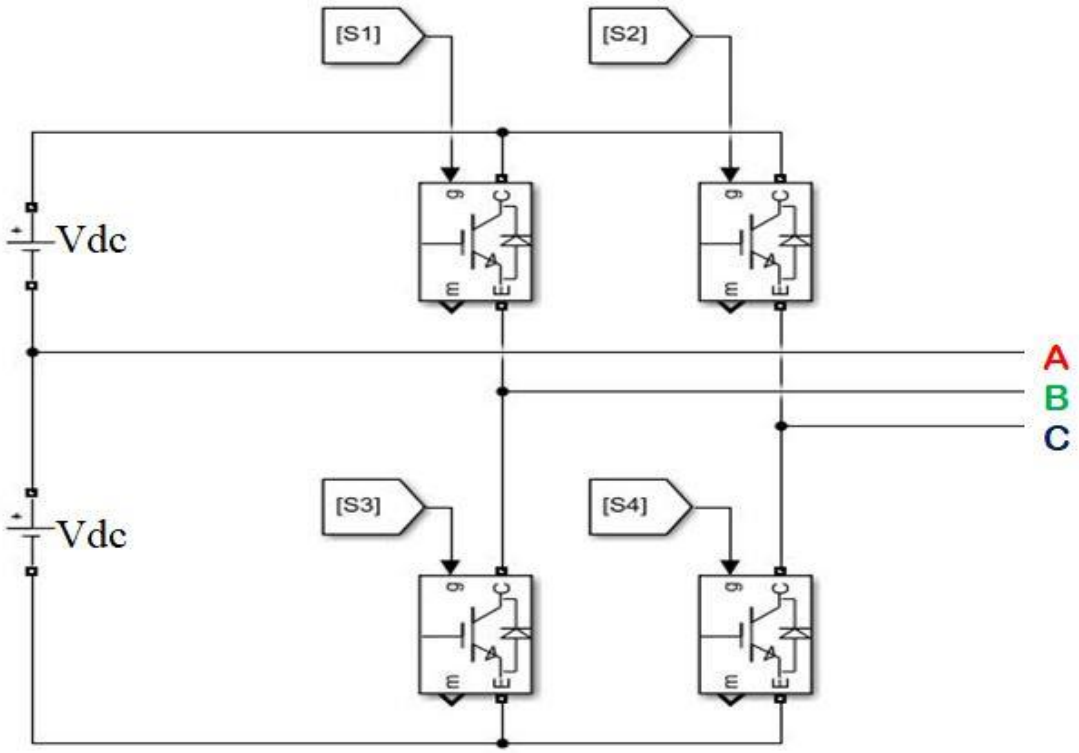

Fig.5.2 Four Switch Three Phase Inverter with constant dc-link Voltages

Fig.5.2 shows the simulated model of Four Switch Three Phase Inverter, where two phases, Phase B and Phase C are derived from the two inverter legs and the third phase, Phase A is taken from the mid-point of two dc-link voltages with both have constant and equal magnitude V_{dc}, Space Vector method is used for switch timings and three output phases from the topology are feeding the induction motor so that performance of ac drive can be analyzed and effectiveness of Space Vector technique can be described for proposed topology.

5.2.3 FS3P Inverter topology with Split Capacitors

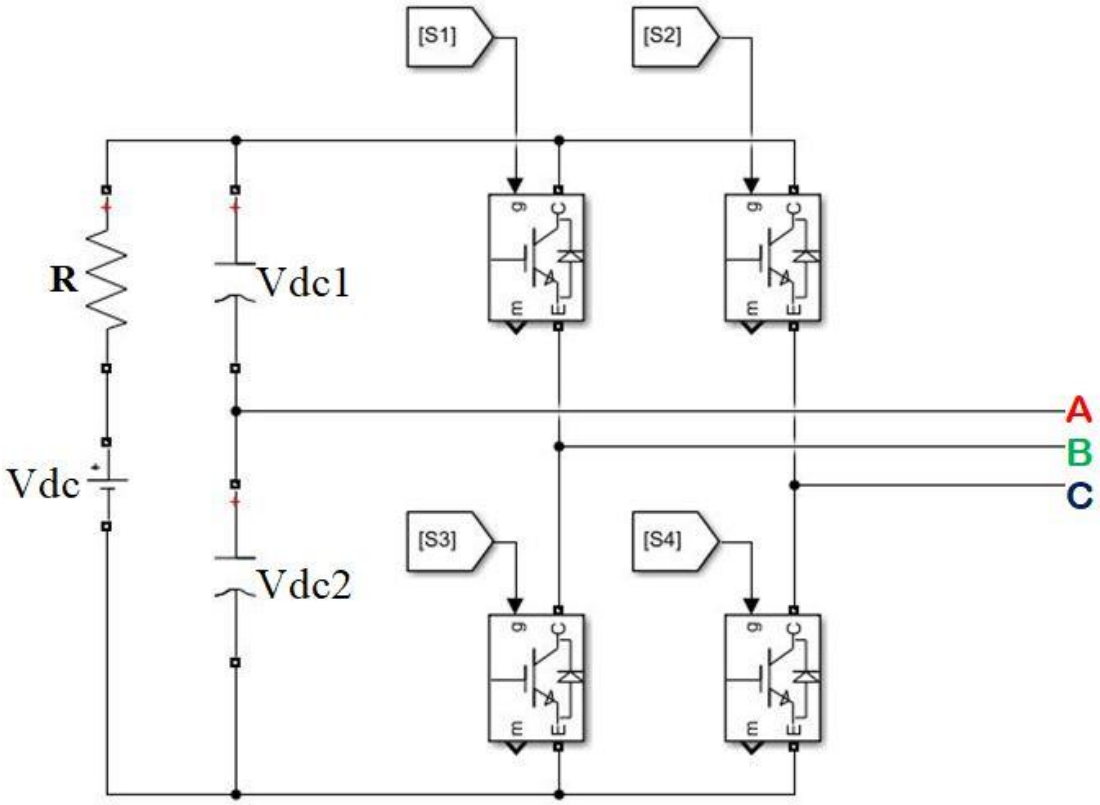

Fg.5.3 FS3P Inverter with dc-link Capacitors

Fig.5.3 shows the simulated model of FS3P Inverter with split capacitors for dc-link creation. Unlike fig.5.2 the third phase, Phase A has been taken from the mid-point of two split capacitors creating the link. Due to capacitors used for dc-link creation, voltage ripples arises (i.e $V_{dc1} \neq V_{dc2}$) which are responsible for unbalancing in the output currents thus, Adaptive Carrier-Bases PWM method is used here for gating pulses of switches as it compensates the voltage oscillations between the two capacitors. Similar as in fig.5.2 IM drive is used as a load and performance is recorded to comment on the effectiveness of the given technique. Also small resistance R is connected with ideal dc source before connecting dc-link capacitors in parallel to it directly for practical implication.

5.3 The Phase Locked Loop

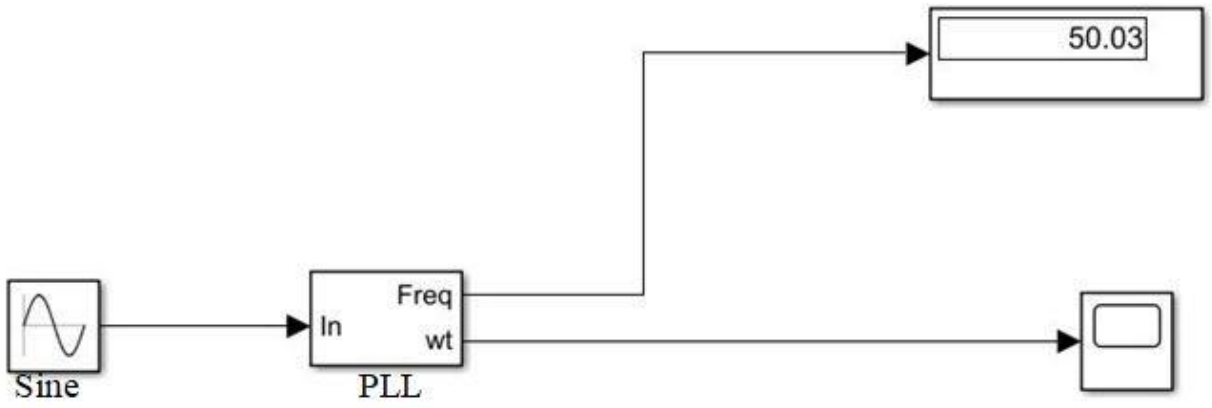

Fig.5.4 The PLL Block

The Phase Locked Loop can be used on a variable frequency sinusoidal sgnal or one can also use it for constant frequency sinusoidal signal. The first output of PLL in measured frequency in Hz i.e $\omega/2\pi$ and the second output of PLL is ramp signal with magnitude varies from 0 to 2π in a period of 0.02 seconds i.e it generates a ramp signal with peak is 2π and frequency of signal is 50Hz. The output of PLL can be used further for sector selection purpose.

5.4 Sector Selection

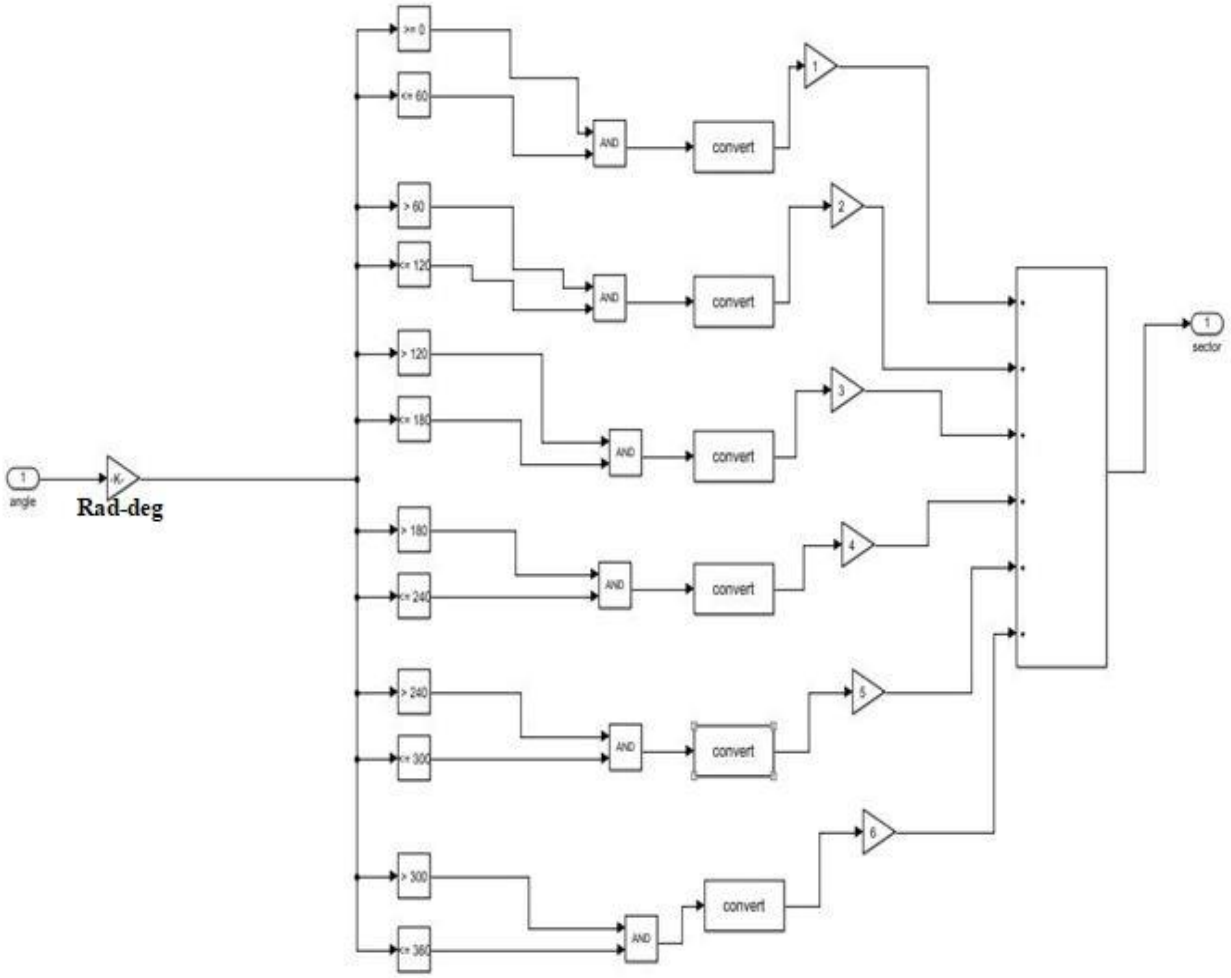

Fig.5.5 Selection of Sectors for Vectors V_1 to V_6

Fig.5.5 shows the selection of six sectors in a period of "0 to 360" degree. The period of each sector is 60 degree, the first sector being at "0 to 60" degree, second when angle goes from "60 to 120" degree, third being when angle at "120 to 180" degree and so on. The input here is second output from PLL block which gives us angle in radians, then conversion of radians to degree is done for easy implementation of sector selection.

5.5 Function Block

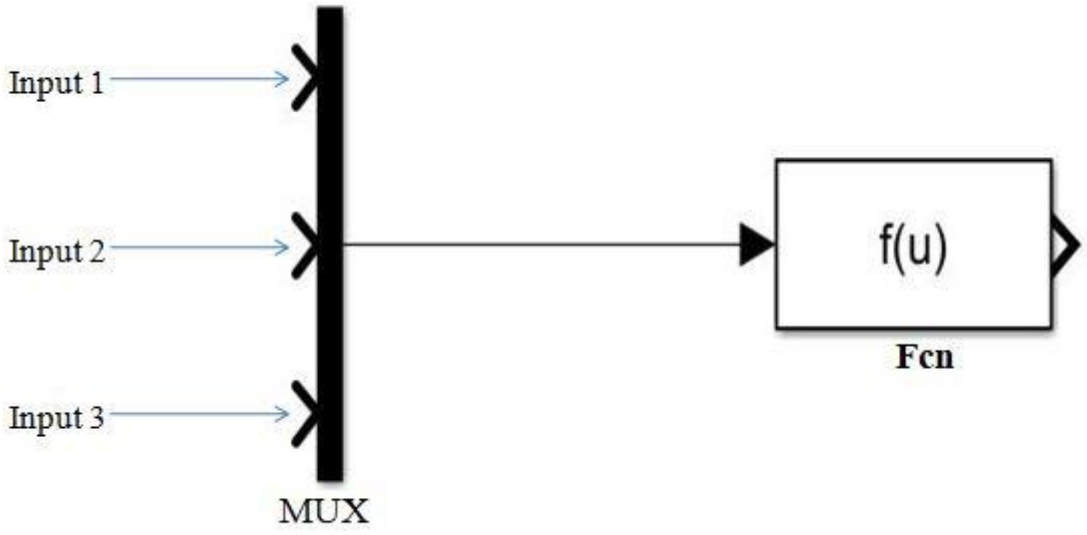

Fig.5.6 Functional Block

Fig.5.6 shows the functional block which is used to generate the timings. This is a general expression block which uses "u" as the input variable name. Since the inputs can be more than one thus, this is achieved using a Mux as shown in fig.5.6

For Example:

Input 1 : "t"

Input 2 : 'α' angle in radians

And the function to be implemented is:

$f(x) = e^{-t} \sin \alpha$

Then expression should be:

Exp(-u(1))*sin(u(2))

Thus the timings as given by various expressions in Chapter 2, Chapter 3 and Chapter 4 is achieved using this functional block.

5.6 Multiport Switch

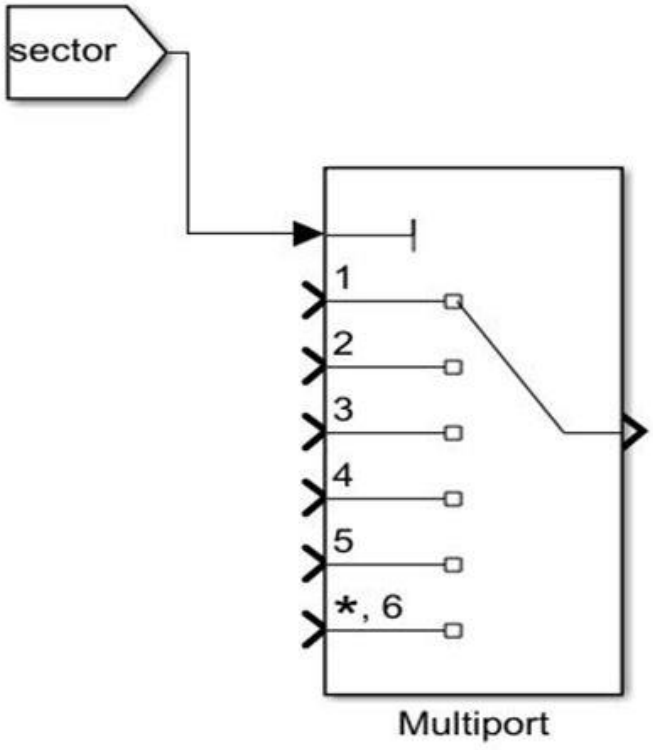

Fig.5.7 Multiport Switch

Fig.5.7 shows the multiport switch. Here, inputs are numbered as top to bottom and the first input is the control input and other input ports are data ports. The control input used here is sector and the data inputs are timings of a particular switch in its respective sector. For example "$T_1 + T_0/2$" is the timing for switch S_1 at sector 3, then multiport switch for S_1 will pass "$T_1 + T_0/2$" at output when sector 3 arrived at the control input required that "$T_1 + T_0/2$" must be connected at data port 3. Since there are six sectors and each sector have particular timings for a particular switch thus total data ports are 6 and corresponding timings must be connected to each data port, so that when particular sector arrives at control input then that required timing will pass to the output. One multiport switch describes one switch of inverter.

5.7 α-β Transformation

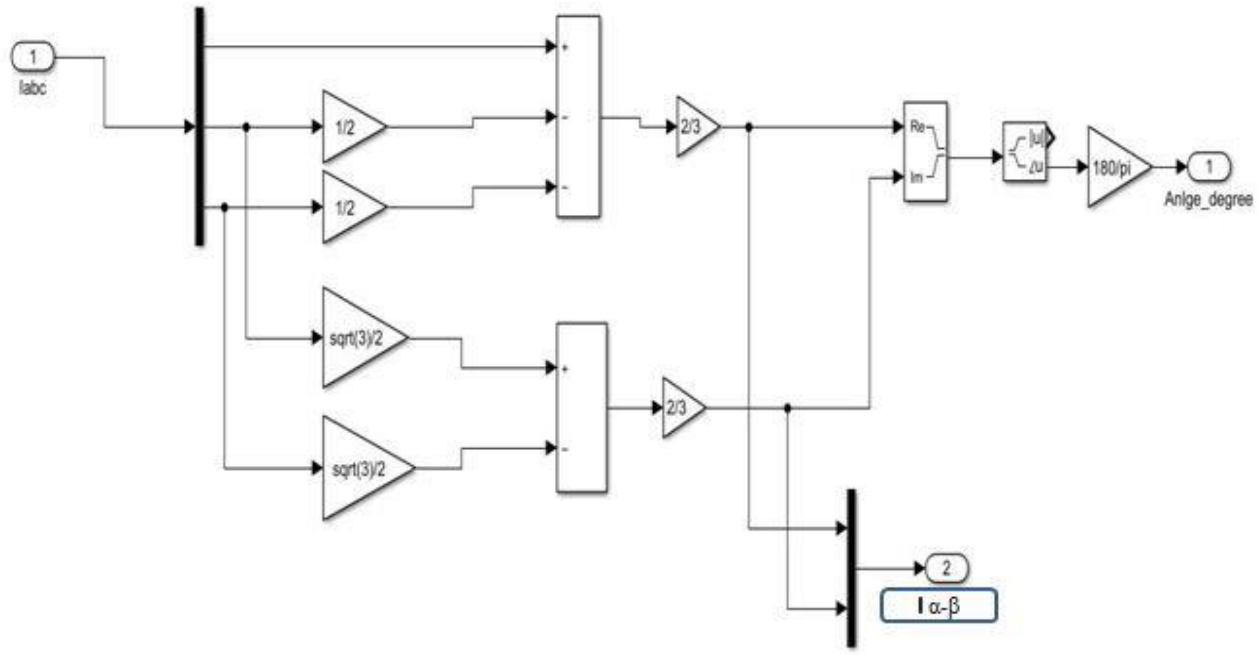

Fig.5.8 Conversion From 3-axis abc frame to 2-axis α-β Plane

Fig.5.8 shows how the simulation of α-β transformation is carried. Here basically the Clark's equation for α-β transformation is implemented. It gives d-axis and q-axis flux of an induction motor when transformation of three phase current to d-q frame is carried out. The d-axis and q-axis flux are phase shifted by 90 degree thus when these fluxes are input to the X-Y plot it gives the trajectory of circle, which can be used for verification purpose of successfully implementation of technique. A perfect implementation will output the d-q axis flux sinusoidal varying and phase shifted by 90 degree, which gives a locus of a circle in X-Y plot,

As

$$(\sin x)^2 + (\cos x)^2 = 1 \tag{5.1}$$

Implies

$$(\sin x)^2 + (\sin(90 - x))^2 = 1 \tag{5.2}$$

Which is a locus of circle of radius 1 and X-Y plot generate the locus of X-Y values input to it.

Fig.5.9 shows the block of X-Y plotter used in Simulink model.

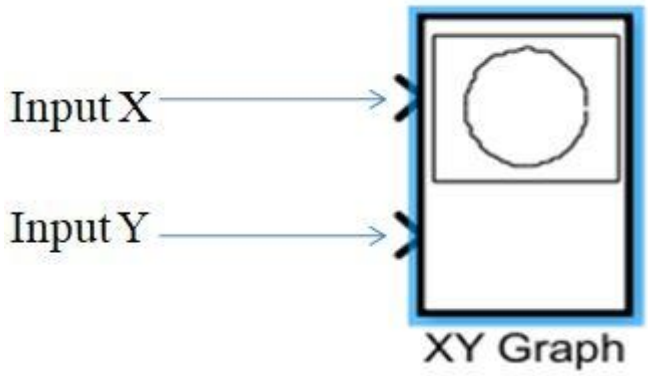

Fig.5.9 X-Y Plotter

5.8 Asynchronous Machine

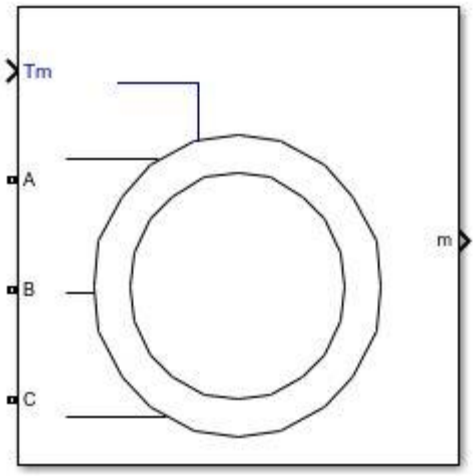

Fig.5.10 Three Phase Induction Motor Drive

Fig.5.10 shows the block of induction motor drive whuch is used as load in FS3P inverter topology. It is modeled in a selectable dq frame (rotor, Stator or synchronous) which is rotor is this cse. The stator and rotor windings are connected in wye to an internat neutral point. The squirrel cge rotor type is being selected here. The mechanical input to the motor is torgue T_m or load torque, this could be constant half rated, rated, step changing depending uon the value given t the motor mechanical input.

The motor ratings are:

Rated Power: 5.4 HP (4KW)

Rated Voltage: 400 V

Frequency: 50 Hz

Rated speed: 1430 RPM

Rated Torque: 26.73 N-m

Thus, in this chapter it is discussed that implementation of Matlab Simulink model of proposed topology is being done using the essential blocks discussed earlier in this chapter and how equations needed for the technique is modeled in the Matlab Simulink model. Also some basic blocks such as adder, logical and relational operators, gain etc have been used to meet the logic and concept behind the technique.

CHAPTER 6

FS3P TOPOLOGY WITH DC-DC BOOST CONVERSION

6.1 Introduction

FS3P Inverter topology for induction motor drive is very cost effective and reliable configuration in case if a fault occurs in any of the leg of six switch three phase inverter running induction motor drive. The reduction in interface circuits, switching losses makes it acceptable for emergency situations or use of it as primary when cost and complexity reduction is the weighted criteria for deciding the inverter-motor system.

Chapter 3 and Chapter 4 discussed the FS3P topology using SVPWM switching technique, since Space Vector Pulse Width Modulation produces more percentage of voltage at output along with the less THD in output line currents. But the major drawback in FS3P topology is that FS3P inverter requires two times the rated voltage battery compared to conventional inverter feeding the motor drive with equal ratings to generate the same amount of power at output. Employing DC-DC boost conversion with existing topology solves the problem of employing large size and high rated voltage batteries at the input, keeping the considerations of Ampere-Hour ratings of the battery.

6.2 Concept

In FS3P topology each DC Link voltage must be 350 volts at 0.986 modulation index (4KW, 400V Drive), also normally available households batteries are 48 volts and 150Ah, it means if motor requires 5A rated current (which is same in our case) then this battery would provide it for 30 hours. But input to the motor requires 350 volts at each DC-link, this creates the question and initiates the idea of employing a method which can boost dc voltage to value required at the input of FS3P inverter.

To boost a voltage from a low voltage to such a high value requires a transformer, but at the same time the available voltage is in the form of DC, thus firstly conversion need to be take place from dc to ac, it is achieved by simple square wave inverter which will convert a dc of constant 48 volts to alternating ac voltage of square wave having max and min value to be +48 volts and -48 volts respectively. This available ac voltage would now be stepped up using full bridge rectifier with centre tapped transformer. So, the centre-tapped transformer we are employing requires more number of turns at secondary such that it generates $700/\sqrt{2}$ volts rms at output. Also, since input to the FS3P inverter requires a dc voltage, it is then achieved by full bridge rectifier whose output voltage gives 700 volts at output and to achieve two dc link voltages, two capacitors of high value are connected in series as split capacitors creating the dc-link voltage for FS3P inverter. Fig 6.1 shows the block diagram of the proposed system.

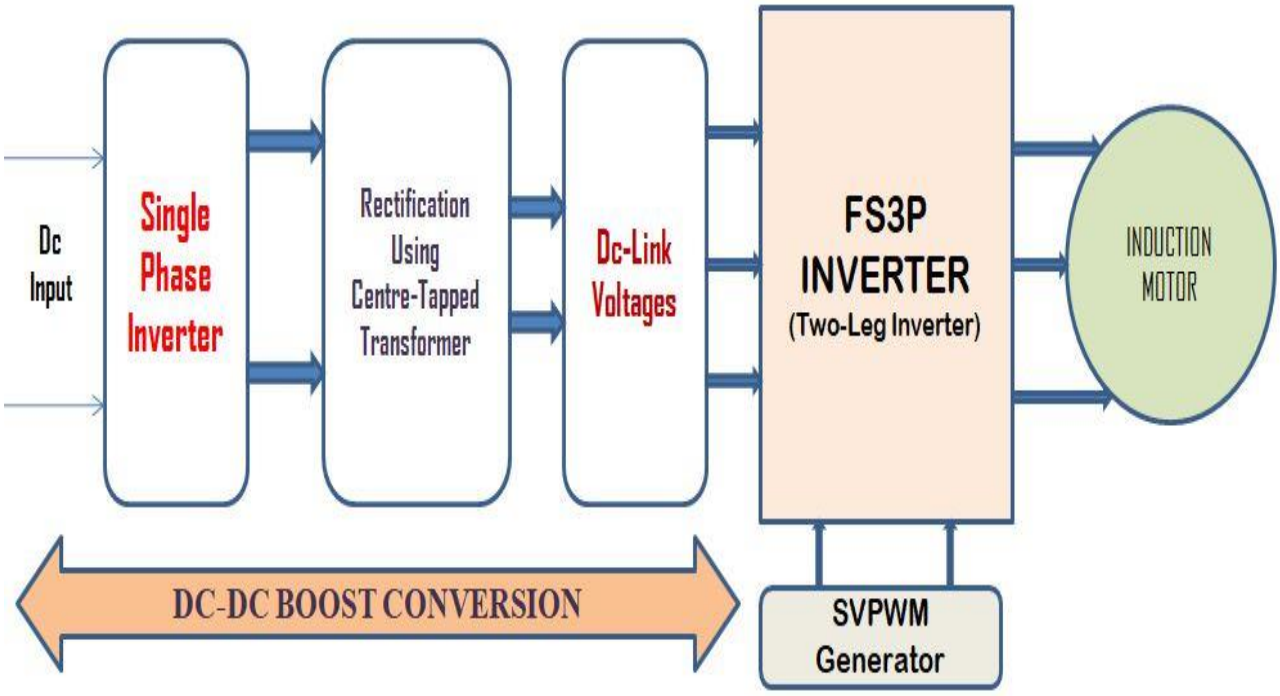

Fig.6.1 Block Diagram of Proposed System

From fig.6.1 it can be infer that our proposed system is divided into three sections, the first section being the DC conversion from low voltage to high voltage meeting the space vector demand to generate the rated voltage for motor drive, the second part being the FS3P inverter to generate the three phase voltage and current required by the load and the third section includes the drive load whose performance analysis is essential criteria to comment on the effectiveness of proposed technique and suggested system.

6.3 MATLAB Implementation of DC-DC Boost Conversion

6.3.1 Single Phase Square Wave Inverter

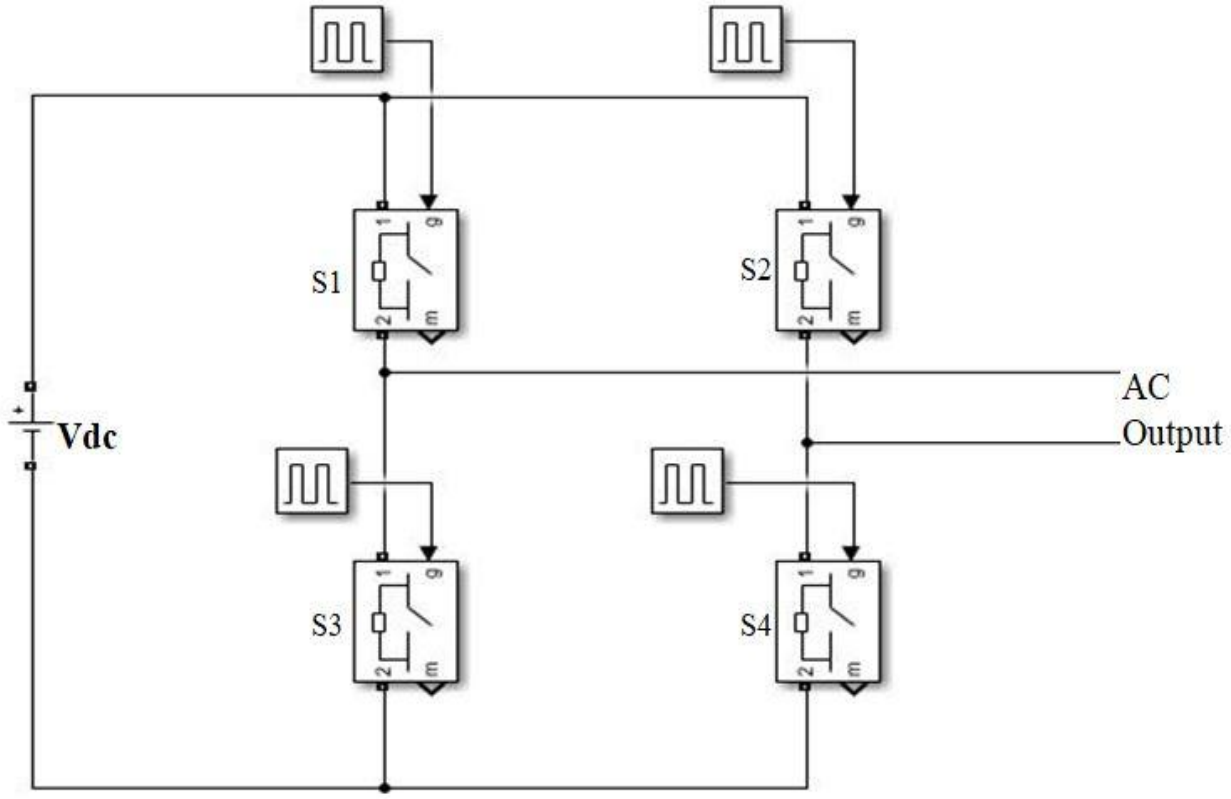

Fig.6.2 Simulation Model of Single Phase Inverter

Fig.6.2 shows the single phase square wave inverter in matlab. The pulses for the switches are conventional using pulse generator with time period of 0.02 seconds (i.e 50Hz frequency). The pulses to switches S_1 and S_2 are at 0.01 phase delay with S_4 following the same pattern as S_1 and S_3 following the same pulsing pattern as S_2 to generate the square wave voltage with max value to be +48 volts and min value to be -48 volts as the input dc voltage given to the inverter is 48 volts.

6.3.2 Stepping-Up and Rectification of Proposed System

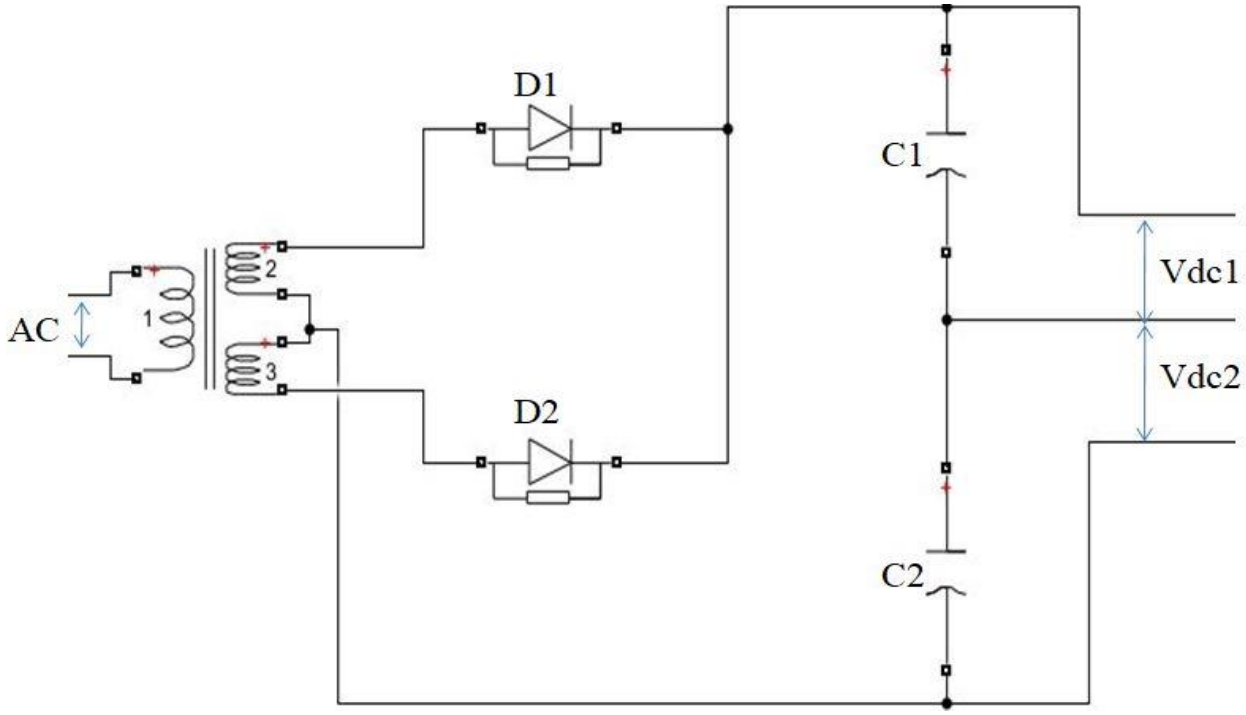

Fig.6.3 Rectification and Amplification

Fig.6.3 shows the simulink model of full bridge diode rectifier with centre tapped transformer which is used for stepping up the the ac voltage output from single phase square wave inverter to the high value required at the dc link. Winding turns of transformer are chosen by considering the ac voltage of 48 volts peak at input and 700 volts peak at output of each windings of transformer, so that it generate the dc voltage of 700 volts at output after rectification.

Thus,

Winding 1 turns are:

$N_1 = 48/\sqrt{2} = 34$

Winding 2 turns are:

$N_2 = 700/\sqrt{2} = 496$

Winding 3 turns are:

$N_3 = 700/\sqrt{2} = 496$

Since rating of induction motor drive used is 4KW thus considering 0.8 power factor the VA rating of centre taped transformer is 5000VA.

The diode bridge is considered for rectification part of proposed system which is producing the 700 volts dc output which is required for FS3P topology. The output of rectifier is connected with two capacitors of 1000μF each in series as shown in fig.6.3 which will be utilized as split capacitors for creating the dc link at input of the FS3P inverter.

CHAPTER 7

INDUCTION MOTOR MODELLING

7.1 INTRODUCTION

Whenever there is change in parameters of stator and rotor for example voltage and current will change other parameters also due to inherent coupling effect in induction motor due to its construction. Both torque and flux are functions of voltage or current and frequency, and due to increase in torque, flux tends to decrease implying that one parameter affects the other which is not desirable.

By modeling of induction motor, the parameters which were earlier interdependent due to coupling effect of induction will become independent due to parameters de-coupling. So by controlling the parameters the current or voltage, frequency, the output torque and seed can be controlled without effecting the other parameters or induction motor modeling helps to control each parameter separately.

7.2 Modeling

Three phase voltages supplied to the motor are as follows:

$$V_{as} = V_m \sin(\omega_e t) \tag{7.1}$$

$$V_{bs} = V_m \sin\left(\omega_e t - \frac{2\pi}{3}\right) \tag{7.2}$$

$$V_{cs} = V_m \sin\left(\omega_e t + \frac{2\pi}{3}\right) \tag{7.3}$$

Where, V_m is the amplitude of the terminal or peak of the supply voltage, and ω_e is the supply frequency.

The three-phase to two-phase transformation is needed in order to develop the dynamic model of induction motor,

Using Clark's Transformation, a three phase stationary reference frame variables V_{as}, V_{bs}, V_{cs} can be transformed in to two phase stationary frame variables "V_{qs}^s and V_{ds}^s", the superscript 's' denotes the stationary frame;

$$\begin{bmatrix} V_{qs}^s \\ V_{ds}^s \end{bmatrix} = \frac{2}{3}\begin{bmatrix} 1 & \frac{-1}{2} & \frac{-1}{2} \\ 0 & \frac{-\sqrt{3}}{2} & \frac{\sqrt{3}}{2} \end{bmatrix}\begin{bmatrix} V_{as} \\ V_{bs} \\ V_{cs} \end{bmatrix} \tag{7.4}$$

Let us transform the two phase stationary reference frame variables (V_{qs}^{s} and V_{ds}^{s}) into two phase synchronously rotating reference frame variables "V_{qs} and V_{ds}" by using the following equation:

$$V_{qs} = V_{qs}^{s} \cos\theta_e - V_{ds}^{s} \sin\theta_e \tag{7.5}$$

$$V_{ds} = V_{qs}^{s} \sin\theta_e + V_{ds}^{s} \cos\theta_e \tag{7.6}$$

Here, $\theta_e = \omega_e t$ is the angle of rotating frame with respect to stationary frame and ω_e is the synchronous speed at which the rotating frames rotates.

The stator circuit equations in stationary frame are given as:

$$V_{qs}^{s} = R_s i_{qs}^{s} + \frac{d\varphi_{qs}^{s}}{dt} \tag{7.7}$$

$$V_{ds}^{s} = R_s i_{ds}^{s} + \frac{d\varphi_{ds}^{s}}{dt} \tag{7.8}$$

Similarly rotor circuit equations in stationary frame are given by:

$$V_{qr}^{s} = R_r i_{qr}^{s} + \frac{d\varphi_{qr}^{s}}{dt} \tag{7.9}$$

$$V_{dr}^{s} = R_r i_{dr}^{s} + \frac{d\varphi_{dr}^{s}}{dt} \tag{7.10}$$

Where φ_{qs}^{s} and φ_{ds}^{s} are stator flux linkages of q-axis and d-axis respectively and φ_{qr}^{s} and φ_{dr}^{s} are rotor flux linkages of q-axis and d-axis in the stationary reference frame respectively.

After converting the above equations from stationary frame to synchronously rotating reference frame we get:

$$V_{qs} = R_s i_{qs} + \frac{d\varphi_{qs}}{dt} + \omega_e \varphi_{ds} \tag{7.11}$$

$$V_{ds} = R_s i_{ds} + \frac{d\varphi_{ds}}{dt} - \omega_e \varphi_{qs} \tag{7.12}$$

And the rotor circuit equations are given by,

$$V_{qr} = R_r i_{qr} + \frac{d\varphi_{qr}}{dt} + \omega_e \varphi_{dr} \tag{7.13}$$

$$V_{dr} = R_r i_{dr} + \frac{d\varphi_{dr}}{dt} - \omega_e \varphi_{qr} \tag{7.14}$$

But rotor actually moves at speed 'ω_r', therefore the d-q axis fixed on the rotor moves at speed '$\omega_e - \omega_r$' relative to the synchronously rotting frame, therefore in synchronously rotating d-q frame i.e 'd^e-q^e frame' the actual rotor equations are written as follows:

$$V_{qr} = R_r i_{qr} + \frac{d\varphi_{qr}}{dt} + (\omega_e - \omega_r)\varphi_{dr} \tag{7.15}$$

$$V_{dr} = R_r i_{dr} + \frac{d\varphi_{dr}}{dt} - (\omega_e - \omega_r)\varphi_{qr} \tag{7.16}$$

Now to develop the dynamic model of induction motor it is necessary to define flux linkage variables:

$$F_{qs} = \omega_b \varphi_{qs} \tag{7.17}$$

$$F_{qr} = \omega_b \varphi_{qr} \tag{7.18}$$

$$F_{ds} = \omega_b \varphi_{ds} \tag{7.19}$$

$$F_{dr} = \omega_b \varphi_{dr} \tag{7.20}$$

Where, ω_b is the base frequency of the machine.

Now assuming $V_{qr} = V_{dr} = 0$ and substituting equations (7.17)-(7.20) in equations (7.11), (7.12), (7.15) and (7.16) we have;

$$V_{qs} = R_s i_{qs} + \frac{1}{\omega_b}\frac{dF_{qs}}{dt} + \frac{\omega_e}{\omega_b}F_{ds} \tag{7.21}$$

$$V_{ds} = R_s i_{ds} + \frac{1}{\omega_b}\frac{dF_{ds}}{dt} - \frac{\omega_e}{\omega_b}F_{qs} \tag{7.22}$$

$$0 = R_r i_{qr} + \frac{1}{\omega_b}\frac{dF_{qr}}{dt} + \frac{(\omega_e - \omega_r)}{\omega_b}F_{dr} \tag{7.23}$$

$$0 = R_r i_{dr} + \frac{1}{\omega_b}\frac{dF_{dr}}{dt} - \frac{(\omega_e - \omega_r)}{\omega_b}F_{qr} \tag{7.24}$$

The Flux linkage equations in terms of currents can be written as follows:

$$\varphi_{qs} = L_{ls} i_{qs} + L_m\left(i_{qs} + i_{qr}\right) \tag{7.25}$$

$$\varphi_{qr} = L_{lr} i_{qr} + L_m\left(i_{qr} + i_{qs}\right) \tag{7.26}$$

$$\varphi_{qm} = L_m\left(i_{qs} + i_{qr}\right) \tag{7.27}$$

$$\varphi_{ds} = L_{ls} i_{ds} + L_m (i_{ds} + i_{dr}) \quad (7.28)$$

$$\varphi_{dr} = L_{lr} i_{dr} + L_m (i_{ds} + i_{dr}) \quad (7.29)$$

$$\varphi_{dm} = L_m (i_{ds} + i_{dr}) \quad (7.30)$$

Now multiplying the equations (7.25)-(7.30) by ω_b on both sides, the flux linkage equations can be written as:

$$F_{qs} = \omega_b \varphi_{qs} = X_{ls} i_{qs} + X_m (i_{qs} + i_{qr}) \quad (7.31)$$

$$F_{qr} = \omega_b \varphi_{qr} = X_{lr} i_{qr} + X_m (i_{qs} + i_{qr}) \quad (7.32)$$

$$F_{qm} = \omega_b \varphi_{qm} = X_m (i_{qs} + i_{qr}) \quad (7.33)$$

$$F_{ds} = \omega_b \varphi_{ds} = X_{ls} i_{ds} + X_m (i_{ds} + i_{dr}) \quad (7.34)$$

$$F_{dr} = \omega_b \varphi_{dr} = X_{lr} i_{dr} + X_m (i_{ds} + i_{dr}) \quad (7.35)$$

$$F_{dm} = \omega_b \varphi_{dm} = X_m (i_{ds} + i_{dr}) \quad (7.36)$$

Where,

$X_{ls} = \omega_b L_{ls}$ = Stator leakage reactance

$X_{lr} = \omega_b L_{lr}$ = Rotor leakage reactance

$X_m = \omega_b L_m$ = Magnetizing reactance

Now equation (7.31), (7.32), (7.34) and (7.35) can be written as:

$$F_{qs} = X_{ls} i_{qs} + F_{qm} \quad (7.37)$$

$$F_{qr} = X_{lr} i_{qr} + F_{qm} \quad (7.38)$$

$$F_{ds} = X_{ls} i_{ds} + F_{dm} \quad (7.39)$$

$$F_{dr} = X_{lr} i_{dr} + F_{dm} \quad (7.40)$$

So, now currents can be expressed in terms of flux linkages as follows:

$$i_{qs} = \frac{F_{qs} - F_{qm}}{X_{ls}} \quad (7.41)$$

$$i_{qr} = \frac{F_{qr} - F_{qm}}{X_{lr}} \quad (7.42)$$

$$i_{ds} = \frac{F_{ds} - F_{dm}}{X_{ls}} \tag{7.43}$$

$$i_{dr} = \frac{F_{dr} - F_{dm}}{X_{lr}} \tag{7.44}$$

From equation (7.33), (7.41) and (7.42) we have

$$F_{qm} = X_m \left(\frac{F_{qs} - F_{qm}}{X_{ls}} + \frac{F_{qr} - F_{qm}}{X_{lr}} \right)$$

$$F_{qm} = \frac{X_m}{X_{ls}} F_{qs} - \frac{X_m}{X_{ls}} F_{qm} + \frac{X_m}{X_{lr}} F_{qr} - \frac{X_m}{X_{lr}} F_{qm}$$

$$F_{qm} \left(1 + \frac{X_m}{X_{ls}} + \frac{X_m}{X_{lr}} \right) = \frac{X_m}{X_{ls}} F_{qs} + \frac{X_m}{X_{lr}} F_{qr}$$

$$F_{qm} \left(\frac{X_{ls}X_{lr} + X_m X_{lr} + X_m X_{ls}}{X_{ls}X_{lr}} \right) = \frac{X_m}{X_{ls}} F_{qs} + \frac{X_m}{X_{lr}} F_{qr}$$

$$F_{qm} \left(\frac{X_{ls}X_{lr} + X_m X_{lr} + X_m X_{ls}}{X_{ls}X_{lr}X_m} \right) = \frac{1}{X_{ls}} F_{qs} + \frac{1}{X_{lr}} F_{qr}$$

$$F_{qm} = \frac{X_{m1}}{X_{ls}} F_{qs} + \frac{X_{m1}}{X_{lr}} F_{qr} \tag{7.45}$$

Similarly,

$$F_{dm} = \frac{X_{m1}}{X_{ls}} F_{ds} + \frac{X_{m1}}{X_{lr}} F_{dr} \tag{7.46}$$

Where,

$$X_{m1} = \frac{X_{ls}X_{lr}X_m}{X_{ls}X_{lr} + X_m X_{lr} + X_m X_{ls}} \tag{7.47}$$

Now the stator and rotor voltage equations can be written by substituting equations (7.41)-(7.44) in equations (7.21)-(7.24)

$$V_{qs} = \frac{R_s}{X_{ls}} \left(F_{qs} - F_{qm} \right) + \frac{1}{\omega_b} \frac{dF_{qs}}{dt} + \frac{\omega_e}{\omega_b} F_{ds} \tag{7.48}$$

$$V_{ds} = \frac{R_s}{X_{ls}} \left(F_{ds} - F_{dm} \right) + \frac{1}{\omega_b} \frac{dF_{ds}}{dt} - \frac{\omega_e}{\omega_b} F_{qs} \tag{7.49}$$

$$0 = \frac{R_r}{X_{lr}}\left(F_{qr} - F_{qm}\right) + \frac{1}{\omega_b}\frac{dF_{qr}}{dt} + \frac{(\omega_e - \omega_r)}{\omega_b}F_{dr} \tag{7.50}$$

$$0 = \frac{R_r}{X_{lr}}\left(F_{dr} - F_{dm}\right) + \frac{1}{\omega_b}\frac{dF_{qr}}{dt} - \frac{(\omega_e - \omega_r)}{\omega_b}F_{qr} \tag{7.51}$$

Now equation (7.48) can be modified as:

$$\frac{1}{\omega_b}\frac{dF_{qs}}{dt} = V_{qs} - \frac{\omega_e}{\omega_b}F_{ds} - \frac{R_s}{X_{ls}}\left(F_{qs} - F_{qm}\right)$$

From equation (7.45)

$$\frac{1}{\omega_b}\frac{dF_{qs}}{dt} = V_{qs} - \frac{\omega_e}{\omega_b}F_{ds} - \frac{R_s}{X_{ls}}\left(F_{qs} - \left(\frac{X_{m1}}{X_{ls}}F_{qs} + \frac{X_{m1}}{X_{lr}}F_{qr}\right)\right)$$

$$\frac{1}{\omega_b}\frac{dF_{qs}}{dt} = V_{qs} - \frac{\omega_e}{\omega_b}F_{ds} + \frac{R_s}{X_{ls}}\left(\frac{X_{m1}}{X_{ls}}F_{qs} + \frac{X_{m1}}{X_{lr}}F_{qr} - F_{qs}\right)$$

$$\frac{1}{\omega_b}\frac{dF_{qs}}{dt} = V_{qs} - \frac{\omega_e}{\omega_b}F_{ds} + \frac{R_s}{X_{ls}}\left(F_{qs}\left(\frac{X_{m1}}{X_{ls}} - 1\right) + \frac{X_{m1}}{X_{lr}}F_{qr}\right)$$

$$\frac{dF_{qs}}{dt} = \omega_b\left(V_{qs} - \frac{\omega_e}{\omega_b}F_{ds} + \frac{R_s}{X_{ls}}\left(F_{qs}\left(\frac{X_{m1}}{X_{ls}} - 1\right) + \frac{X_{m1}}{X_{lr}}F_{qr}\right)\right) \tag{7.52}$$

Equation (7.52) is modified in state space form and is used to develop the sub-model for obtaining F_{qs}.

Similarly,

$$\frac{dF_{ds}}{dt} = \omega_b\left(V_{ds} + \frac{\omega_e}{\omega_b}F_{qs} + \frac{R_s}{X_{ls}}\left(F_{ds}\left(\frac{X_{m1}}{X_{ls}} - 1\right) + \frac{X_{m1}}{X_{lr}}F_{dr}\right)\right) \tag{7.53}$$

$$\frac{dF_{qr}}{dt} = \omega_b\left(-\frac{(\omega_e - \omega_r)}{\omega_b}F_{dr} + \frac{R_r}{X_{lr}}\left(F_{qr}\left(\frac{X_{m1}}{X_{lr}} - 1\right) + \frac{X_{m1}}{X_{ls}}F_{qs}\right)\right) \tag{7.54}$$

$$\frac{dF_{dr}}{dt} = \omega_b\left(\frac{(\omega_e - \omega_r)}{\omega_b}F_{qr} + \frac{R_r}{X_{lr}}\left(F_{dr}\left(\frac{X_{m1}}{X_{lr}} - 1\right) + \frac{X_{m1}}{X_{ls}}F_{ds}\right)\right) \tag{7.55}$$

Equations (7.53), (7.54) and (7.55) are also in state space form and used to develop sub-model to obtain F_{ds}, F_{qr} and F_{dr}.

Now, Once the Variables F_{qs}, F_{ds}, F_{qr} and F_{dr} are calculated and further from it we can find F_{qm} and F_{dm} using (7.45) and (7.46). So after calculating all these variables we can find q-axis stator and rotor currents using equations (7.41) and (7.42) and d-axis stator and rotor currents using equations (7.43) and (7.42).

After finding F_{ds}, F_{qs}, i_{ds} and i_{qs} the electromagnetic torque produced by the motor is found by following equation:

$$T_e = \frac{3}{2}\frac{P}{2}\frac{1}{\omega_b}\left(F_{ds}i_{qs} - F_{qs}i_{ds}\right) \tag{7.56}$$

Once the torque from equation (7.56) is found, the speed of the Motor can be calculated by the equation:

$$(T_e - T_l) = \frac{2}{P}J\frac{d\omega_r}{dt} \tag{7.57}$$

Where,

T_l = Load Torque

J = rotor Inertia

P = number of poles

ω_r = rotor angular electrical speed

also

$$\omega_m = \frac{2}{P}\omega_r \tag{7.58}$$

Where,

ω_m = Rotor Mechanical (angular) Speed.

CHAPTER 8

RESULTS AND DISCUSSIONS

8.1 Introduction

In this chapter simulation results are discussed for our proposed topologies that are involved to fed three-phase induction motor drive. The first topology that is considered is six-switch three phase inverter fed induction motor drive and the gating pulses are obtained through SVPWM, this is conventional topology and results are obtained for rotor mechanical speed, electromagnetic torque, line currents I_{abc} to comment on the performance of given drive, current THD is also mentioned in order to obtain the effectiveness of given technique.

The results are taken for three drives as shown in table 8.1 to test the performance of different drives with proposed topology and modulation technique used.

Table 8.1 Induction Motor Drives for Test

S.No	Power Rating	Voltage Rating	Rated Torque	Rated Speed (RPM)	Connection
1	1 HP	380 V	4.97 N-M	1500	Star
2	3 HP	220 V	14.25 N-M	1500	Delta
3	5 HP	400 V	26.72 N-M	1430	Star

The second topology is FS3P VSI Fed IM drive, the motor is run from no-load to full-load and variation in electromagnetic torque, rotor speed, line currents is observed through simulation results and discussion over the performance is presented for its reliability in case of emergency situations if one leg of six-switch inverter becomes inactive during fault situations.

If efforts are made for making a FS3P VSI Fed IM drive as a primary method to reduce the cost and complexity of interfacing circuits, results of third topology involving dc-boost conversion to obtain dc-link voltage in FS3P inverter are presented and discussion over the drive performance considering rotor speed, electromagnetic torque, line currents for three drives given in table 8.1.

In all three topologies motor is run from no-load to full-load to observe the effects of different output parameters and comparative discussion between the conventional and proposed topology is presented to comment on the reliability of suggested cost effective inverter topology.

8.2 Six-Switch VSI Fed IM Drive

8.2.1 SVPWM Output

8.2.1.1 PLL Output

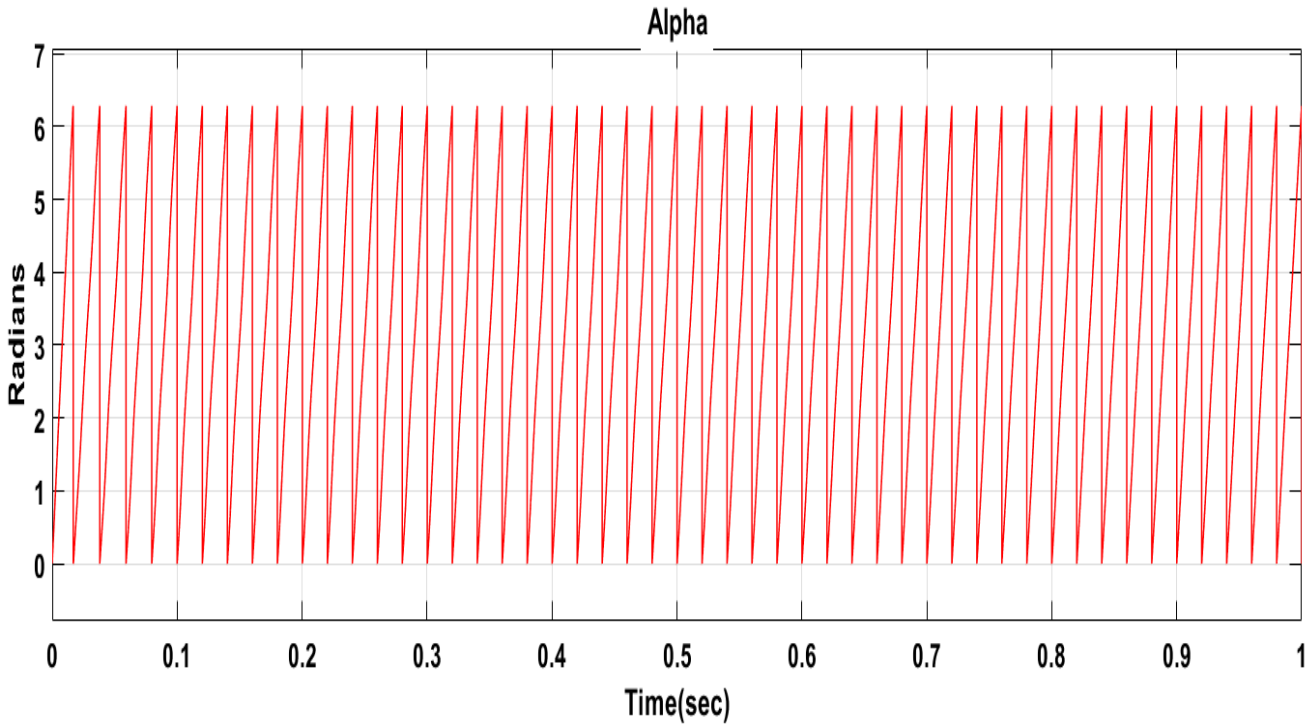

Fig.8.1 PLL Output in radians

Fig.8.1 shows the output of a PLL, the input to the PLL block is sine wave with frequency 50 Hz, in return it produces output of value 0 to 2π radians in a particular period. For example for a frequency of 50 Hz it produces value 0 at time 0 seconds which varies linearly and at 0.02 second gives value 2π radians, so output of a PLL is our angle alpha in the Space Vector synthesis.

8.2.1.2 Sector Selection

Fig.8.2 shows the selection of sectors. Any two consecutive vectors displaced by each other at a angle of 60 degrees and Space Vector synthesis demands 6 active vectors (two consecutive vectors are responsible for V_{ref} synthesis depending upon the sector in which alpha lies), therefore total 6 sectors are divided in space. When alpha vary from 0-60 degree sector 1 is selected, from 60-120 degree sector 2 is selected depending upon the value of angle alpha made by Vref with the X-axis.

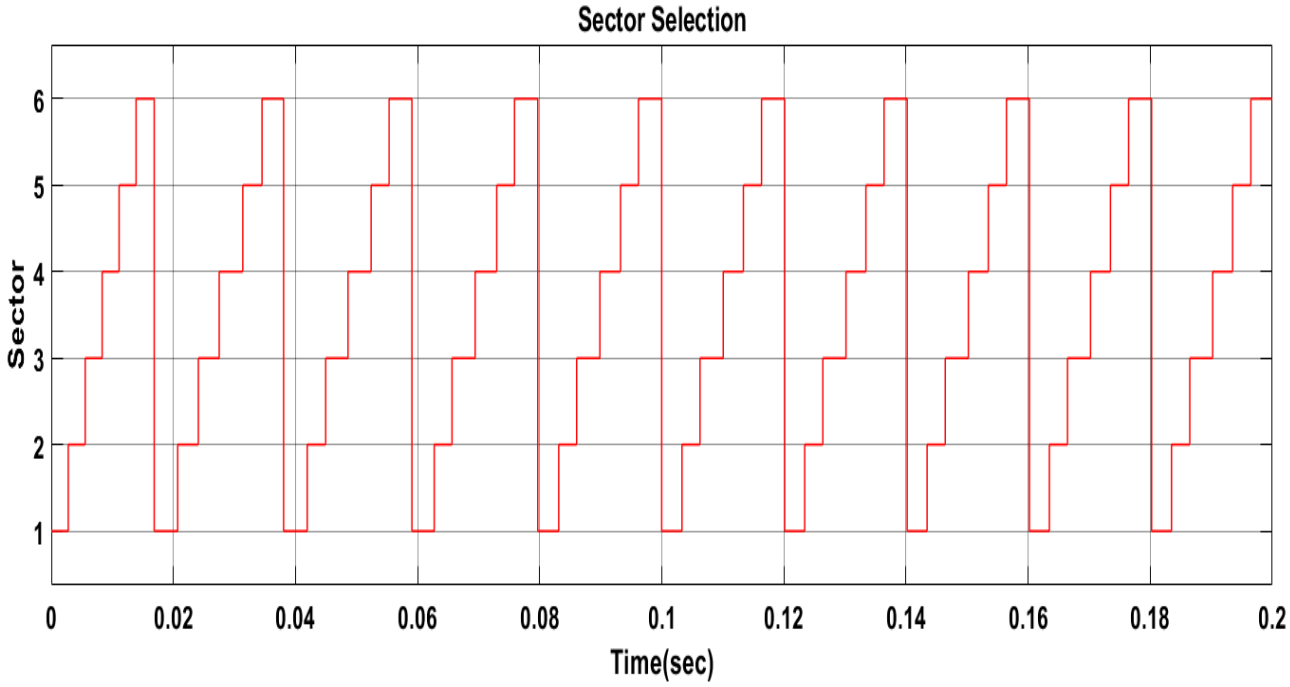

Fig.8.2 Sector selection in a period of 0.02 seconds

It can be seen from fig.8.2 that total of 6 sectors are generated in a period of 0.02 seconds in which sector 1 is selected for time 0 to 60/360*0.02 seconds, sector 2 is for time 60/360*0.02 to 120/360*0.02 seconds and so on.

8.2.1.3 Switch Timings

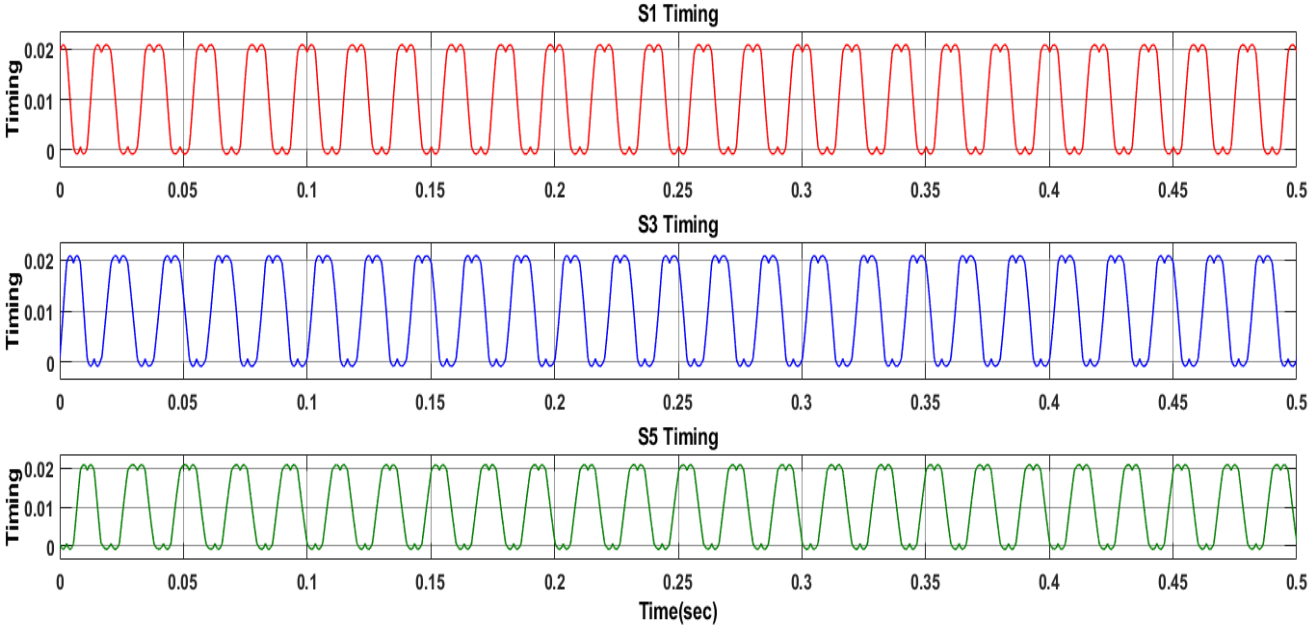

Fig.8.3 Gate Switching Time for three phase inverter switches

Fig.8.3 shows the gate switching times for switch S_1, S_3 and S_5, these timing waveforms are compared with ramp signal of 2Khz frequency as a result pulses will be generated that will be fed to respective Switches. The fundamental component of pulses obtained constitutes the waveforms as shown in fig.8.3, thus switches S_1, S_3 and S_5 is getting respective timing waveforms as shown.

8.2.1.4 Gate Pulses

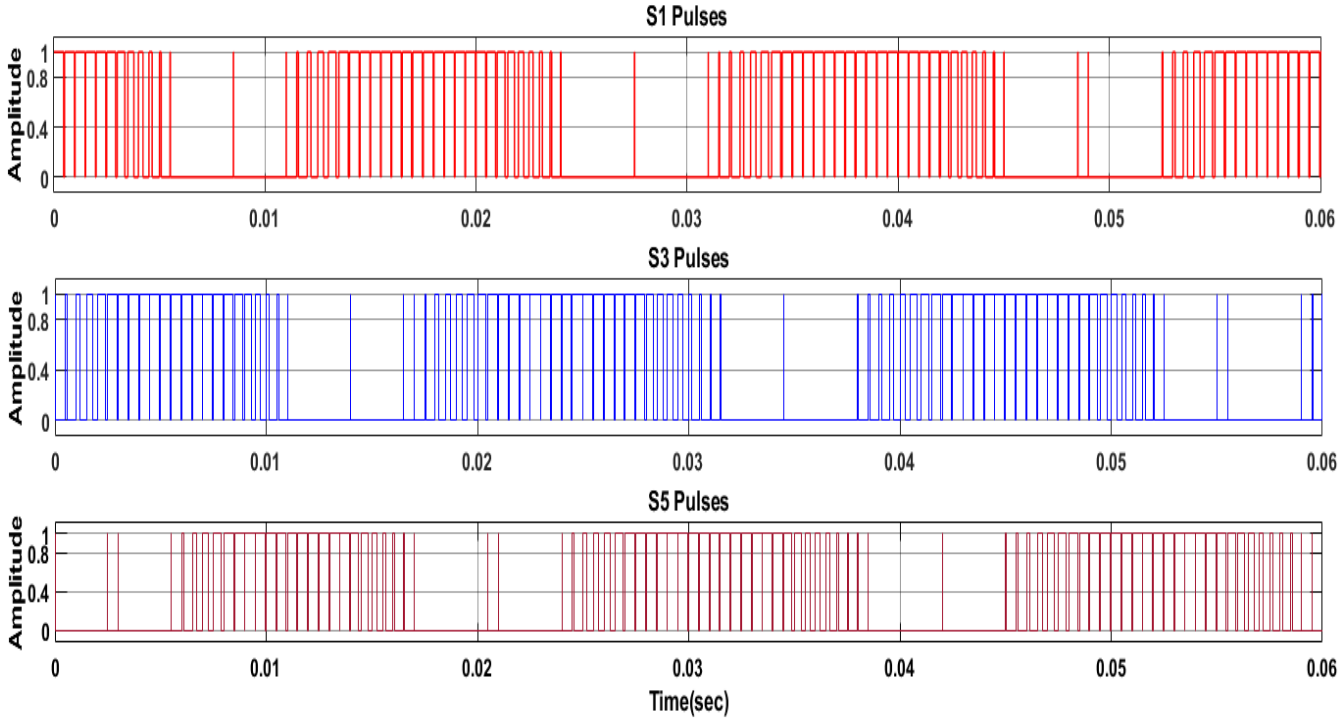

Fig.8.4 Gating Pulses for three phase inverter switches

Fig.8.4 shows the pulses obtained by comparing waveforms of fig.8.3 with ramp signal. The pulses are given to the switches which therefore generate the three phase output voltages or current according to the SVPWM theory.

8.2.2 Performance analysis of 1HP, 380 V Star Connected IM Drive

Performance analysis of given IM Drive is done on the basis of stator or line current, electromagnetic torque and rotor mechanical speed, along with the THD in line currents. The torque input given to the motor is summarized in table 8.2 and effects in different motor parameters with changing load are analyzed.

Table.8.2 Load Torque to 1HP motor fed with SS3P Inverter

Time(sec)	Load Torque (N-m)
0-1	0
1-2	1
2-3	2
3-4	3
4-5	4
5-6	5

8.2.2.1 Rotor Mechanical Speed

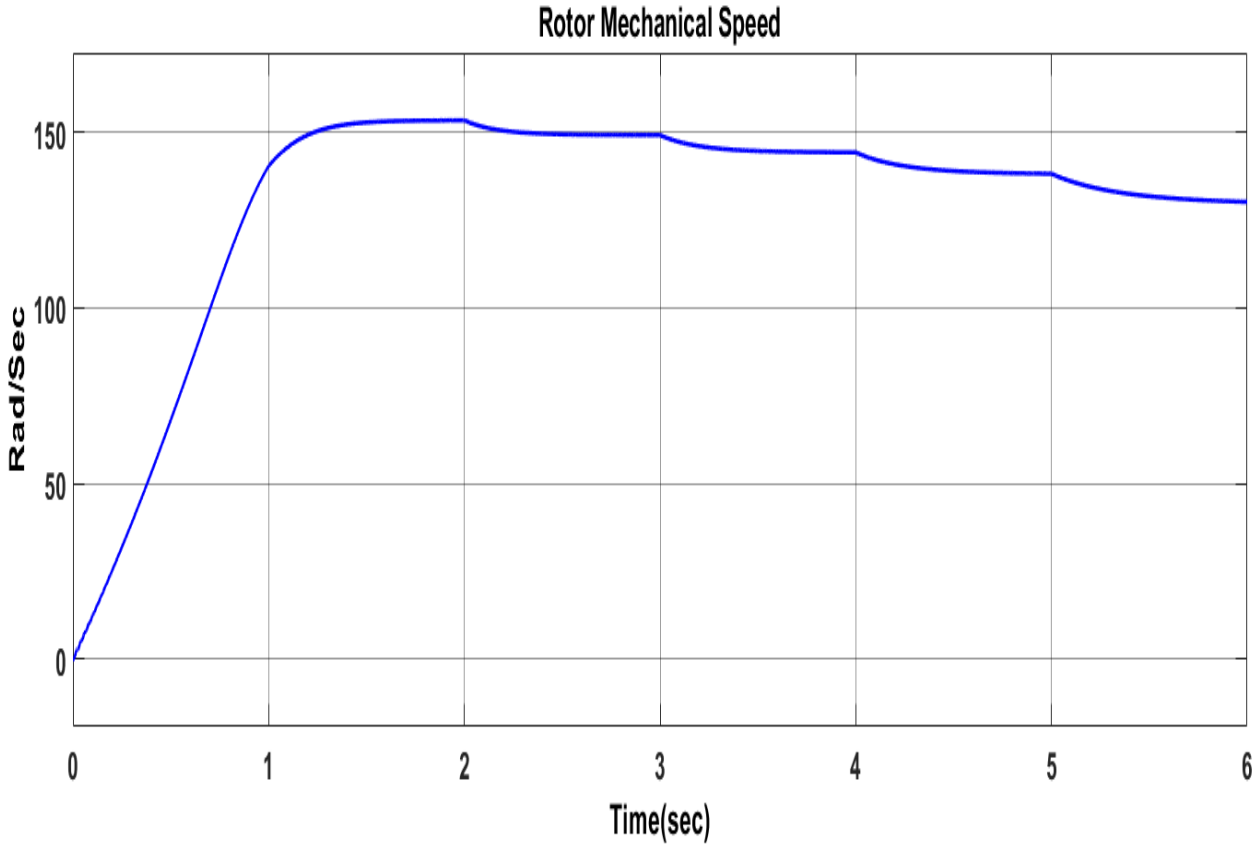

Fig.8.5 Rotor Speed of 1HP Motor fed with SS3P Inverter

Fig.8.5 shows the behavior of motor speed at different loadings to the motor. When load torque increases the dip in speed is observed which settles to a constant value after some settling period of time. The rotor speed at different load torque is summarized in table 8.3

Table 8.3 Rotor Speed at different input load of 1HP Motor fed with SS3P Inverter

Time(sec)	Torque (N-m)	Motor Speed (rad/sec)
0-1	0	-
1-2	1	153.5
2-3	2	149.3
3-4	3	144
4-5	4	138
5-6	5	130

Table 8.3 gives the conclusive idea of behavior of rotor speed at different loadings. From time (0-1) seconds i.e when there is no load, motor speed is increasing linearly during this period and settles to a constant value of 153.5 rad/sec when load 1N-m is applied at 1 seconds. With increase in load, speed is decreasing and settles to a constant value as given in table 8.3.

8.2.2.2 Electromagnetic Torque

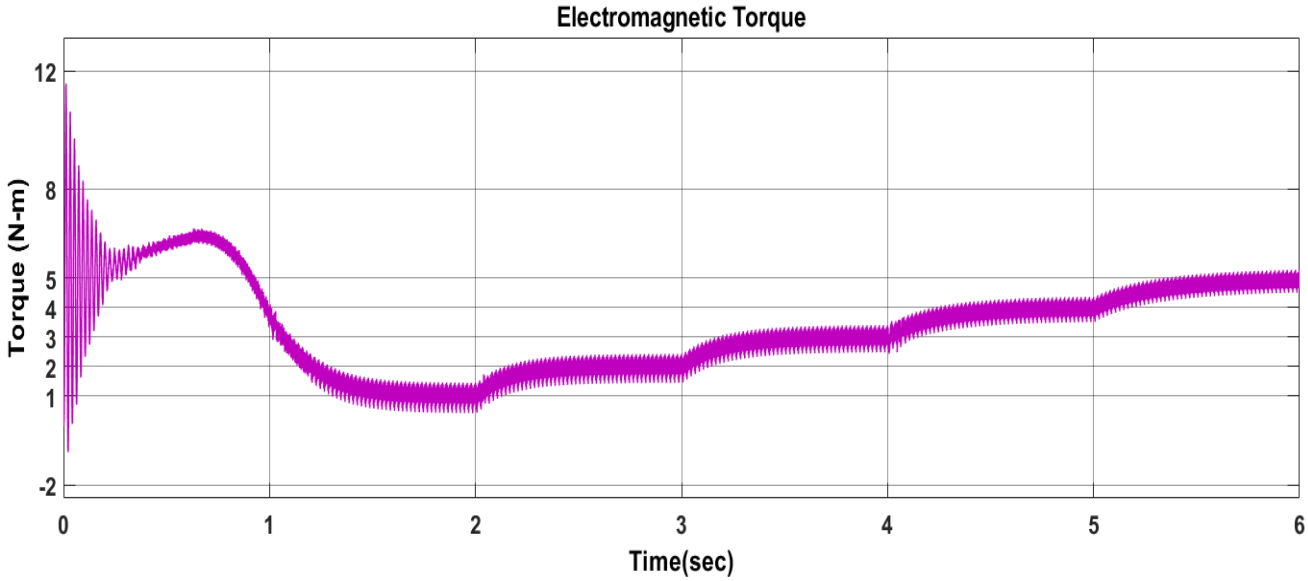

Fig.8.6 Electromagnetic Torque of 1HP Motor fed with SS3P Inverter

Fig.8.6 shows the electromagnetic torque of the motor at different timings, since with timings the mechanical torque is changed from no-load to full load as shown in table.8.2, the fig.8.6 shows that electromagnetic torque generated is tracing the mechanical torque given at the input of the motor.

8.2.2.3 Stator Current

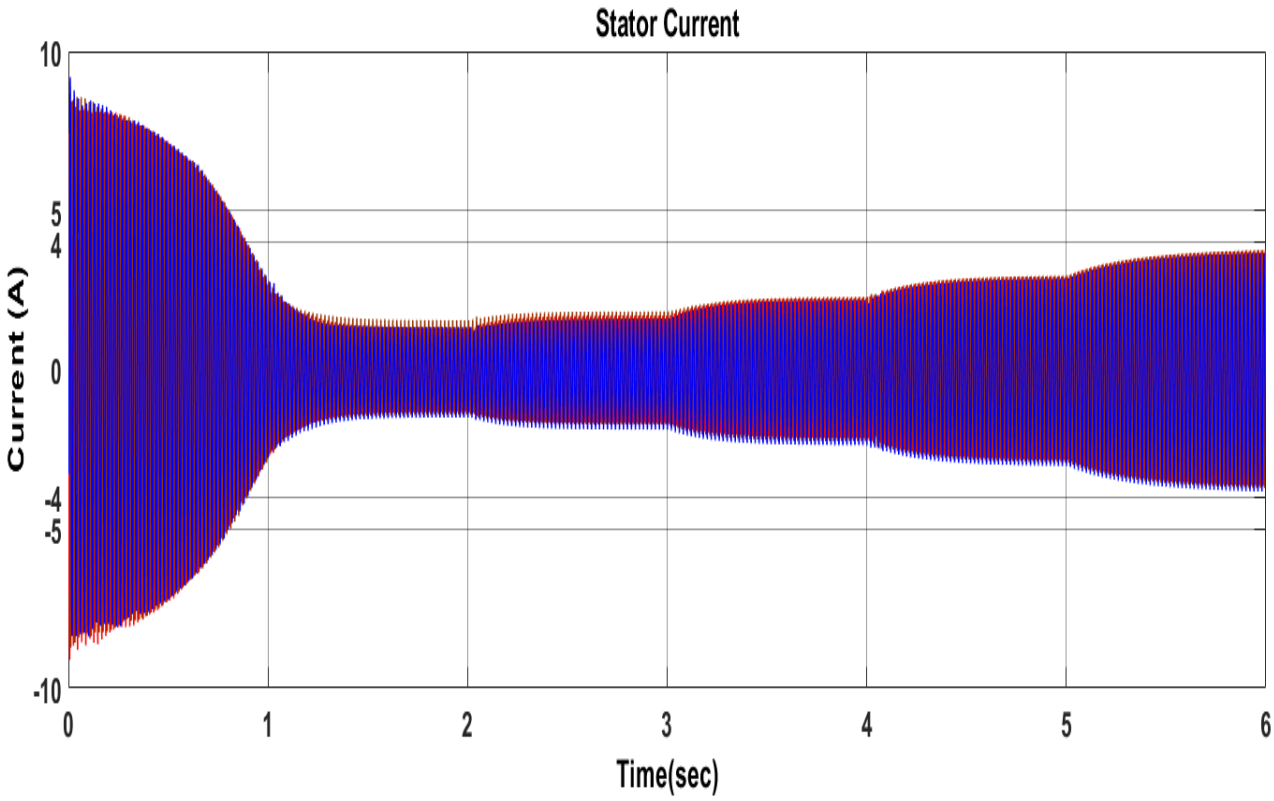

Fig.8.7 Stator Current of 1HP Motor fed with SS3P Inverter

The behavior of stator current can be seen from fig.8.7 at different intervals of time according to the mechanical input given to the motor. From (0-1) seconds there is no load to the motor, the starting currents are high and stabilizes according to the given load. When load is increasing the stator current is also increasing in accordance with the given mechanical input. From (5-6) seconds, rated torque of 5N-m is given to the motor and peak value of current is 3.5A which implies 2.3A of current is flowing at rated load. Also fig.8.8 shows three phase stator current waveforms when rated mechanical load is applied to the given drive.

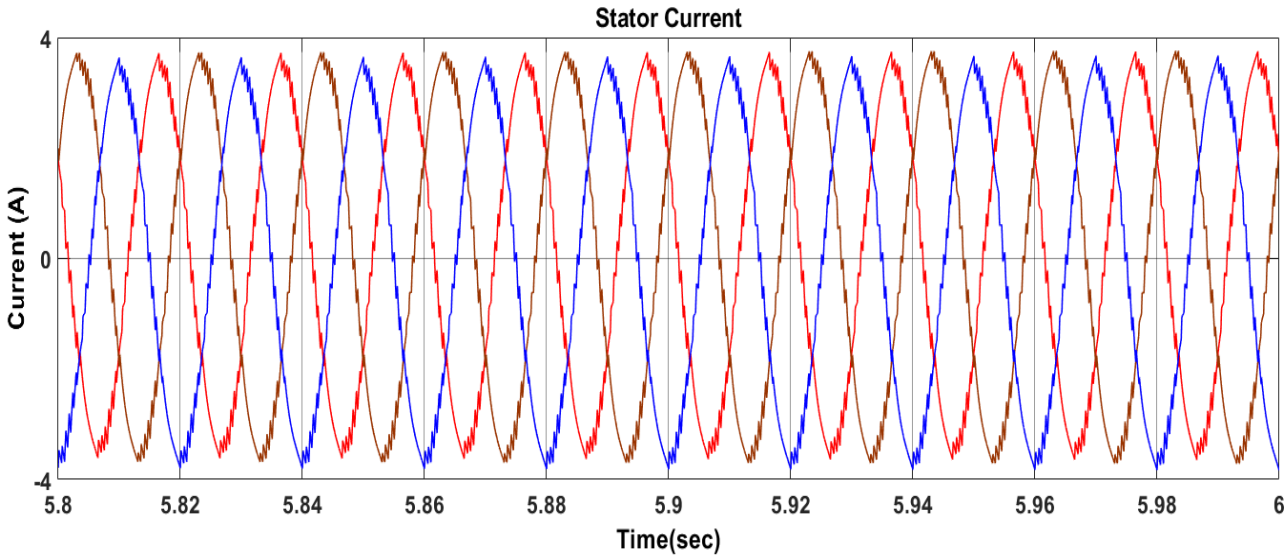

Fig.8.8 Stator Current at rated torque period of 1HP Motor fed with SS3P Inverter

Fig.8.8 shows the three phase line current waveforms at rated torque, it can be seen that waveforms are sinusoidal in nature and to get the effectiveness in generating the three phase voltage of SVPWM technique that is used here, the FFT Analysis tool result is shown in fig.8.9 which shows the stator current THD at rated load torque.

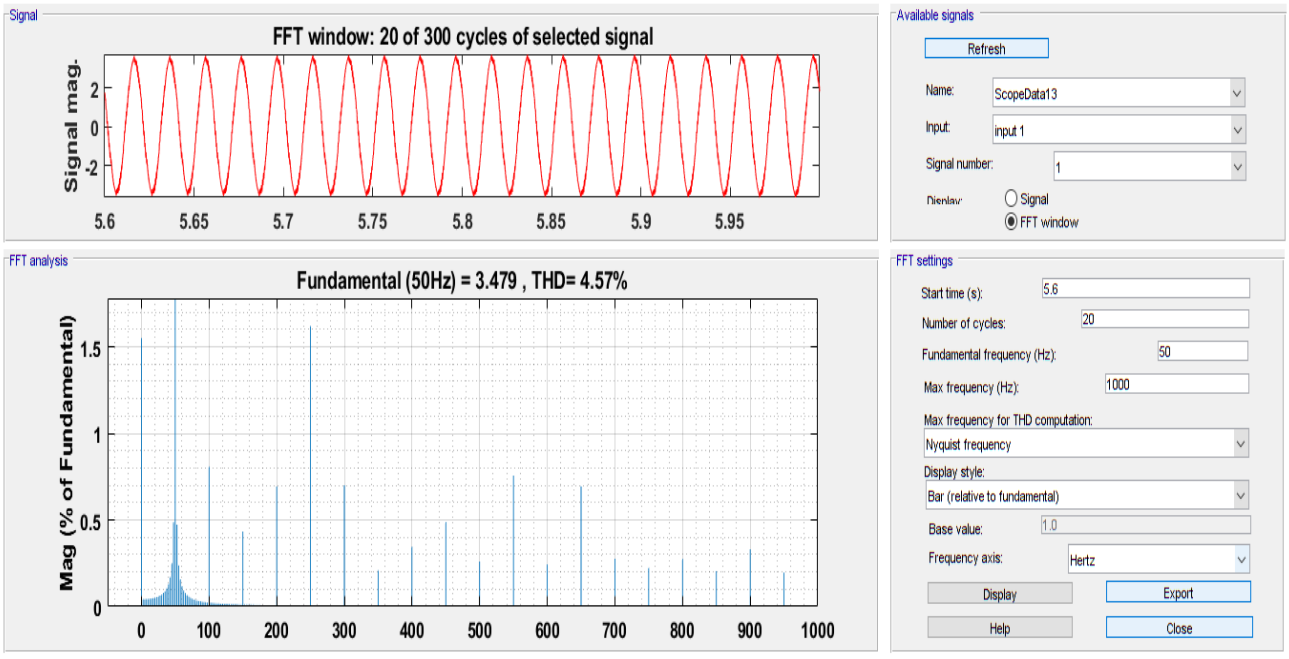

Fig.8.9 Stator Current THD of 1HP Motor fed with SS3P Inverter

The stator current THD at rated torque is 4.57% which is in harmonic distortion limits.

In order to verify the successful implementation of space vector technique the X-Y plot for q-d axis stator current is taken into account. The q-d axis currents are phase displaced by 90 degrees due to which there X-Y plot would be a circle, the successful implementation of SVPWM technique results in exactness of circle. The fig.8.10 shows the X-Y plot for q-d axis stator currents at rated load and it can be seen that the space vector technique is successfully implemented.

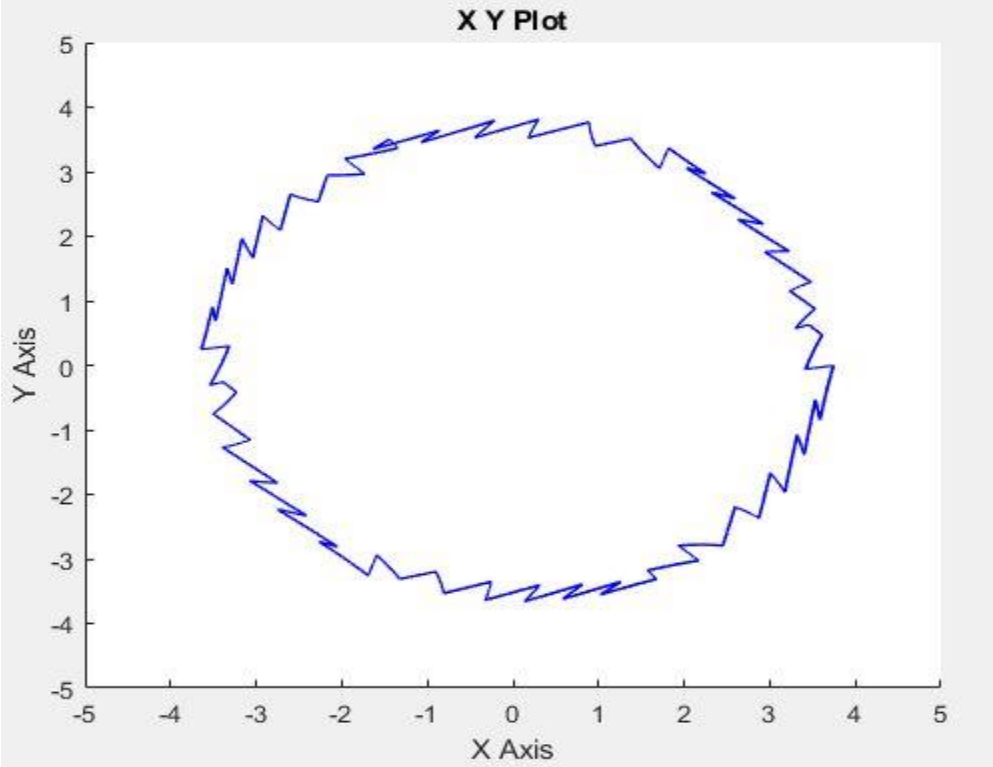

Fig.8.10 X-Y Plot for q-d Axis Stator Currents of 1HP Motor fed with SS3P Inverter

8.2.3 Performance analysis of 3HP, 220 V Delta Connected IM Drive

The effectiveness of SVPWM technique is tested on the basis of performance of given drive. The drive is directly fed from 6-Switch VSI based inverter and stator currents, electromagnetic torque and rotor mechanical speed are recorded. The rated torque of given IM Drive is 14.25N-m, motor is run from (0-15) N-m as mechanical input i.e from no load to full load. Table 8.4 shows the torque input to the motor at different intervals of time.

Table.8.4 Mechanical input to the motor for 3HP Motor fed with SS3P Inverter

Time(sec)	Load Torque (N-m)
(0-1)	0
(1-2)	3
(2-3)	6
(3-4)	9
(4-5)	12
(5-6)	15

8.2.3.1 Rotor Speed

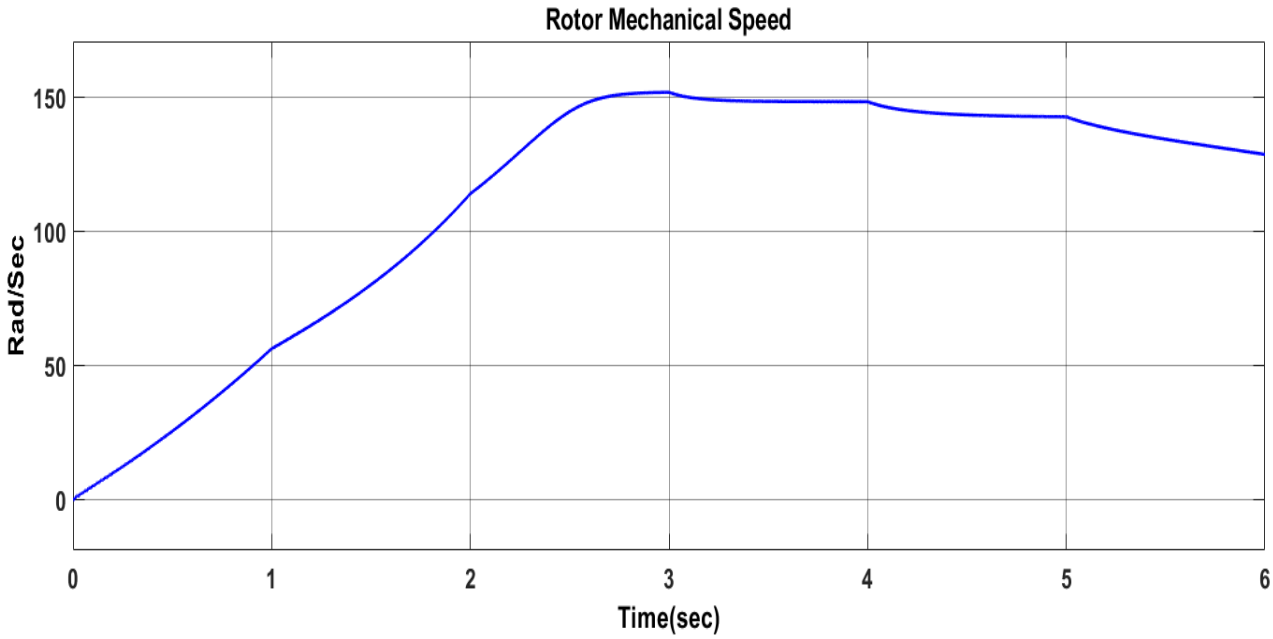

Fig.8.11 Rotor Mechanical Speed of 3HP Motor fed with SS3P Inverter

The behavior of rotor mechanical speed is shown in fig.8.11. The inertia of 3HP motor is high due to which rotor speed is taking more time to settle at a constant value. With increase in the load from no load to full load, the speed is decreasing and settling to a constant value. Table 8.5 summarizes the rotor speed at different loadings in different intervals of time.

Tbale.8.5 Rotor Mechanical Speed of 3HP Motor fed with SS3P Inverter

Time (sec)	Load Torque (N-m)	Rotor Speed (rad/sec)
(0-1)	0	-
(1-2)	3	-
(2-3)	6	152
(3-4)	9	148.5
(4-5)	12	143
(5-6)	15	125

The motor speed is increasing linearly from (0-2.6) seconds and settling to constant value of 152 rad/sec. when motor is run at 15N-m load it is observed that speed is continuously decreasing and settles to a value of 125 rad/sec after some time.

8.2.3.2 Electromagnetic Torque

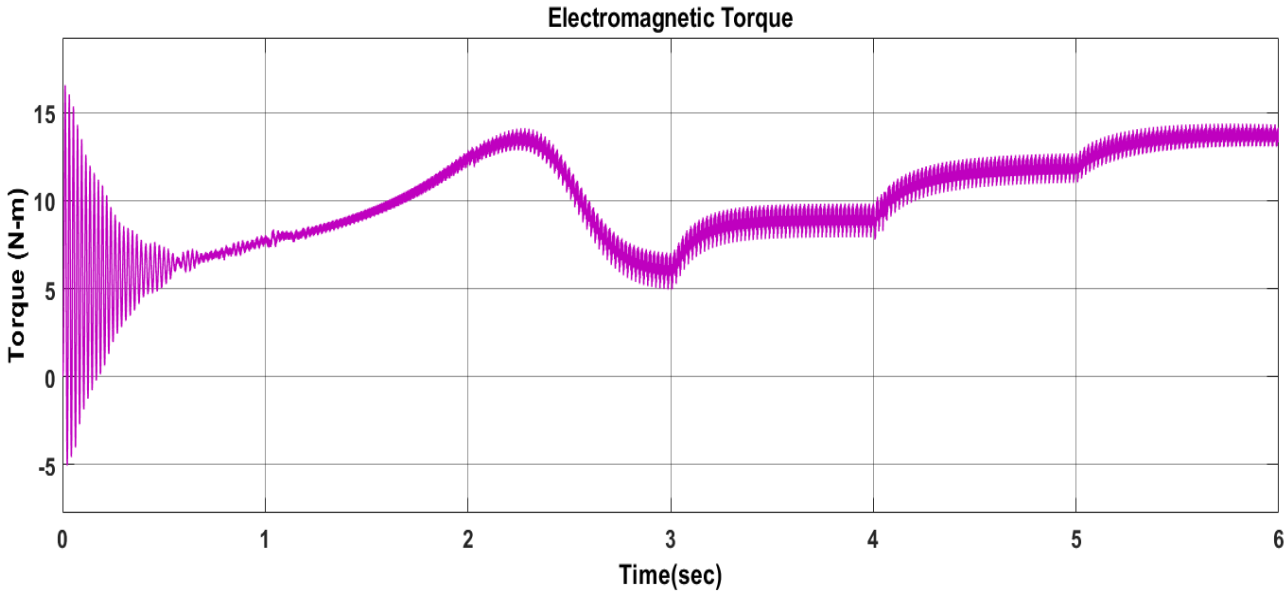

Fig.8.12 Electromagnetic Torque of 3HP Motor fed with SS3P Inverter

The behavior of electromagnetic torque for given IM Drive is shown in fig.8.12. The torque increases initially and then follows the values given at input to the motor as load. Electromagnetic torque is taking approximately 2.6 seconds to settle and after tracing the mechanical torque input of the motor.

8.2.3.3 Stator Current

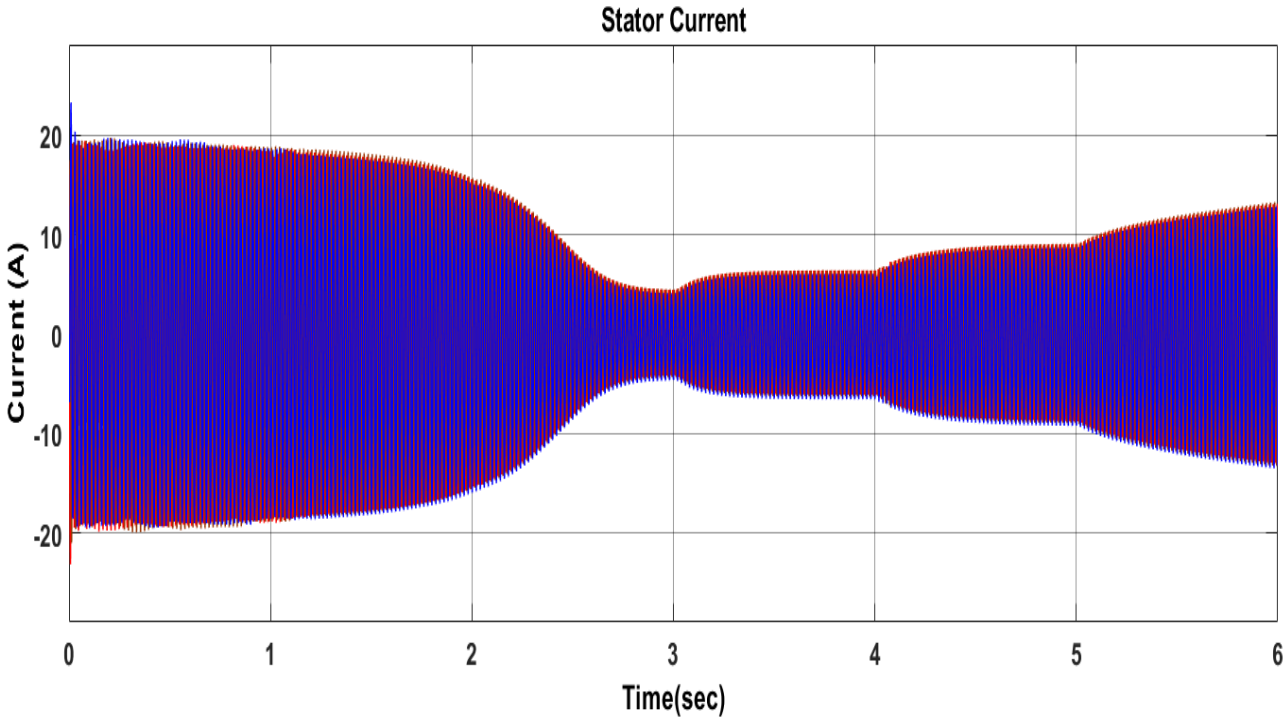

Fig.8.13 Stator Current of 3HP Motor fed with SS3P Inverter

The existence of starting currents for given drive is longer and exist approximately for 2.6 seconds as shown in fig.8.13. The value of current is increasing according to the load given at input to the motor. For a period of (5-6) seconds the torque input to the motor is 15N-m i.e rated and behavior of stator current for this period can be seen in fig.8.14, which shows the sinusoidal waveforms of three-phase stator current.

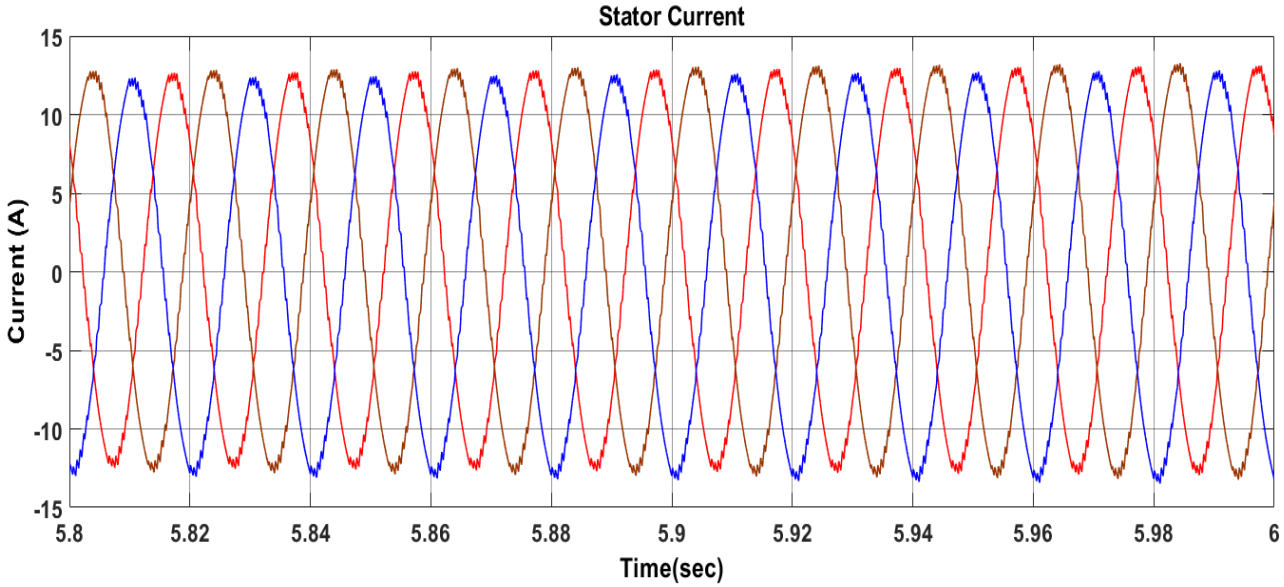

Fig.8.14 Three Phase Stator Current at 15N-m Load for 3HP Motor fed with SS3P Inverter

In order to test the harmonic distortion in stator current waveforms at rated load the THD is calculated using FFT analysis tool in Matlab and results are shown in fig.8.15.

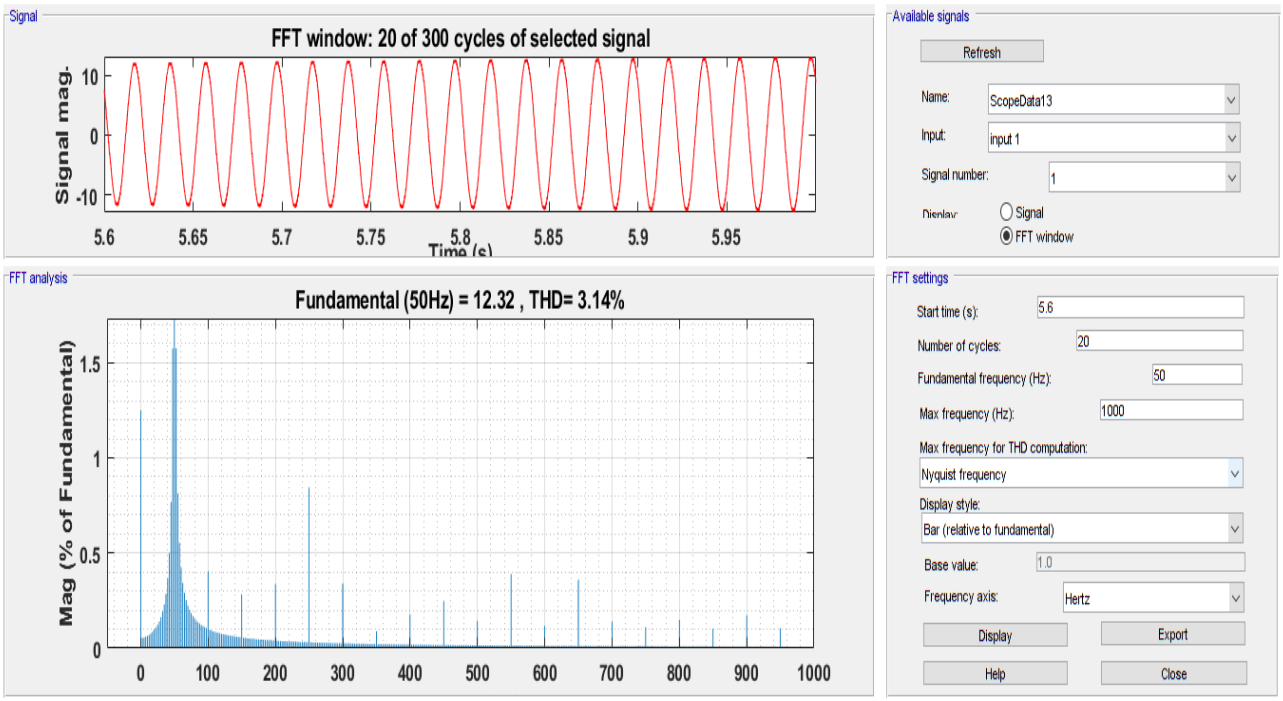

Fig.8.15 THD Calculation Using FFT analysis Tool for 3HP Motor fed with SS3P Inverter

Also the XY plot for q-d axis stator current is shown in fig.8.16. The trajectory of q-d axis stator current in XY plane is circle, which implies that flux polygon would also be a circle thus fig8.16 shows the successful implementation of space vector technique.

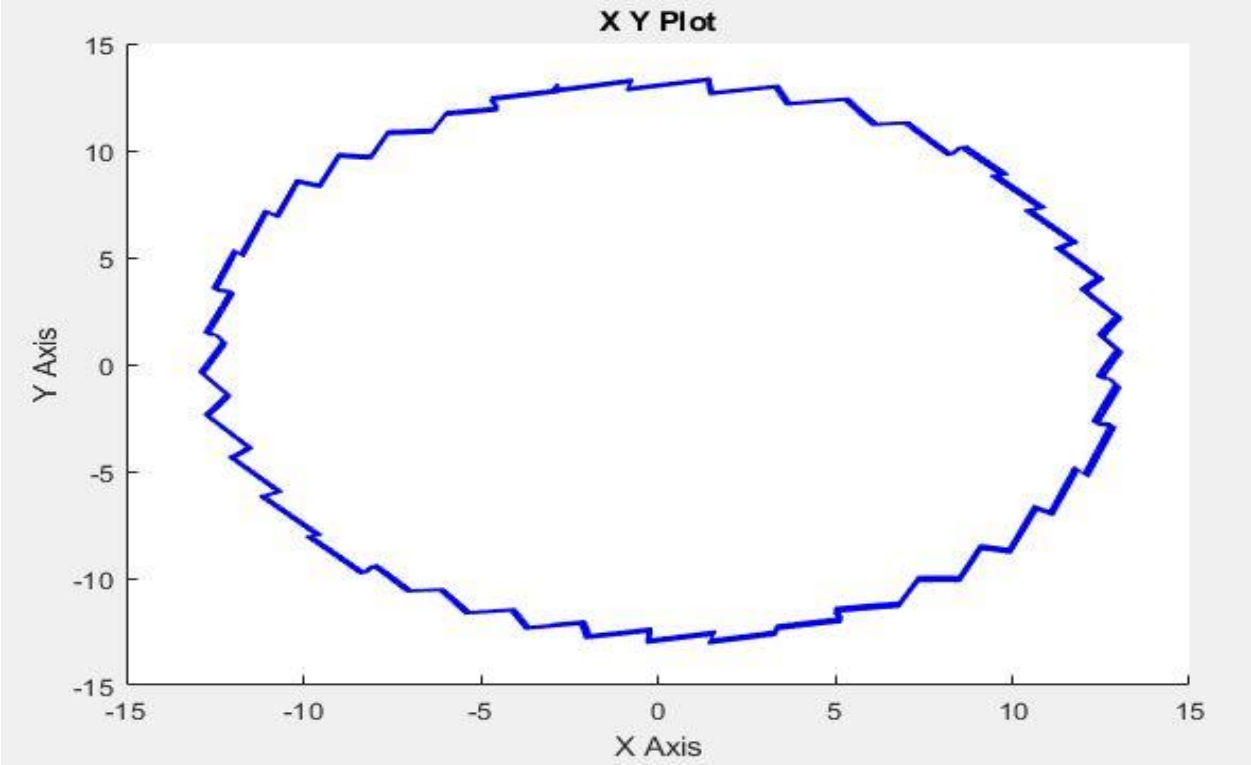

Fig.8.16 Trajectory of q-d axis stator currents in XY plane of 3HP Motor fed with SS3P Inverter

8.2.4 Performance analysis of 5.4 HP, 400 V Star Connected IM Drive

The six switch three phase inverter is connected with given IM Drive as load. The effectiveness of modulation technique is now tested over high rated IM Drive and results are noted. The torque input here is again from no load to full load as given in table 8.6 at different intervals.

Table.8.6 Mechanical torque input to 5.4HP Motor fed with SS3P Inverter

Time (sec)	Load Torque (N-m)
(0-1)	0
(1-2)	5
(2-3)	10
(3-4)	15
(4-5)	20
(5-6)	26

With these loadings at different intervals the effects in stator current, electromagnetic torque and rotor speed is studied as following.

8.2.4.1 Rotor Speed

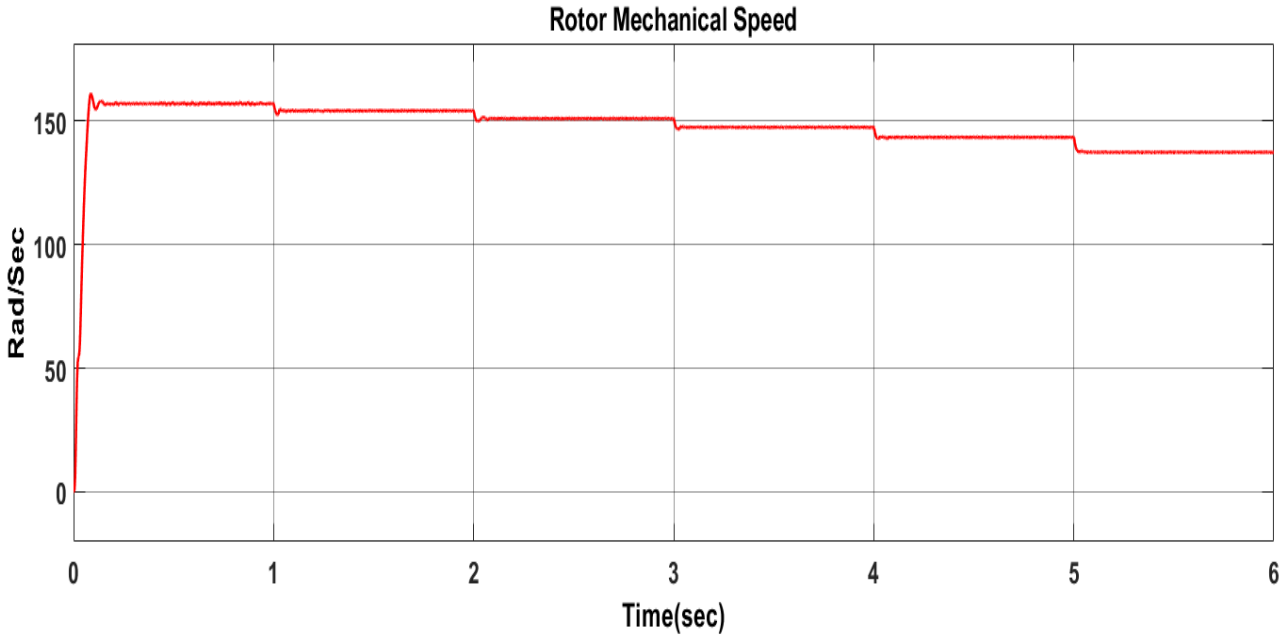

Fig.8.17 Motor Speed at different loadings of 5.4HP Motor fed with SS3P Inverter

Fig.8.17 shows the rotor speed at different time intervals with loading varied from no load to full load. It can be seen from figure that speed decreases and reaches to a constant value as load to the motor increases. Table 8.7 shows different speed of motor at different loading given at input to the motor.

Table .8.7 Rotor Mechanical Speed of 5.4HP Motor fed with SS3P Inverter

Time (sec)	Load Torque (N-m)	Rotor Speed (rad/sec)
(0-1)	0	157
(1-2)	5	154
(2-3)	10	151
(3-4)	15	147.5
(4-5)	20	143
(5-6)	26	137

8.2.4.2 Electromagnetic Torque

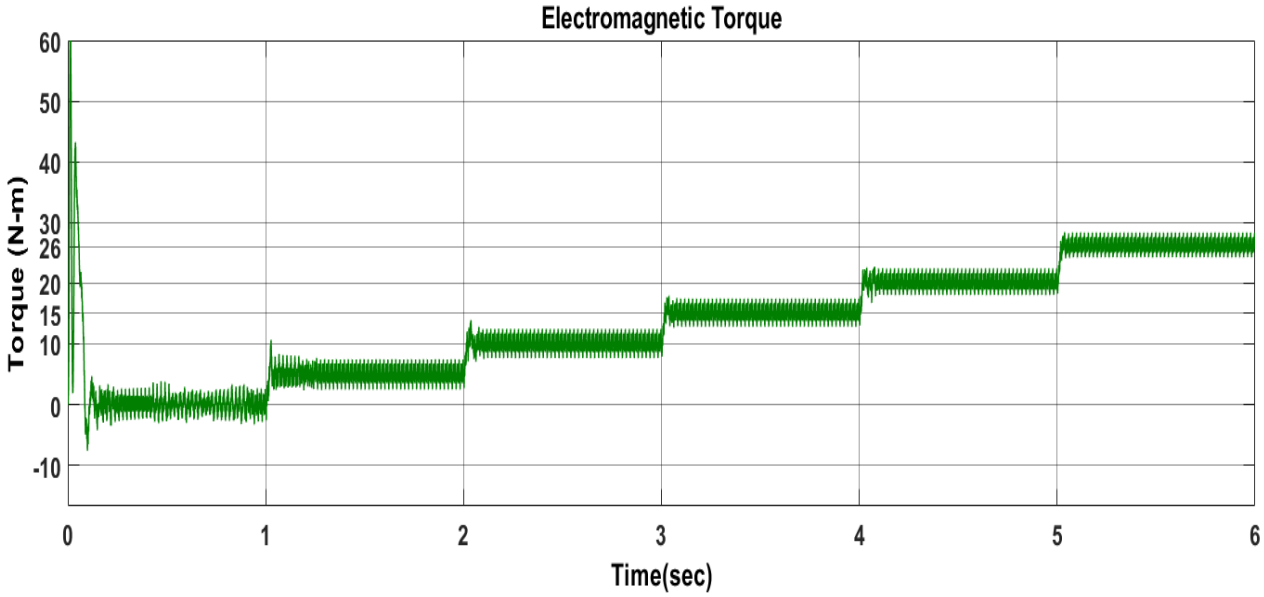

Fig.8.18 Electromagnetic torque of 5.4HP Motor fed with SS3P Inverter

The electromagnetic torque generated by given IM Drive is shown in fig.8.18. The load input given to the motor is summarized in table 8.6. It can be infer that electromagnetic torque generated is tracing load input given to the motor at each interval.

8.2.4.3 Stator Current

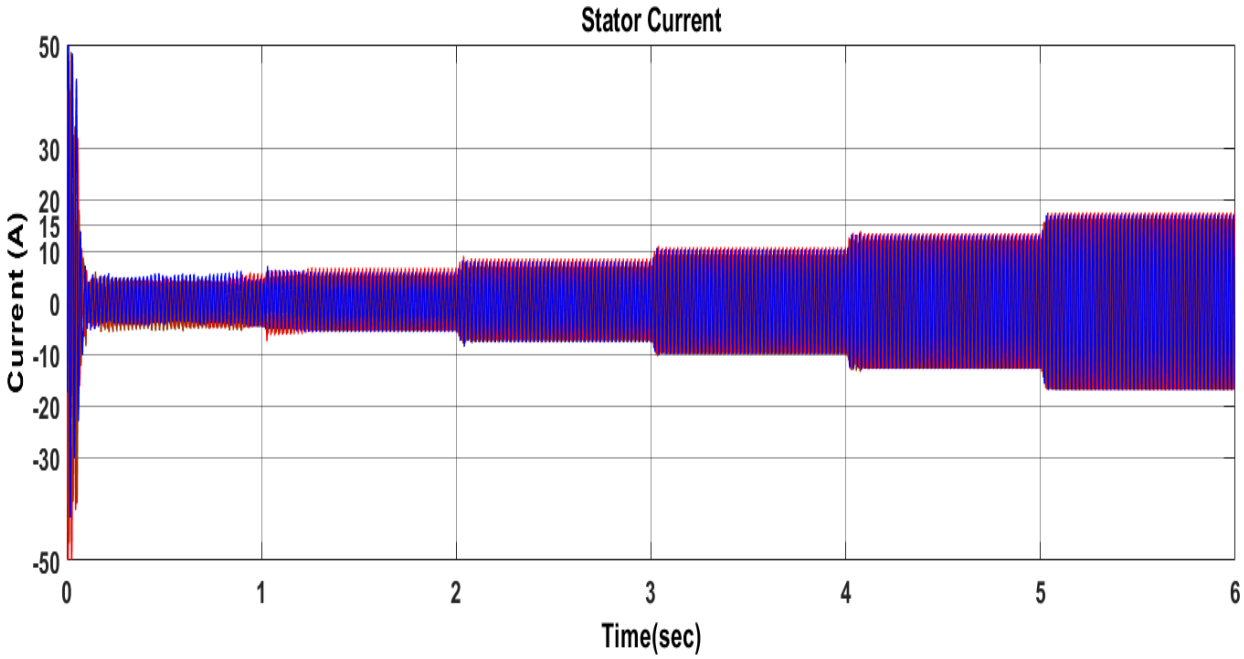

Fig.8.19 Stator Current of 5.4HP Motor fed with SS3P Inverter

Fig.8.19 shows the stator current or line current of the motor. As the load increases the stator current also increases to generate the flux. The behavior is observed from no load to full load with rated torque of the motor is 26N-m. The Calculated current at rated torque is 6A and figure shows 10A when this motor is run at rated load. The waveforms of three phase stator currents can be seen in fig.8.20 at rated load period.

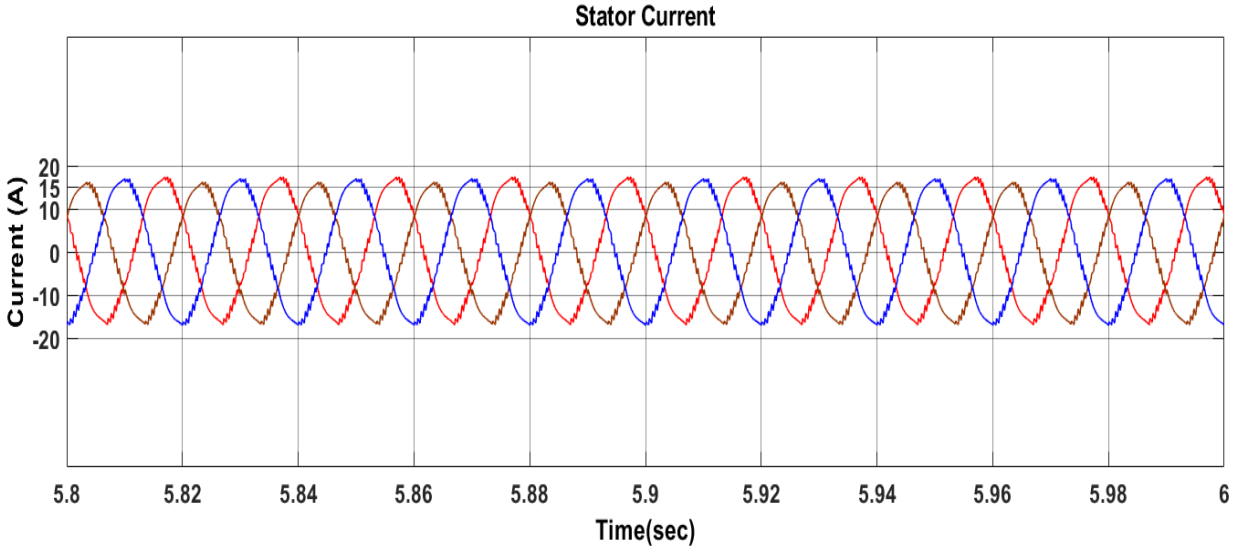

Fig.8.20 Stator Current waveforms of 5.4HP Motor fed with SS3P Inverter

The stator current THD is calculated using FFT tool analysis to calculate harmonics affecting the stator currents waveforms. The calculated THD can be shown in fig.8.21

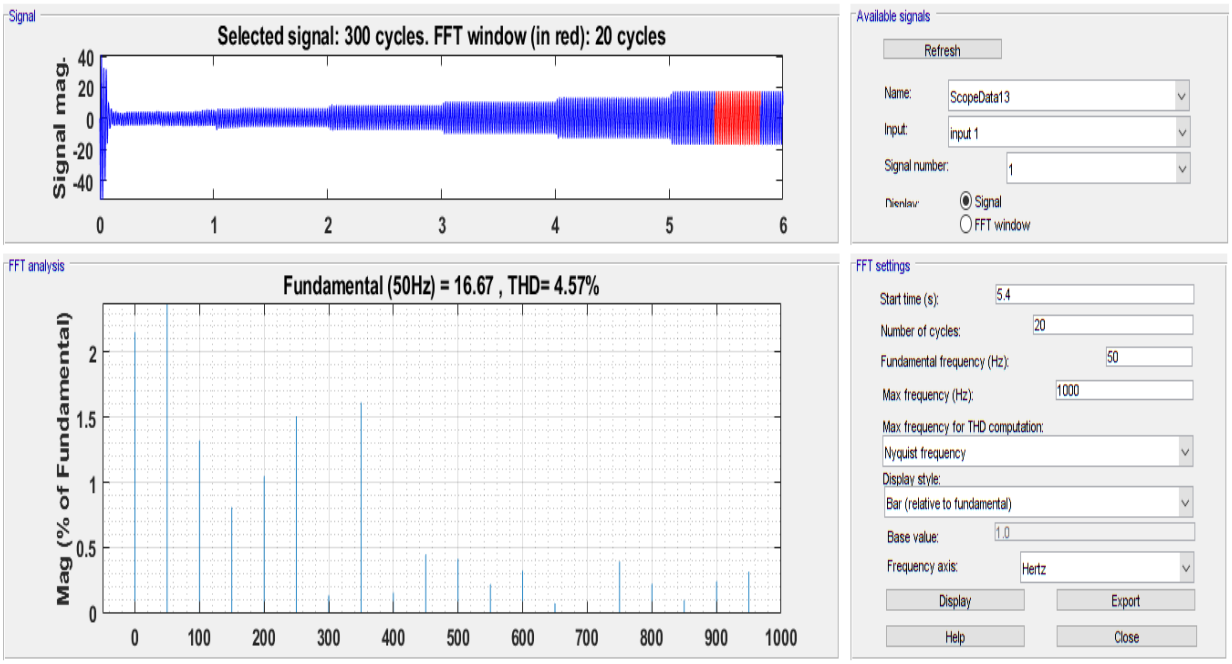

Fig.8.21 THD analysis of stator currents for 5.4HP Motor fed with SS3P Inverter

The calculated THD is 4.57% which can be tolerated and method can be used further.

8.3 Four Switch Three Phase VSI Fed IM Drive

This is proposed scheme for our induction motor drive. With this scheme induction motor will be fed through four-switch inverter, generating two phases from the two legs and third phase from the two dc link voltages. SVPWM technique is used to pulse the switches of two leg inverter to generate the three phase voltages as studied in chapter 3. The effectiveness of proposes scheme is studied using performance analysis of three IM Drives given in table 8.1

8.3.1 SVPWM Output

8.3.1.1 Switch Timings and Gate Pulses

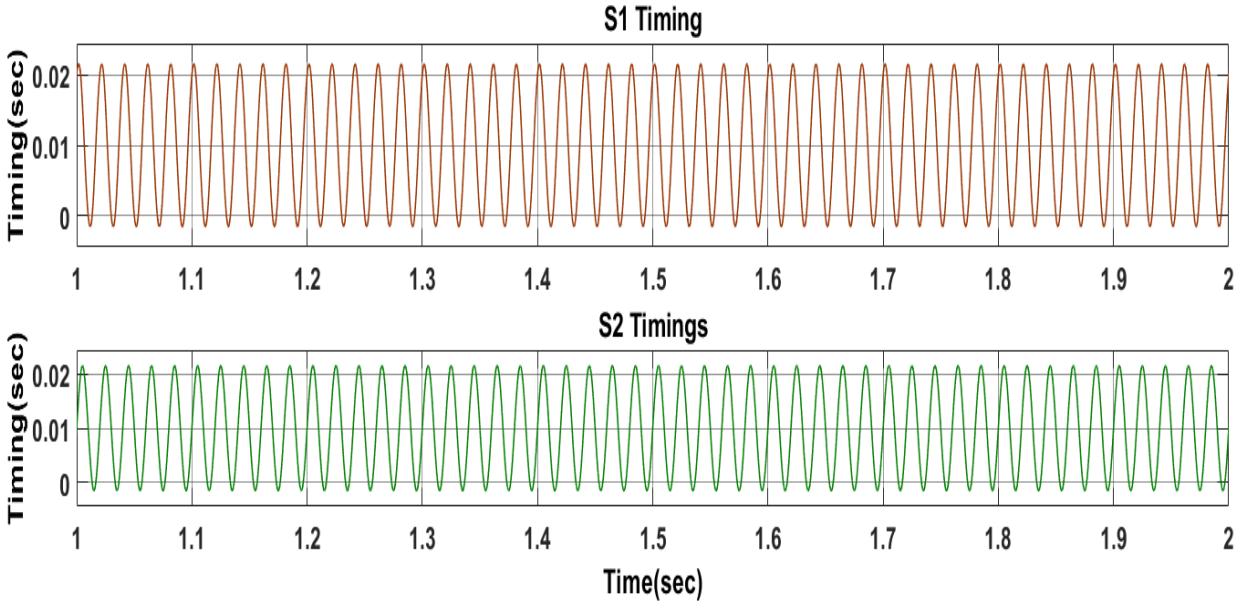

Fig.8.22 Timing pattern for Switches in FS3P Topology

Fig.8.22shows the timings for the switches S_1 and S_2 of the four switch inverter. When switches are operated according to the timings shown in fig.8.22 three phase output voltages will be generated. These timings are compared with the ramp signal to generate the pulses which regulates the switching of the two switches S_1 and S_2. The pulses to the two inverter switches are shown in fig.8.23.

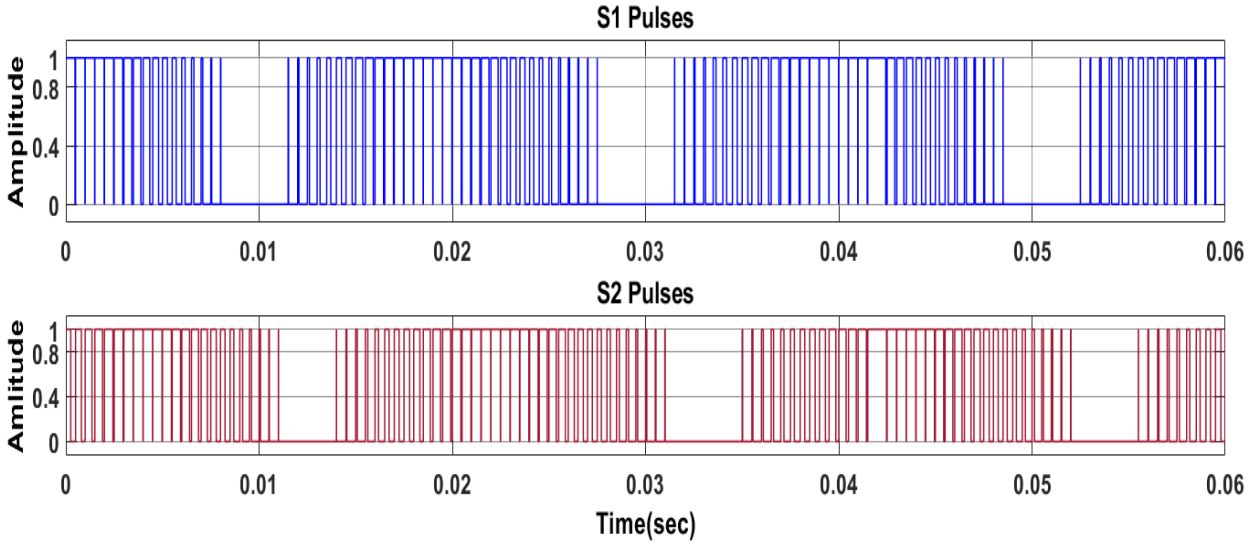

Fg.8.23 Gating Pulses of Inverter switches S_1 and S_2

8.3.2 Performance Analysis of 1HP, 380 V Star Connected IM Drive

The given IM Drive is fed with FS3P VSI based inverter which is proposed scheme and effectiveness of the proposed topology to fed three-phase IM Drive is studied with behavior of stator current, electromagnetic torque and rotor mechanical speed. The THD of stator current and XY Plot for q-d axis stator current is also shown to comment on the effectiveness of proposed scheme for given drive. The motor is run from no load to full load as given in table 8.2.

8.3.2.1 Rotor Speed

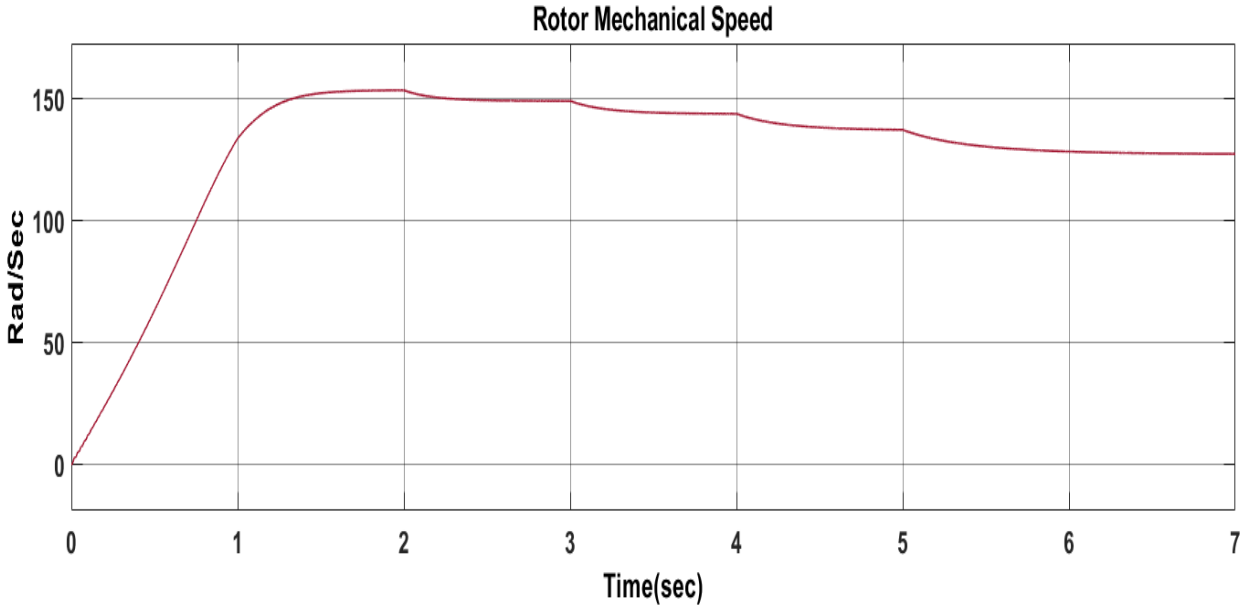

Fig.8.24 Rotor Speed of 1HP Motor fed with FS3P Inverter

Fig.8.24 shows the behavior of rotor speed at different intervals of time when run from no-load to full load. It can be seen from figure that rotor speed is decreasing when load torque to the motor increases and settles to a constant value, the motor speed at different loads is summarized in table 8.8.

Table.8.8 Rotor Mechanical Speed of 1HP Motor fed with FS3P Inverter

Time (sec)	Input Torque (N-m)	Rotor Speed (rad/sec)
(0-1)	0	-
(1-2)	5	153
(2-3)	10	148.5
(3-4)	15	143.5
(4-5)	20	137
(5-7)	26	127

8.3.2.2 Electromagnetic Torque

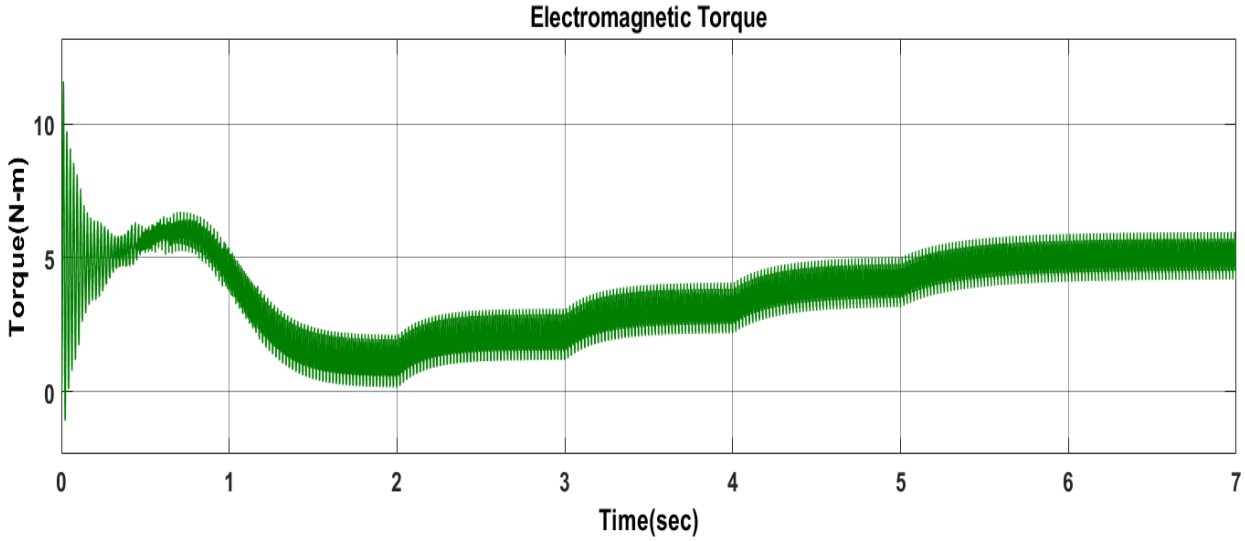

Fig.8.25 Generated Electromagnetic Torque of 1HP Motor fed with FS3P Inverter

Fig.8.25 shows the electromagnetic torque generated by the motor from proposed topology. The generated torque is tracing the load torque given at the input to the motor at each intervals of time from no load to full load.

8.3.2.3 Stator Current

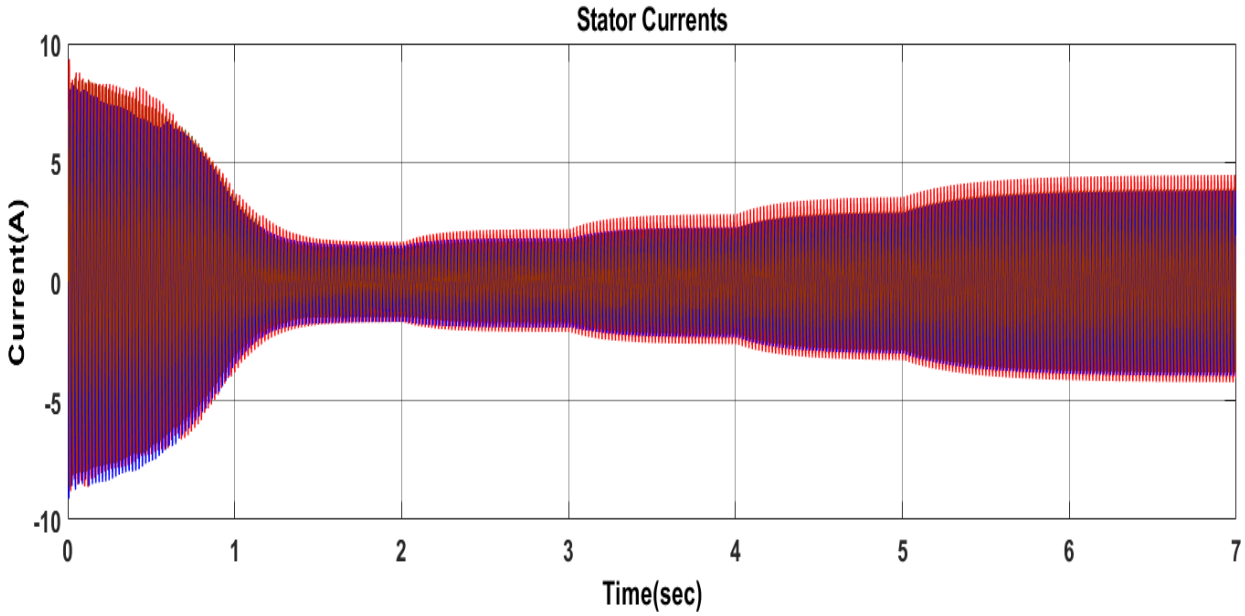

Fig.8.26 Stator Current of 1HP Motor fed with FS3P Inverter

The behavior of stator current from the proposed topology for given IM Drive is shown in fig.8.26. The given motor is run from no load to full load and stator currents are increasing at each interval in accordance with load input. The peak current at rated load 3.5A which implies rms current at the rated load in 2.47A from given topology and rated current is 1.9A. the effectiveness of proposed topology is also studied in terms of stator current waveforms at rated load as shown in fig.8.27

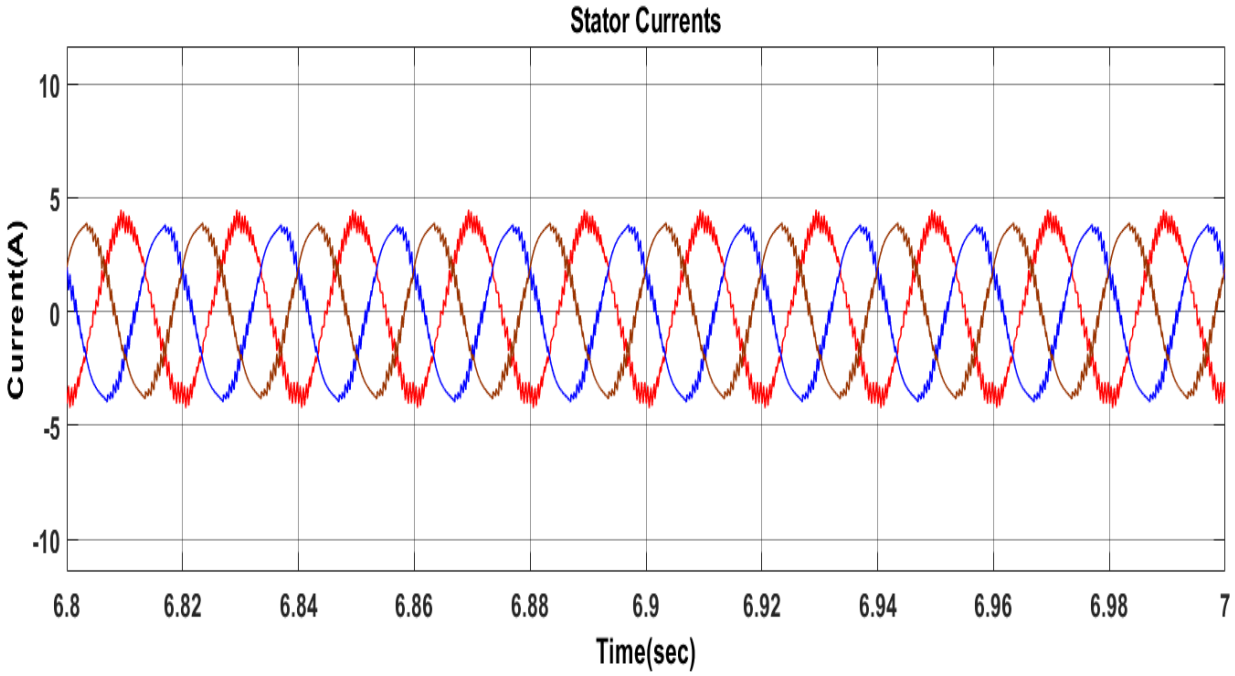

Fig.8.27 Stator current waveforms at rated load for 1HP Motor fed with FS3P Inverter

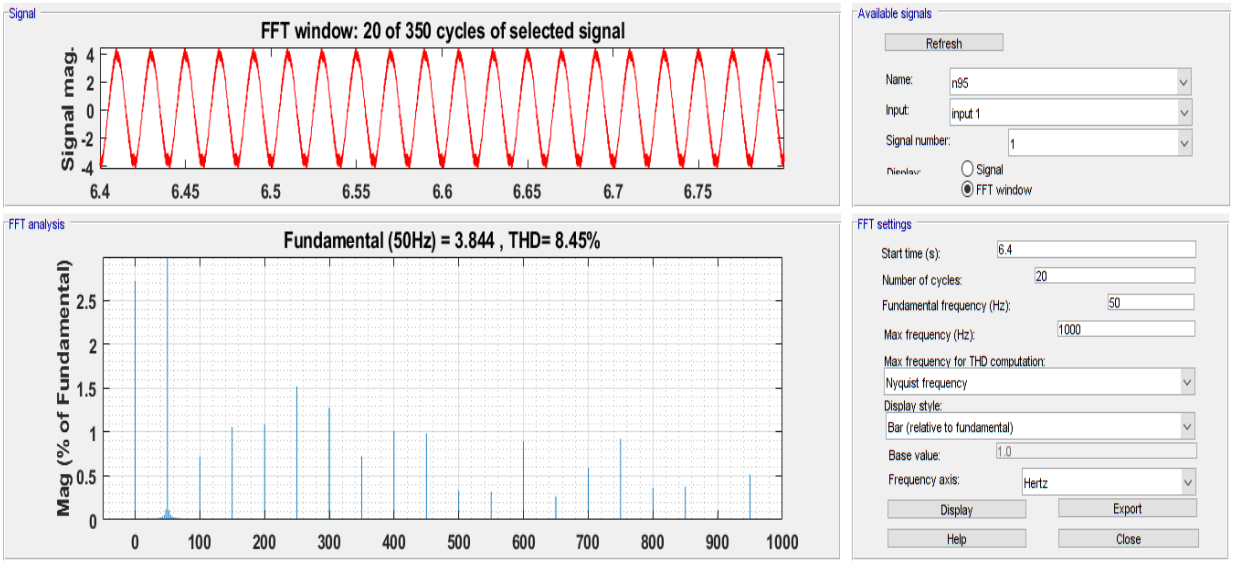

Fig.8.28 FFT analysis of stator current for 1HP Motor fed with FS3P Inverter

THD is being calculated using the FFT tool analysis to get the calculation of amount of harmonics that are affecting the stator current waveforms. The calculated THD is 8.45% from the given topology as shown in fig.8.28. Also q-d axis stator current is also seen in XY Plot to get the effectiveness of SVPWM technique in proposed topology. The XY plot is shown in fig.8.29 and the locus or trajectory is coming out to be circle. However, THD is distorting the locus to some extent.

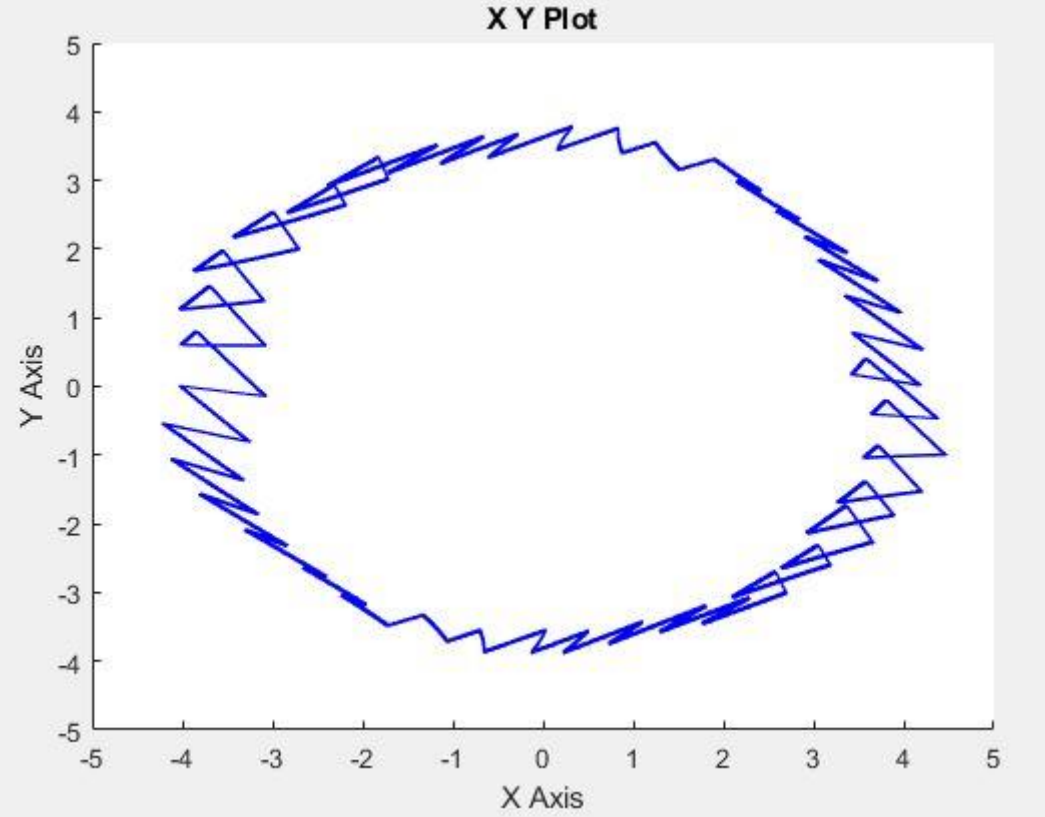

Fig.8.29 XY Plot for q-d axes stator Current of 1HP Motor fed with FS3P Inverter

8.3.3 Performance Analysis of 3HP, 220 V Delta Connected IM Drive

Induction motor drive of high inertia and rating is now tested with proposed topology. The loads are varied from no-load to 13.5N-m load (Full load) in different intervals of time as summarized in table 8.9.

Table.8.9 Load torque to 3HP Motor fed with FS3P Inverter

Time (sec)	Load Torque (N-m)
(0-1)	0
(1-2)	3
(2-3)	6
(3-4)	8
(4-5)	10
(5-7)	13.5

Performance of given drive is being noted in terms of taking behavior of stator current, electromagnetic torque and motor speed into account.

8.3.3.1 Rotor Speed

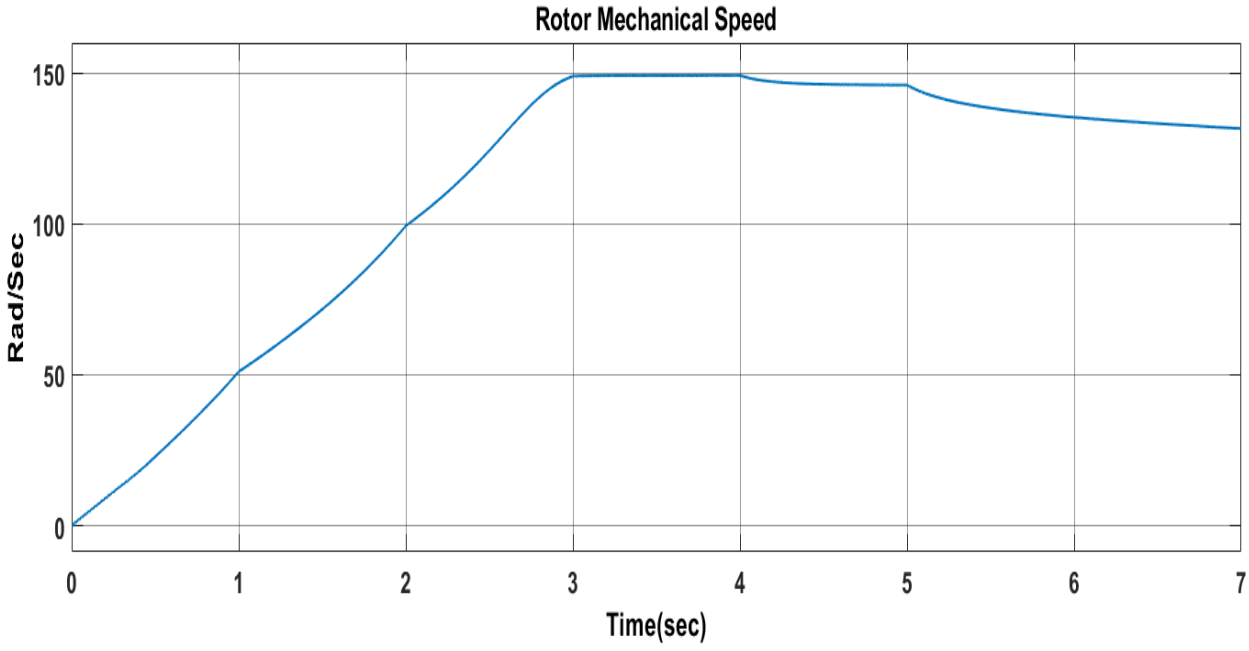

Fig.8.30 Rotor Mechanical Speed for 3HP Motor fed with FS3P Inverter

Fig.8.28 shows the rotor speed with FS3P topology. The behavior here is same as studied in previous sections i.e speed is decreasing and settles to a constant value with increase in load at each interval. The motor speed is increasing linearly for 3 seconds which is long and then settles to a constant value. The motor speed change behavior is conventional after 3 seconds as observed earlier i.e speed dip is present with increase in the load. Table 8.10 shows the rotor speed at different intervals from no load to full load.

Table 8.10 Rotor speed of 3HP Motor fed with FS3P Inverter

Time(sec)	Load Torque (N-m)	Rotor Speed (rad/sec)
(0-1)	0	-
(1-2)	3	-
(2-3)	6	-
(3-4)	8	149
(4-5)	10	146
(5-6)	13.5	130

8.3.3.2 Electromagnetic Torque

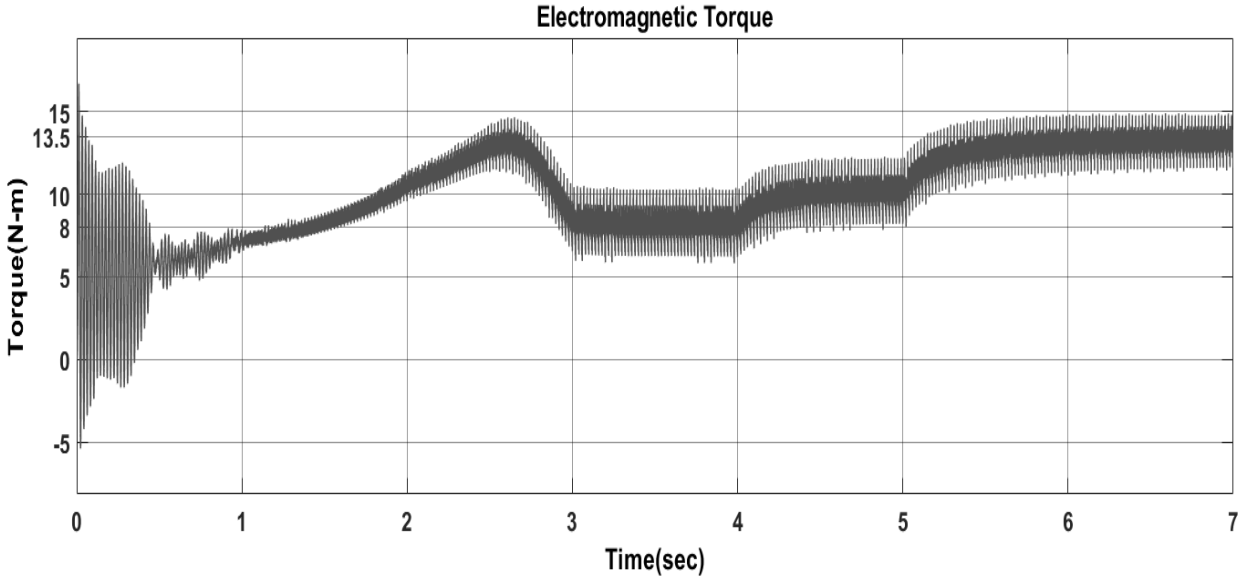

Fig.8.31 Generated Electromagnetic torque of 3HP Motor fed with FS3P Inverter

Generated electromagnetic torque for given IM Drive can be seen from fig.8.29. The load inputs to the motor at different intervals are given in table 8.9. From 3seconds onwards the electromagnetic torque is tracing the load input to the motor in each interval however, some deviations about mean can be observed.

8.3.3.3 Stator Current

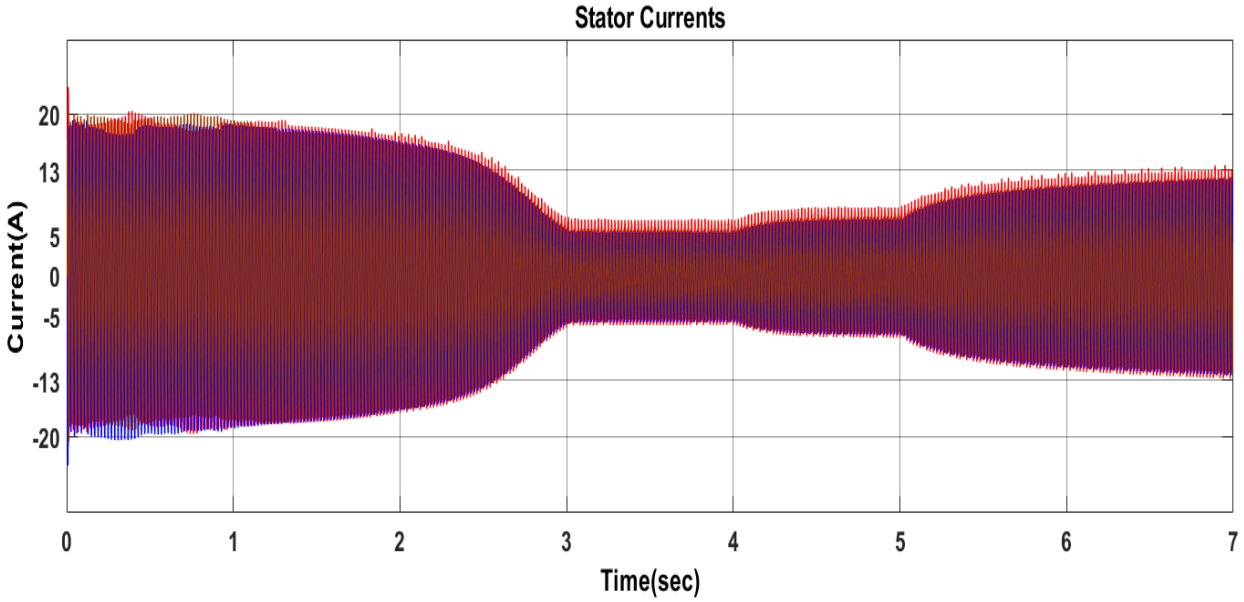

Fig.8.32 Three Phase Stator Current of 3HP Motor fed with FS3P Inverter

The behavior of stator current for FS3P VSI fed IM Drive can be seen from fig.8.30. The stator current is increasing as load is increasing, as it can be seen from figure for each interval. Motor inertia affecting the starting currents and they exist for longer time for the given motor specifications. The rated torque of given motor is 14N-m and maximum load applied here is 13.5 N-m which for interval (5-7) seconds. Fig.8.31 shows the stator current waveforms at maximum load given to the motor. The calculation is also being done at rated load using FFT analysis tool and results are shown in fig.8.32.

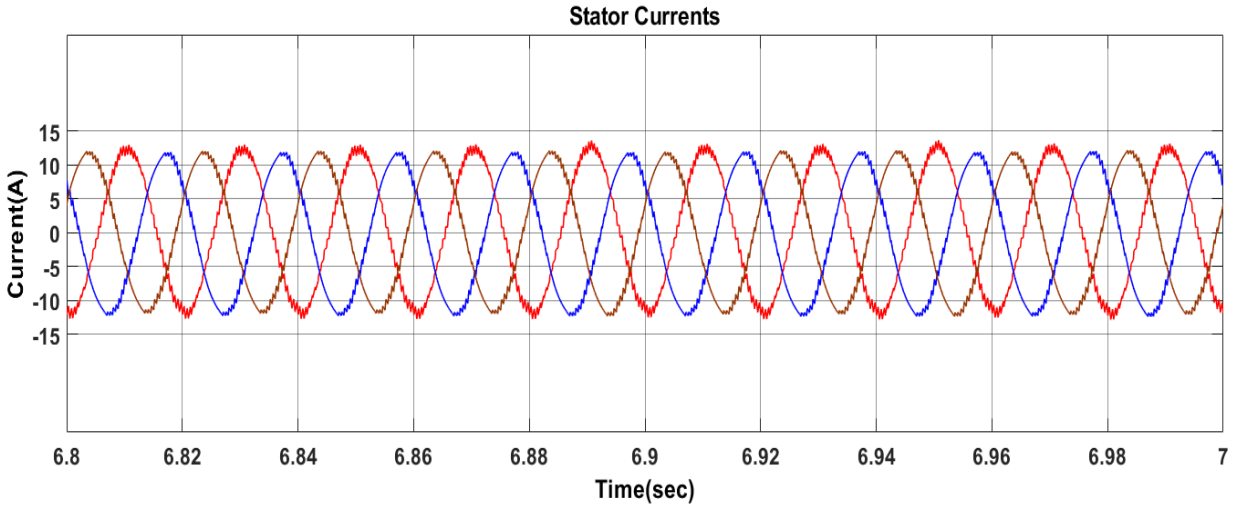

Fig.8.33 Stator Current Waveforms at 13.5 N-m load for 3HP Motor fed with FS3P Inverter

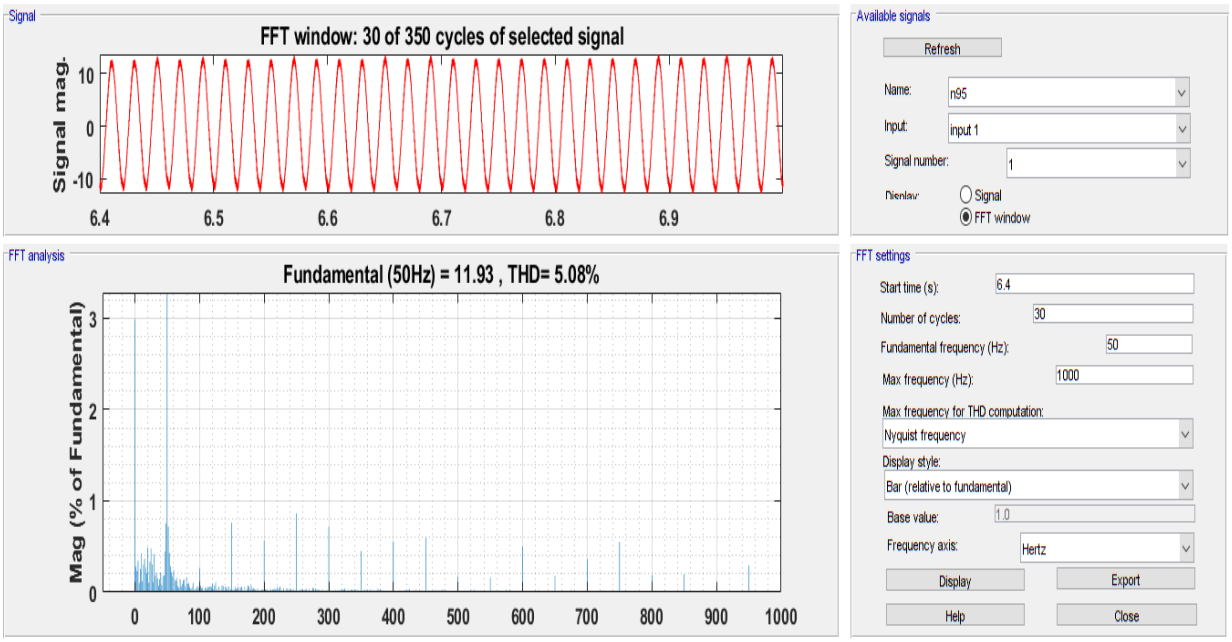

Fig.8.34 FFT analysis tool calculation of 3HP Motor fed with FS3P Inverter

The calculated THD for stator current is 5.08% at rated load which is acceptable for the proposed system consideration, also XY plot for q-d axes stator current is also shown in fig.8.33 which shows the successful implementation of SVPWM technique in proposed method and behavior of q-d fluxes of the motor can also be inferred from it as trajectory of circle shows that q-d flux are 90 degree displaced which is requirement for successful working of induction motor drive.

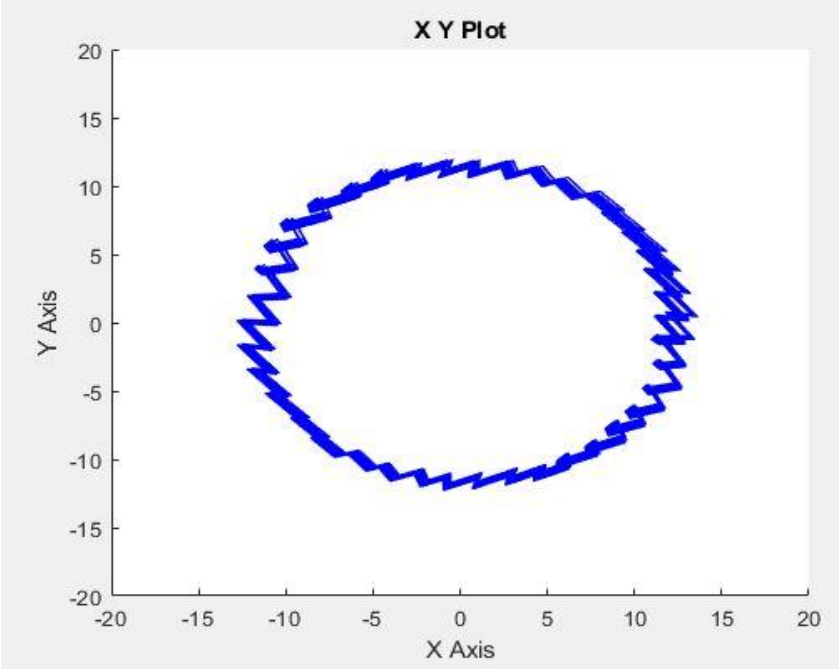

Fig.8.35 q-d axes stator current in XY plane for 3HP Motor fed with FS3P Inverter

8.3.4 Performance Analysis of 5.4HP, 400 V Star Connected IM Drive

Motor of further high rating is taken into account to consider the effectiveness of proposed scheme which feds IM Drive. The behavior of stator current, electromagnetic torque and rotor speed is studied when drive is run from no load to full load torque of 27N-m. Table 8.11 shows the load torque at each interval that is input to the motor.

Table 8.11 Loads given to 5.4HP Motor fed with FS3P Inverter

Time (sec)	Load Torque (N-m)
(0-1)	0
(1-2)	5
(2-3)	10
(3-4)	15
(4-5)	20
(5-6)	27

8.3.4.1 Rotor Speed

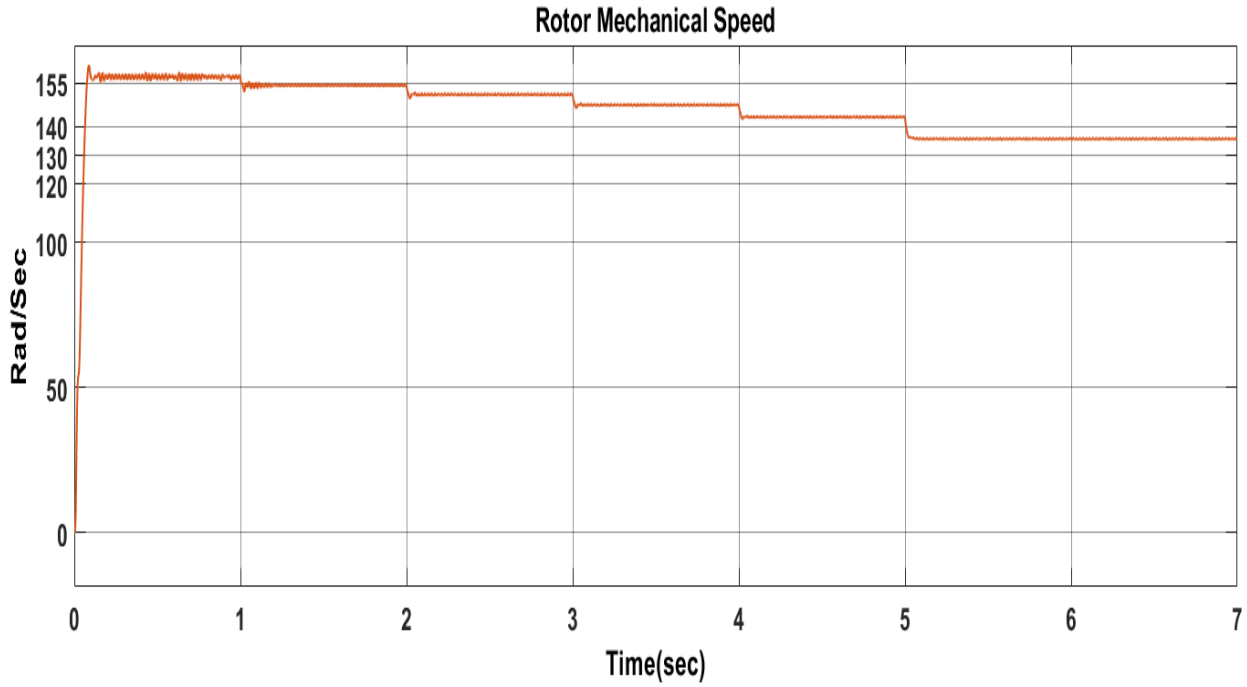

Fig.8.36 Rotor mechanical Speed of 5.4HP Motor fed with FS3P Inverter

The variation in the rotor speed can be seen from the fig.8.34. Variation as dip is observed when load increases, the speed settles to a constant value in each intervals which is summarized in table 8.12

Table 8.12 Rotor Speed for 5.4HP Motor fed with FS3P Inverter at different loads

Time (sec)	Load Torque (N-m)	Rotor Speed (rad/sec)
(0-1)	0	157
(1-2)	5	154
(2-3)	10	151
(3-4)	15	147
(4-5)	20	143
(5-6)	27	135.5

8.3.4.2 Electromagnetic Torque

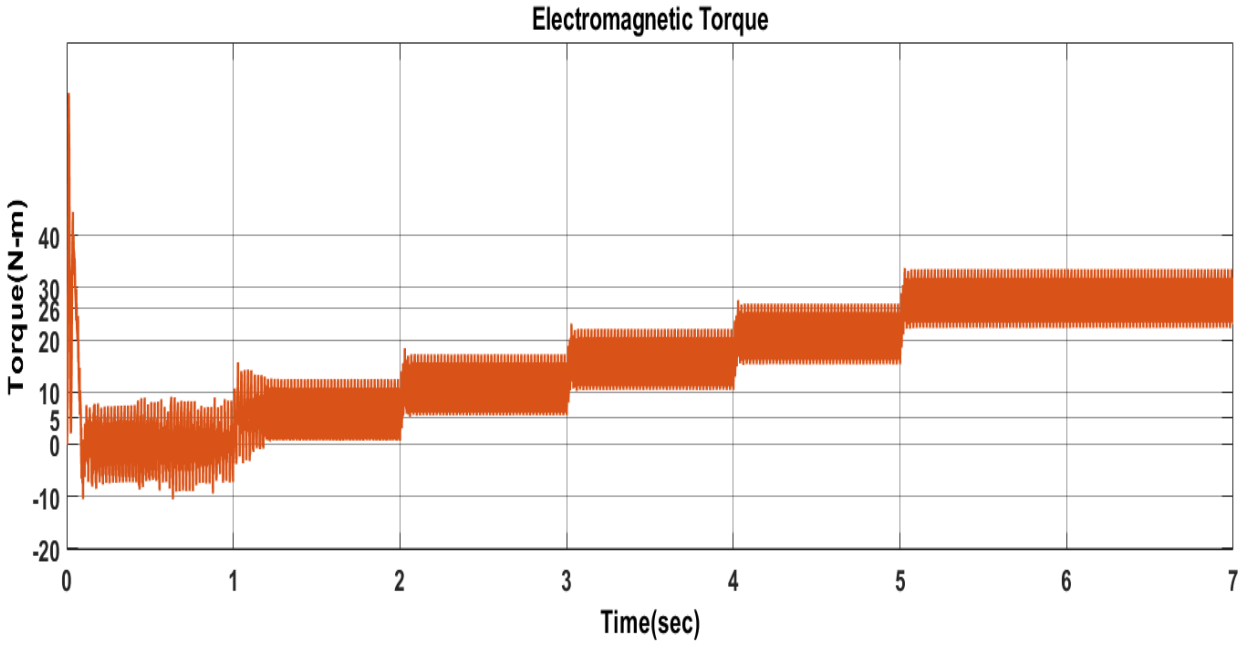

Fig.8.37 Generated Electromagnetic Torque of 5.4HP Motor fed with FS3P Inverter

Fig.8.35 shows the generated electromagnetic torque for 5.4HP rated motor. The spikes of high amplitude in electromagnetic can be observed during starting and then settles to a constant values governed by the load input to the motor. However, values are not constant and deviating about mean to about as $T_e = (T_L$ +/- 2N-m).

8.3.4.3 Stator Current

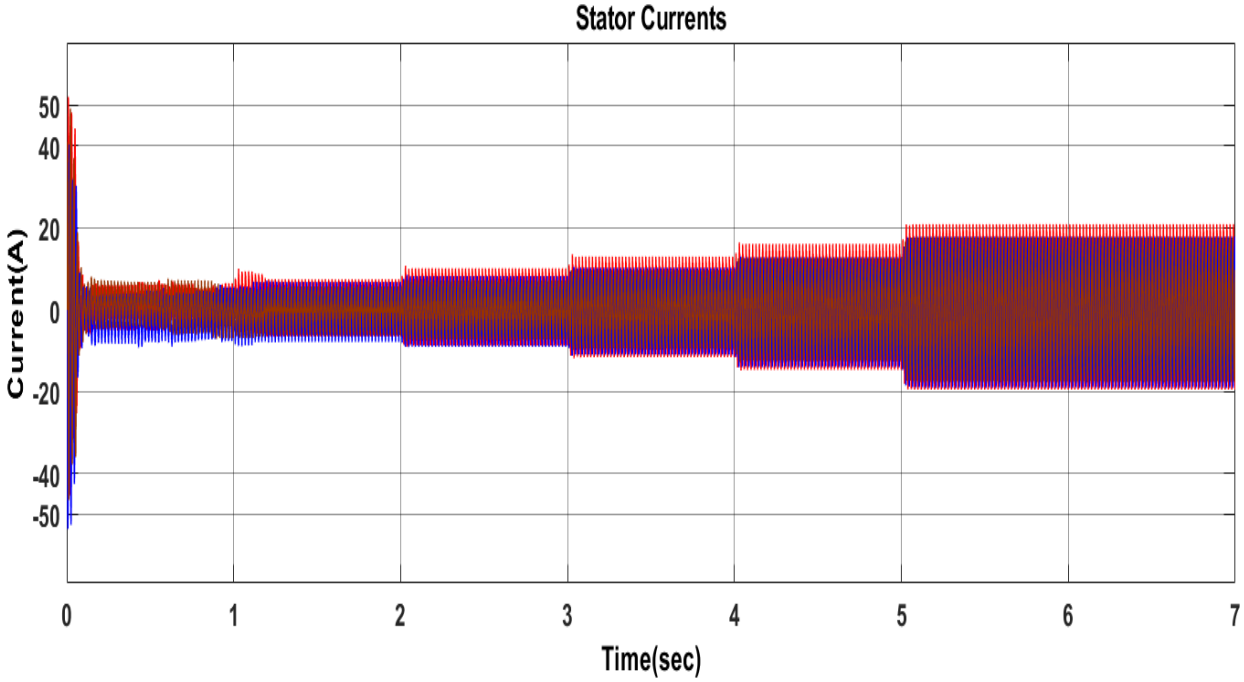

Fig.8.38 Three Phase Stator Current of 5.4HP Motor fed with FS3P Inverter

The stator current behavior can be seen in fig.8.36 which increases in each interval as load input increases. The waveform for three phase stator current can be seen in fig.8.37 for rated load.

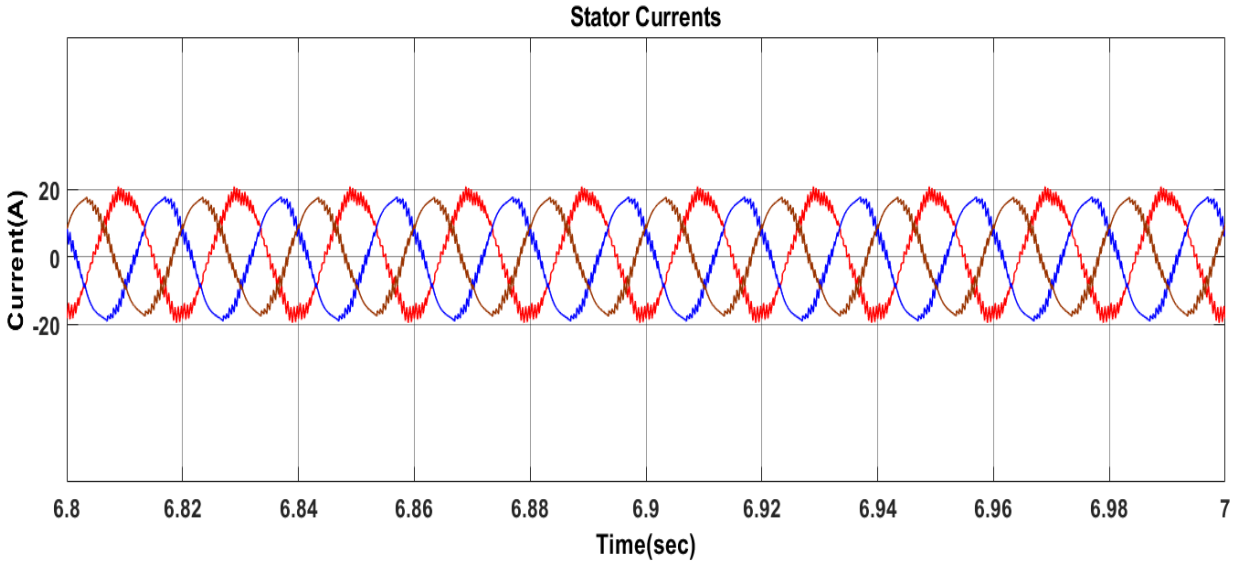

Fig.8.39 Stator Current Waveforms at 27N-m Load for 5.4HP Motor fed with FS3P Inverter

FFT tool The THD is being calculated to study the affect of harmonics in stator current waveforms using analysis and result can be shown in fig.8.38.

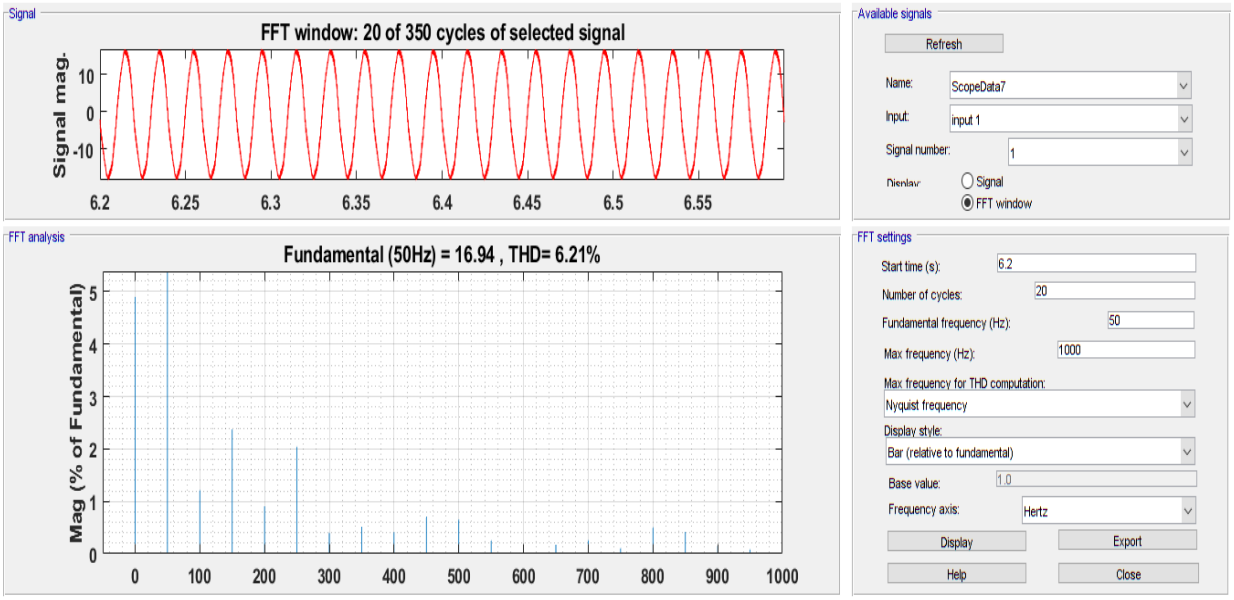

Fig.8.40 THD calculation at rated load of 5.4HP Motor fed with FS3P Inverter

The trajectory for q-d axes stator current in using XY plotter is also studied and from fig.8.39 it can be seen that q-d axes current trajectory is circle which shows the successful implementation of SVPWM technique and 90 degree displacement of q-d reference framed stator fluxes.

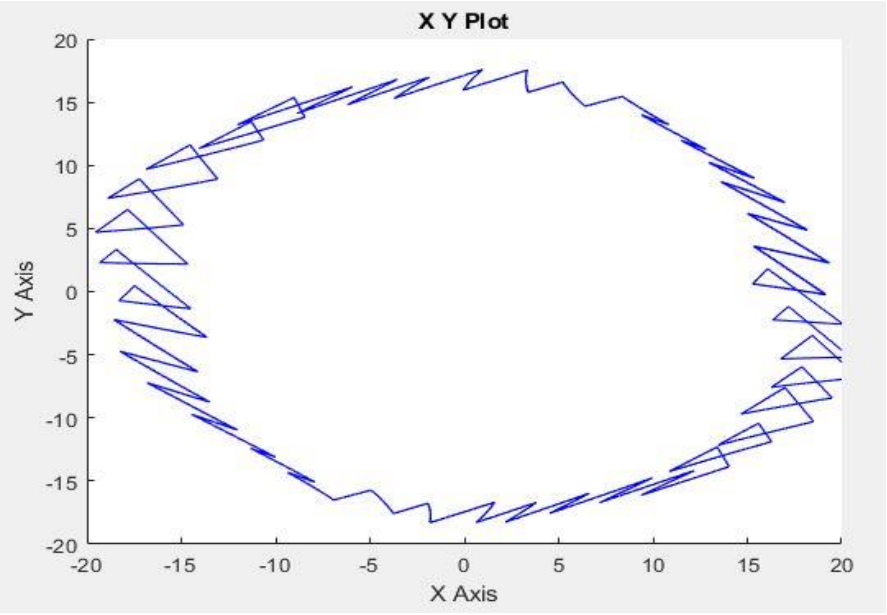

Fig.8.41 XY Plot for q-d axes stator current of 5.4HP Motor fed with FS3P Inverter

8.4 Comparative analysis between Six Switch Three Phase and Four Switch Three Phase Inverter Fed IM Drive

Four-switch three-phase inverter topology is cost effective topology to fed IM drives due to reduction of switches along with driver circuits. Also FS3P increases the reliability of three phase system since continuous run motor can be achieved if six-switch three-phase inverter find a fault and system is shifted to FS3P system. However, some modifications must be there and more importantly is to look for motor performance in FS3P topology i.e performance should not be compromised to a high extent. Thus analysis is being done between the conventional and proposed topology by taking some parameters into account and recording the deviation from conventional to proposed system.

8.4.1 With 1HP, 380 V Star Connected IM Drive

Table 8.13 Comparison between two topologies with drive 1

Parameters	Six Switch Three Phase Topology	FS3P Inverter Topology
Stator Current THD	4.57%	8.45%
Motor Speed at Rated Load	130 rad/sec	128 rad/sec
Existence time for high starting currents	1 sec	1.2 sec
Current at Maximum input Load	2.61A	2.82A

8.4.2 With 3HP, 220 V Delta Connected IM Drive

Table 8.14 Comparison between two topologies with drive 2

Parameters	Six Switch Three Phase Topology	FS3P Inverter Topology
Stator Current THD	3.14%	5.08%
Motor Speed at Rated Load	125rad/sec	130rad/sec
Existence time for high starting currents	2.5 sec	2.8 sec
Current at Maximum input Load	8.1A	8.2A

8.4.3 With 5.4HP, 400 V Star Connected IM Drive

Table 8.15 Comparison between two topologies with drive 3

Parameters	Six Switch Three Phase Topology	FS3P Inverter Topology
Stator Current THD	4.57%	6.21%
Motor Speed at Rated Load	137rad/sec	135.5rad/sec
Existence time for high starting currents	0.1 sec	0.1 sec
Current at Maximum input Load	10.1A	10.2A

Table 8.13, 8.14 and 8.15 shows the comparison between two topologies that are used to fed IM Drives. The proposed FS3P inverter is compared with six switch three phase inverter by taking some important parameters into account that need to take care of, for example current THD,

rotor speed etc. The comparative analysis is done for three IM Drives to comment on the effectiveness of proposed topology for IM Drives.

The comparative analysis shows that current THD is higher in case of FS3P topology but the difference is not that higher which makes it non-permissible, here $THD_{SS3P} = THD_{FS3P} + 3\%$ for low rated drives and THD difference between the two methods is decreasing as motor rating is going higher, For example difference between THD in two topologies is only 1.54% for 5.4HP motor.

It can be deduce from three tables that shows data of motor performance parameters for two topologies that rotor speed is approximately same for both the topologies and difference is not higher, both provides approximately same speed at their maximum rated load.

The time for existence of high currents during starting is also same approximately but it can be infer that existence time of high starting currents increases with motor inertia. However, this effect is for both the topologies and also the currents at maximum loading are also recorded which shows both the topologies give more or less same value of current at rated load of motor.

These results are taken with modeled IM Drive but saturation effect and friction factor is not taken into account for tested IM Drives. However the data recorded from the performance of IM Drives with two topologies does not shows a high deviation thus making the proposed FS3P system a permissible system from the data that is considered here.

8.5 FS3P Topology with DC-DC Boost Conversion

Space Vector demands two times of dc-voltage in FS3P topology as compared with conventional six switch inverter for two dc-links at input of FS3P inverter. This causes increase in cost thus an effort is made to create two dc-links voltage using dc-dc boost conversion whose concet, methodology and implementation is well described in chapter 6. This section contains a performance analysis of 5.4HP, 220V star connected IM Drive from mentioned topology. The motor is run from no load to full load in different intervals as shown in table 8.6.

Input Voltage = 48 Volts

Winding 1 turns (primary) = 34

Winding 2 turns (secondary) = 496

Winding 3 turns (secondary) = 496

Rating of 3 winding transformer = 5000 VA

Capacitance of DC-Link capacitors = 1000 mF

8.5.1 Rotor Speed

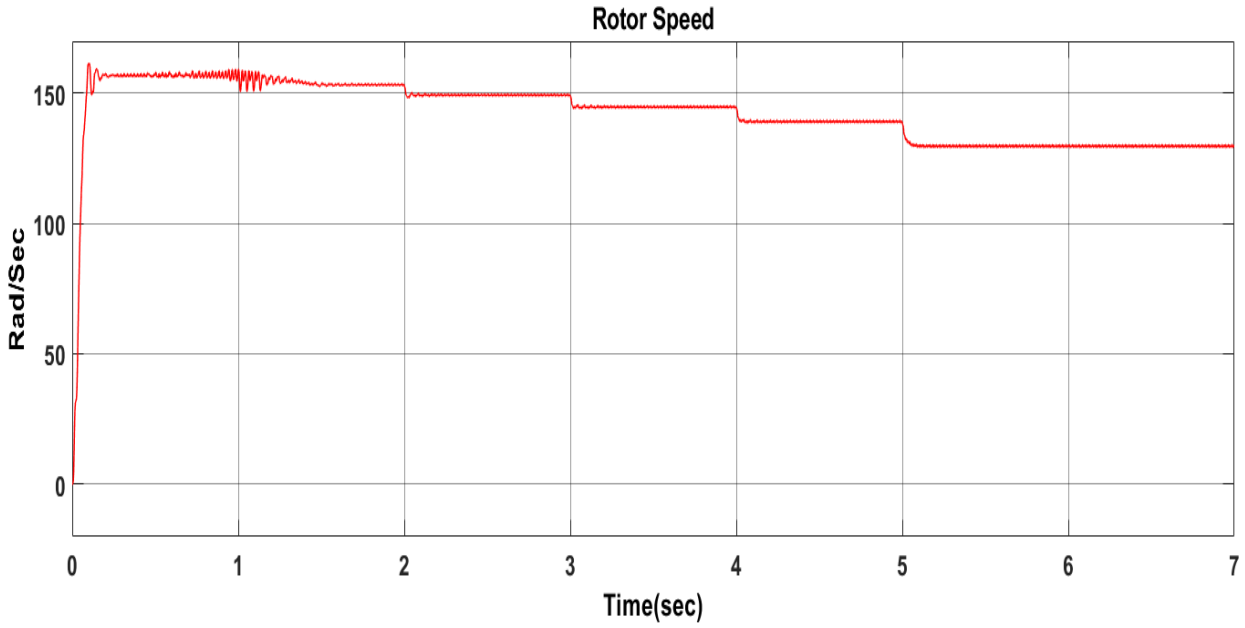

Fig.8.42 Rotor Speed of 5.4HP Motor with dc boost conversion in FS3P Inverter

The behavior of rotor speed can be seen in fig.8.40. With increase in load the speed of motor decreases and settles to a constant value in the same way as seen in previous sections. The fluctuation in the mean value can be seen during (0-2) seconds due to high voltage ripples between two dc-link capacitors. Table 8.15 shows the rotor speed at different loads.

Table 8.16 Rotor Speed for 5.4HP Motor with dc boost conversion in FS3P Inverter

Time (sec)	Load Input (N-m)	Rotor Speed (rad/sec)
(0-1)	0	157
(1-2)	5	153.5
(2-3)	10	149
(3-4)	15	145
(4-5)	20	139
(5-6)	26	129.5

8.5.2 Electromagnetic Torque

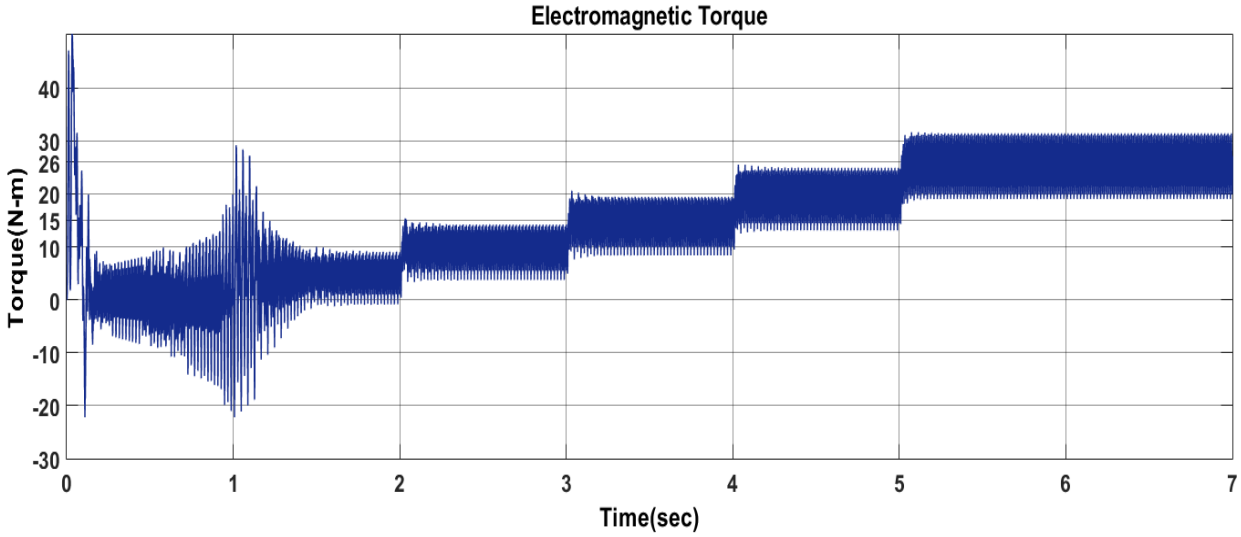

Fig.8.43 Electromagnetic Torque for 5.4HP Motor with dc boost conversion in FS3P Inverter

The electromagnetic torque generated can be shown in fig.8.41. The generated torque is changing in accordance with load torque. During the interval at (0.5-1.5) seconds a high fluctuation is observed which is due to high unequal voltages in the two dc-link capacitors which produce imbalance in the system.

8.5.3 Stator Currents

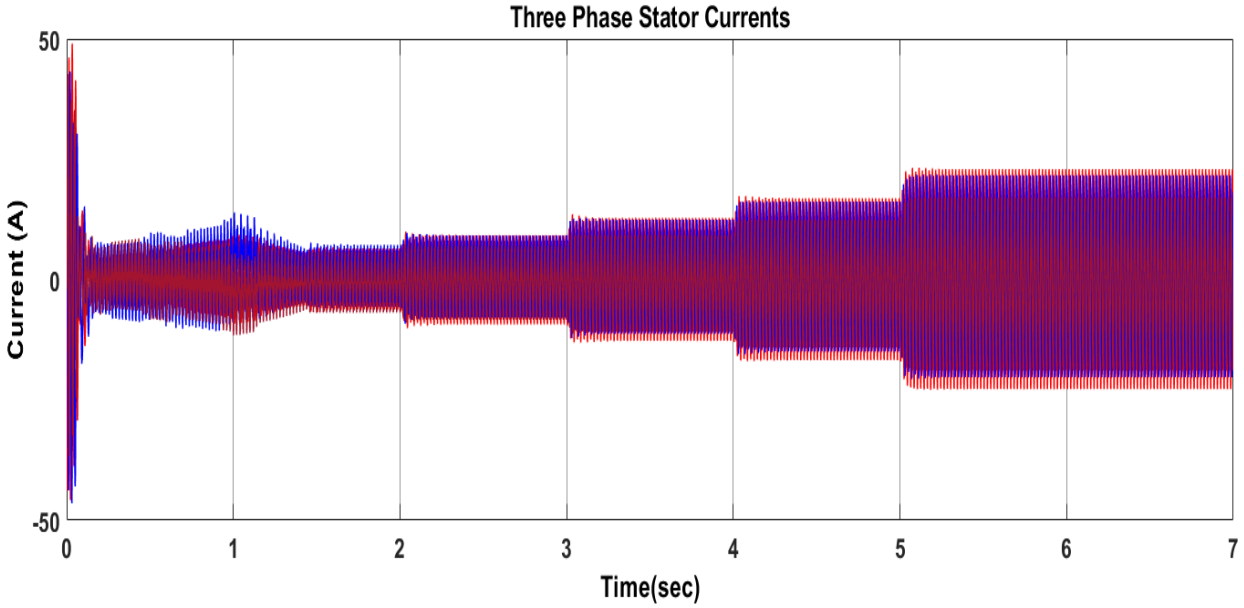

Fig.8.44 Three Phase Stator Currents of 5.4HP Motor with dc boost conversion in FS3P Inverter

The behavior of motor stator current can be seen in fig.8.42 at different loadings to the motor. The stator current is increasing from low value to rated value as load to the motor increases. Fig.8.43 shows the current waveforms when rated load is applied to the motor, the imbalance in the current waveforms for three phase is observed which is due to existence of voltage ripples in two dc-link capacitors i.e unequal voltages between two capacitors which feeds the inverter at input.

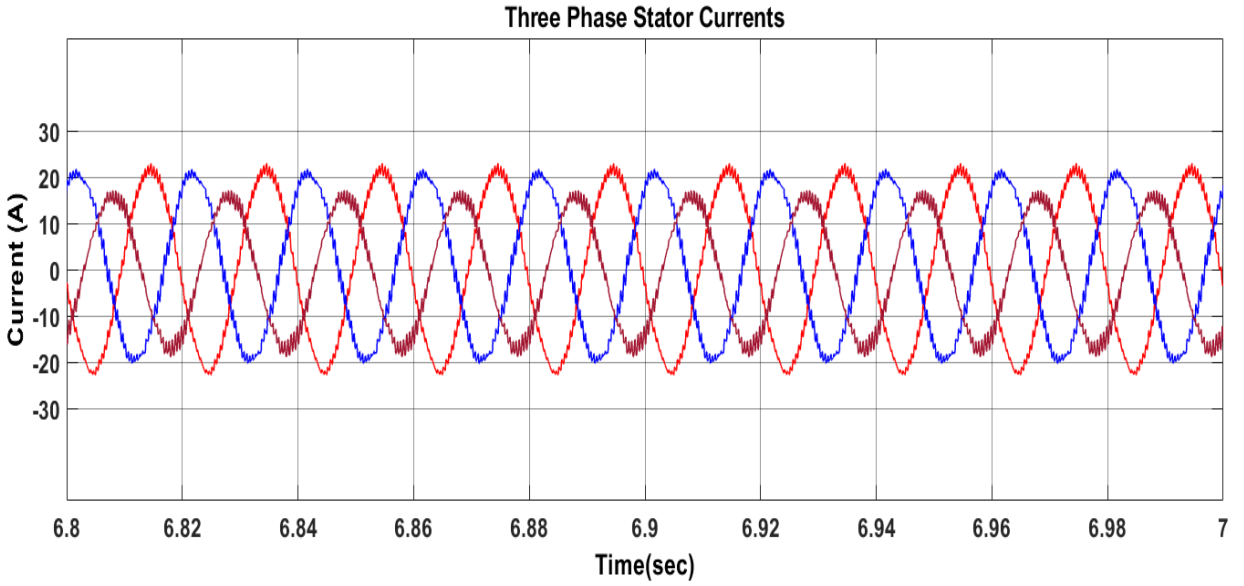

Fig.8.45 Current Waveforms for 5.4HP Motor with dc boost conversion in FS3P Inverter

The THD is also being calculated using FFT analysis tool to comment on the effectiveness of the given method i.e how much our fundamental wave is getting distorted using the proposed method. The Fig.8.44 shows the THD calculation in stator currents at rated load.

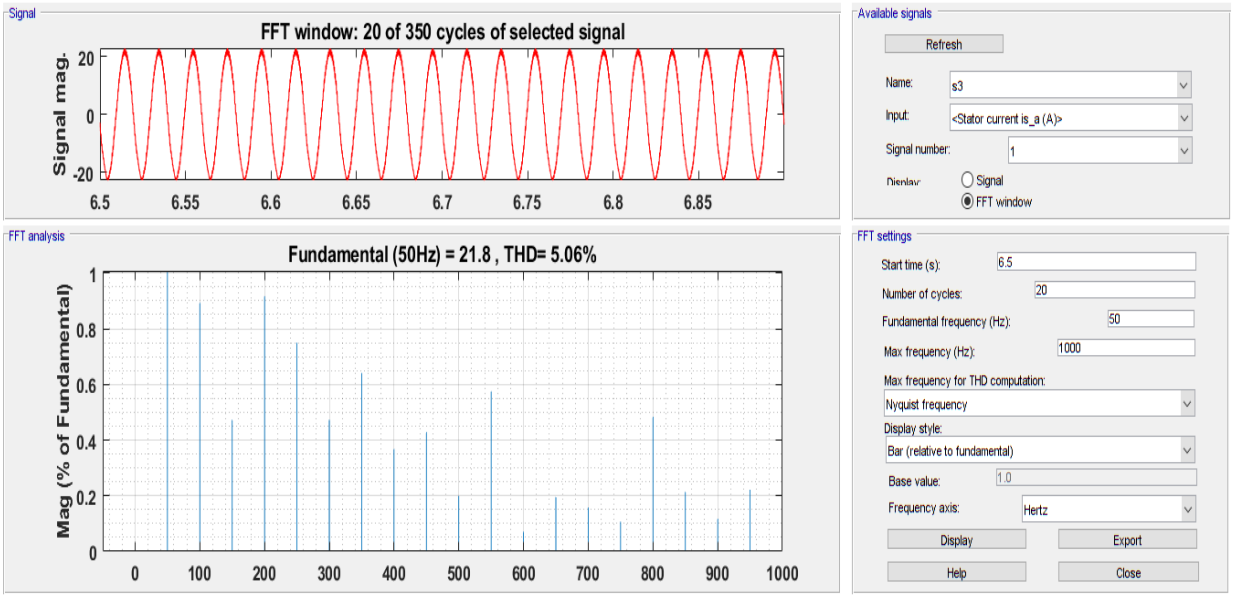

Fig.8.46 THD in currents for 5.4HP Motor with dc boost conversion in FS3P Inverter

The calculated THD is 5.06% which is in permissible limits. The proposed method with dc-dc boost conversion is tested for 5.4HP motor and it shows the comparable results with the previous topologies. This method using dc-dc conversion has advantage of low voltage requirement of the battery but simultaneously its A-h rating must be high to compensate the power demands. The disadvantage in the method is that it creates the voltage and current imbalance in the three phase voltages and currents, compensating the imbalance in the system, the proposed method of dc-dc boost conversion feeding FS3P inverter which further feed IM Drive would hold good.

CHAPTER 9

CONCLUSION AND FUTURE SCOPE

9.1 CONCLUSION

The simulation part for analysis of induction motor drive fed using six-switch three phase inverter, four-switch three phase inverter and FS3P with DC boost conversion is done in Matlab/Simulink. The switching technique used to pulse the inverter switches is SVPWM.

The variation of motor speed, electromagnetic torque and stator currents is observed for three induction motor drives by varying load from no load to full load and results are noted. It is observed that performance of induction motor is approximately same for conventional six-switch and proposed four switch inverter topology, but current THD for FS3P inverter topology is found higher.

FS3P topology with dc-dc boost conversion to fed induction motor is also studied and results are observed. The simulation part for this topology is done with 5.4HP induction motor drive and it is observed that performance of motor matches all the testing parameters with conventional topology but unbalancing in voltage and current is induced due to presence of voltage ripples in dc-link split capacitors.

9.2 FUTURE SCOPE

Some workable recommendations for future work to the work carried out in this dissertation is given below:

- Speed Controllers in FS3P can be designed and simulated.
- Creating dc-link using multi-input and multi-output dc-dc boost converter.
- Compensation of voltage and current unbalance arising due to dc-link split capacitors using voltage ripples compensation techniques.
- The experimental execution of the proposed method to fed induction motor drive can be carried out using dSpace.

REFERENCES

[1] H. W. Van Der Broeck and J. D. Van Wyk, "A Comparative Investigation of a Three-Phase Induction Machine Drive with a Component Minimized Voltage-Fed Inverter under Different Control Options," *IEEE Transactions on Industry Applications*, vol. IA-20, no. 2, pp. 309-320, March 1984.

[2] C. B. Jacobina, E. R. C. da Silva, A. M. N. Lima and R. L. A. Ribeiro, "Vector and scalar control of a four switch three phase inverter," IAS '95. *Conference Record of the 1995 IEEE Industry Applications Conference Thirtieth IAS Annual Meeting*, Orlando, FL, USA, 1995, pp. 2422-2429 vol.3.

[3] S. R. Bowes and D. Holliday, "Comparison of pulse-width-modulation control strategies for three-phase inverter systems, " *IEE Proceedings - Electric Power Applications*, vol. 153, no. 4, pp. 575-584, July 2006.

[4] F. Blaabjerg, S. Freysson, H. -. Hansen and S. Hansen, "A new optimized space vector modulation strategy for a component minimized voltage source inverter," *Proceedings of 1995 IEEE Applied Power Electronics Conference and Exposition - APEC'95*, Dallas, TX, USA, 1995, pp. 577-585 vol.2.

[5] P. N. Enjeti and A. Rahman, "A new single-phase to three-phase converter with active input current shaping for low cost AC motor drives," *IEEE Transactions on Industry Applications*, vol. 29, no. 4, pp. 806-813, July-Aug. 1993, doi: 10.1109/28.231999.

[6] F. Blaabjerg, D. O. Neacsu and J. K. Pedersen, "Adaptive SVM to compensate DC-link voltage ripple for four-switch three-phase voltage-source inverters," *IEEE Transactions on Power Electronics*, vol. 14, no. 4, pp. 743-752, July 1999.

[7] H. W. van der Broeck and H. -. Skudelny, "Analytical analysis of the harmonic effects of a PWM AC drive," *IEEE Transactions on Power Electronics*, vol. 3, no. 2, pp. 216-223, April 1988.

[8] P. N. Enjeti and W. Shireen, "A new technique to reject DC-link voltage ripple for inverters operating on programmed PWM waveforms,"*IEEE Transactions on Power Electronics*, vol. 7, no. 1, pp. 171-180, Jan. 1992.

[9] N. V. Nho, T. H. Phuc and N. X. Bac, "Novel carrier PWM technique with extension range for 4-switch inverter," *2007 7th Internatonal Conference on Power Electronics*, Daegu, 2007, pp. 1056-1061.

[10] S. K. Mondal, B. K. Bose, V. Oleschuk and J. O. P. Pinto, "Space vector pulse width modulation of three-level inverter extending operation into over modulation region," *IEEE Transactions on Power Electronics*, vol. 18, no. 2, pp. 604-611, March 2003.

[11] G. A. Covic, G. L. Peters and J. T. Boys, "An improved single phase to three phase converter for low cost AC motor drives," *Proceedings of 1995 International Conference on Power Electronics and Drive Systems. PEDS 95*, Singapore, 1995, pp. 549-554 vol.1.

[12] P. Q. Dzung, Le Minh Phuong, P. Q. Vinh, N. M. Hoang and T. C. Binh, "New Space Vector Control Approach for Four Switch Three Phase Inverter (FSTPI)," *2007 7th International Conference on Power Electronics and Drive Systems*, Bangkok, 2007, pp. 1002-1008.

[13] H. Lee, P. Q. Dzung, L. D. Khoa and L. M. Phuong, "The development of space vector PWM for four switch three phase inverter fed induction motor with DC - link voltage imbalance," *2009 IEEE International Conference on Industrial Technology*, Gippsland, VIC, 2009, pp. 1-6.

[14] Keliang Zhou and Danwei Wang, "Relationship between space-vector modulation and three-phase carrier-based PWM: a comprehensive analysis [three-phase inverters]," *IEEE Transactions on Industrial Electronics*, vol. 49, no. 1, pp. 186-196, Feb. 2002.

[15] S. R. Bowes and Yen-Shin Lai, "The relationship between space-vector modulation and regular-sampled PWM," *IEEE Transactions on Industrial Electronics*, vol. 44, no. 5, pp. 670-679, Oct. 1997.

[16] D. G. Holmes, "The general relationship between regular-sampled pulse-width-modulation and space vector modulation for hard switched converters," *Conference Record of the 1992 IEEE Industry Applications Society Annual Meeting*, Houston, TX, USA, 1992, pp. 1002-1009 vol.1.

[17] R. Arulmozhiyal, K. Baskaran, N. Devarajan and J. Kanagaraj, "Space Vector Pulse Width Modulation Based Induction Motor Speed Control Using FPGA," *2009 Second International Conference on Emerging Trends in Engineering & Technology*, Nagpur, 2009, pp. 742-747.

[18] Zhang Liwei, Wen Xuhui and Liu Jun, "A novel fundamental voltage amplitude linear output control strategy of SVPWM inverter in the overmodulation region," *31st Annual Conference of IEEE Industrial Electronics Society, 2005. IECON 2005.*, Raleigh, NC, 2005, pp. 4 pp.

[19] Z. Li, M. Zhang, Y. Guo and X. Zhang, "Overmodulation strategy for four-switch three-phase inverter based on virtual voltage vector," *2017 36th Chinese Control Conference (CCC)*, Dalian, 2017, pp. 7364-7369.

[20] V. Kaura and V. Blasko, "A new method to extend linearity of a sinusoidal PWM in the overmodulation region," *IEEE Transactions on Industry Applications*, vol. 32, no. 5, pp. 1115-1121, Sept.-Oct. 1996.

[21] Z. Yuan and J. Cheng, "Research on Space Vector PWM Inverter Based on Artificial Neural Network," *2013 Sixth International Symposium on Computational Intelligence and Design*, Hangzhou, 2013, pp. 80-83.

[22] T. D. Nguyen, H. M. Nguyen and Hong-Hee Lee, "An adaptive carrier-based PWM method for four-switch three-phase inverter," *2009 IEEE International Symposium on Industrial Electronics*, Seoul, 2009, pp. 1552-1557.

[23] D. Joshi, K. S. Sandhu and M. K. Soni, "Constant voltage constant frequency operation for a self-excited induction generator," *IEEE Transactions on Energy Conversion*, vol. 21, no. 1, pp. 228-234, March 2006.

[24] K. S. Sandhu and Vivek Pahwa, "A Novel Approach to Incorporate the Main Flux Saturation Effect in a Three-phase Induction Machine during Motoring and Plugging," *International Journal of Computer and Electrical Engineering* vol. 3, no. 3, pp. 443-448 , 2011.

INDUCTION MOTOR

Induction motor load to test the effectiveness of proposed topology is used in this project. The induction motor is modeled in Matlab/Simulink as shown in following figure.

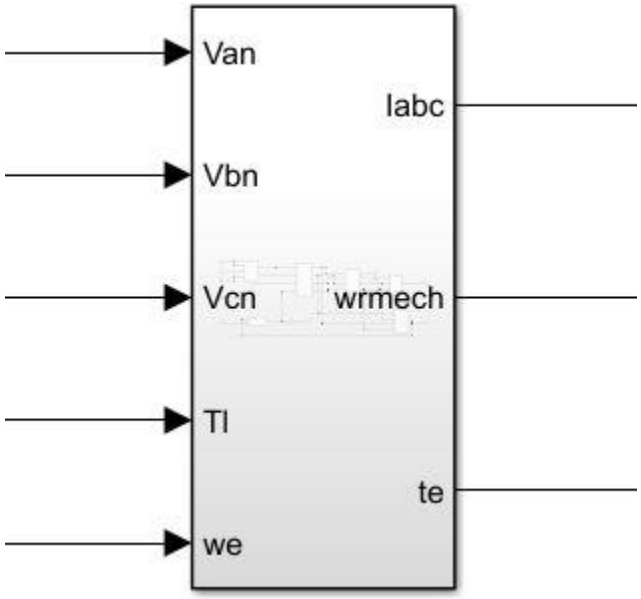

Fig: Modeled Induction Motor Drive

1HP, 380V Star connected induction motor has following parameters

Rated Speed	: 1500 RPM
Stator Resistance (R_s)	: 9.5 Ω
Rotor Resistance (R_r)	: 8.04 Ω
Stator Self Inductance (L_{ls})	: 28.1 mH
Rotor self Inductance (L_{lr})	: 28.1 mH
Magnetizing Inductance (L_m)	: 587.45 mH
Base Frequency (f_b)	: 50 Hz
Number of Poles (P)	: 4
Moment of Inertia (J)	: 0.04 Kg-m^2

3HP, 220V Delta connected induction motor has following parameters

Rated Speed	: 1500 RPM
Stator Resistance (R_s)	: 3.35 Ω
Rotor Resistance (R_r)	: 1.7 Ω
Stator Self Inductance (L_{ls})	: 15.44 mH
Rotor self Inductance (L_{lr})	: 15.44 mH
Magnetizing Inductance (L_m)	: 344.739 mH
Base Frequency (f_b)	: 50 Hz
Number of Poles (P)	: 4
Moment of Inertia (J)	: 0.113 Kg-m^2

5.4HP, 400V Star connected induction motor has following parameters

Rated Speed	: 1500 RPM
Stator Resistance (R_s)	: 1.405 Ω
Rotor Resistance (R_r)	: 1.395 Ω
Stator Self Inductance (L_{ls})	: 5.839 mH
Rotor self Inductance (L_{lr})	: 5.839 mH
Magnetizing Inductance (L_m)	: 172.2 mH
Base Frequency (f_b)	: 50 Hz
Number of Poles (P)	: 4
Moment of Inertia (J)	: 0.0131 Kg-m^2